THESIS/
REPORTS
Richards,
G.N.

FINAL REPORT FOR RESEARCH AGREEMENT
#INT-93847- RJVA
"Analysis of Trace Gases Using New Technology"
THE UNIVERSITY OF MONTANA
FS Contact: Dr. Darold E. Ward
CoOp Contact: Dr. Geoffry Richards

Analysis of Trace Gases Using New Technology

Final Report

To
USDA Forest Service
Intermountain Research Station
Intermountain Fire Sciences Laboratory
Missoula, MT 59807

By
Dr. Geoffrey N. Richards
Dr. Wei Min Hao
Dr. Robert J. Yokelson
Shafizadeh Center for Wood and Carbohydrate Chemistry
University of Montana
Missoula, MT 59812

December 30, 1994

Table of Contents

EXECUTIVE SUMMARY 1

TABLE OF CONTENTS 2

PART 1. AN EVALUATION OF SOME TRACE GAS MEASUREMENT STRATEGIES FOR BIOMASS BURNING AND THE RESULTING RECOMMENDATIONS. 9

INTRODUCTION AND SCOPE OF PROJECT. 10

SURVEY RESULTS. 11

TABLE 1 12

A SUMMARY DESCRIPTION OF THE MOST PROMISING TECHNIQUES. 18

FOURIER TRANSFORM INFRARED SPECTROSCOPY (FTIR). 18

ROOM TEMPERATURE DIODE LASER LONG PATH ABSORPTION. 19

ATMOSPHERIC PRESSURE CHEMICAL IONIZATION MASS SPECTROMETRY (APCIMS). 19

JUSTIFICATION FOR THE INITIAL DECISION TO PURCHASE A FTIR. 20

DETAILS OF THE DEPLOYMENT STRATEGY FOR A FTIR AND A RELATED ASSESSMENT OF THE BEST MODEL TO BUY. 21

HARDWARE CONFIGURATION. 21

PROJECTED SAMPLING LOCATIONS. 22

Laboratory. 22

Field. 22

THE LENGTH OF THE ABSORBING PATH IN SMOKE. 23

EXTERNAL OPTICS. 23

Multipass cell 23

Telescope-retroreflector. 23

DETERMINATION OF THE MOST SUITABLE MODEL OF FTIR. 24

ANALYTICAL METHOD DEVELOPMENT FOR THE FTIR. 24

EXAMPLES OF EXPERIMENTAL PROTOCOLS. 27

SUMMARY 30

APPENDIX 1.1 31

AN ESTIMATE OF PROBABLE CONCENTRATIONS OF TRACE GASES IN BIOMASS SMOKE AND AN ESTIMATE OF THE FTIR DETECTION LIMITS FOR SELECTED COMPOUNDS. 31

How the concentration estimates were derived: *31*

How the detection limits were estimated. *33*

TABLE 2. SOME COMPOUNDS IMPORTANT IN BIOMASS SMOKE THAT CAN BE MEASURED BY FTIR. 34

APPENDIX 1.2 ..... **37**

SOME RECOMMENDATIONS ON ACCESSORIES 37

Detectors. *37*

Beamsplitters. *37*

Windows. *37*

Mirror coatings. *37*

IR source, ADC, Scan Speed. *37*

Resolution. *37*

Filters. *38*

Dedicated Computer. *38*

Manpower. *38*

APPENDIX 1.3 ..... **39**

SOME COST ESTIMATES FOR SPECIFIC SYSTEMS: 39

Bomem *39*

Midac *40*

Idealab *41*

APPENDIX 1.4 ..... **42**

LIST OF MOLECULES ON THE HITRAN DATA BASE. 42

SELECTED REFERENCES **43**

PART 2. SPECIFICATIONS FOR THE DESIGN OF A FTIR SYSTEM OPTIMIZED FOR COMBUSTION EMISSIONS MEASUREMENTS **47**

SUMMARY OF RESEARCH GOALS AND EXPERIMENTAL APPROACH **48**

1.1 SCOPE OF CONTRACT 48

1.2 RESEARCH GOALS. 48

1.3 INTRODUCTION TO EXPERIMENTAL APPROACH. 48

1.3.2 Derivation of technical approach adopted for system design *49*

1.3.2.a Limitations of extractive sampling. *49*

1.3.2.b Limitations of optical remote sensing "fenceline monitoring" systems. 49
1.3.2.c Justification for using optical techniques with a "folded", open optical path. 50
1.3.2.d The need for a custom design for the open, folded optical path. 50

SPECIFICATIONS FOR GAS ANALYSIS SYSTEM FOR FIRE CHEMISTRY PROJECT. 52

2.1 SUMMARY OF CRUCIAL ELEMENTS OF PROPOSED SYSTEM. 52
2.2 DEFINITIONS. 52
2.3 DETAILED SYSTEM SPECIFICATIONS. 52
2.3.2.a Total size of system. 52
2.3.2.b Overall configuration of system components. 53
2.3.2.c Cell: general aspects. 53
2.3.2.d Detectors: speed, amount, sensitivity, and linearity. 54
2.3.2.e Interferometer: attributes. 55
2.3.2.f Source: attributes. 56
2.3.2.g Overall system attributes: 56
2.3.2.h Baseplate: attributes. 57
2.3.2.i Computerized data acquisition and analysis. 58
2.3.2.j Measurement capabilities. 58
TABLE OF DETECTION LIMITS 58
2.3.3. Service, warranty and delivery schedule specifications. 60
2.3.3.b Service: attributes. 60
TERMS: UNCONDITIONAL SATISFACTION GUARANTEED. 61

SCHEMATICS OF GAS ANALYSIS SYSTEM FOR FIRE CHEMISTRY PROJECT. 62

3.1 Schematic of the Optical Configuration of the FTIR and the Cell. 62
3.2 Diagram of the Baseplate. 63
3.3 Diagram of a Deployment Option. 64

SELECTION CRITERIA FOR THE GAS ANALYSIS SYSTEM FOR THE FIRE CHEMISTRY PROJECT 65

RELEVANT INFORMATION FOR STAFF IN OGDEN: NOT TO BE INCLUDED IN BID. 66
Bid Evaluation Panel Membership 66
Government estimate of cost 66
Notes on some vendors contacted regarding project. 68
List of Interested Prospective Bidders 70

ACKNOWLEDGEMENTS. 71

PART 3. RESULTS FROM USE OF A FTIR SYSTEM WITH A DESIGN SIMILAR TO THE PROPOSED SYSTEM 72

ABSTRACT 74

INTRODUCTION 75

METHODS 77

FIRE & FUEL TYPES. 77

EXPERIMENTAL. 78

SPECTRUM ANALYSIS. 79

MALT/CLS based retrievals. 79

Spectral subtraction and peak-height based retrievals. 79

AUXILIARY DATA. 80

ACCURACY & PRECISION OF RESULTS. 80

DERIVED QUANTITIES. 81

CALCULATION OF EMISSION FACTORS. 82

RESULTS AND DISCUSSION 83

TEMPORAL BEHAVIOR OF FIRE EMISSIONS. 84

Interpretative model. 85

Relative fuel consumption by various combustion processes. 88

PRODUCTION OF OXYGENATED ORGANIC COMPOUNDS. 89

Which compounds and how much. 89

Potential effects of oxygenated organic compounds on plume chemistry. 90

PRODUCTION OF REACTIVE NITROGEN-CONTAINING COMPOUNDS. 91

Which compounds are produced. 91

Production levels and relative importance of nitrogen-containing compounds. 92

Potential effects of nitrogen-containing compounds on plume chemistry and sampling. 92

DEPENDENCE OF MEASURED EMISSIONS ON FUEL AND FIRE TYPE. 93

Variation in emission factors in comparison to other uncertainties. 94

COMPARISON OF LABORATORY AND FIELD DATA. 94

Comparison with FTIR field data. 94

Comparison with tower-based integrated canister sampling. 95

Comparison with aircraft grab samples. 96

EMISSION OF SULFUR COMPOUNDS. 96

CONCLUSIONS **96**

ACKNOWLEDGEMENTS **97**

REFERENCES **98**

Figure 1. Experimental arrangement. *104*
Figure 2. Examples of the fitted and measured spectra compared. *105*
Figure 3. Mass balance. *110*
Figure 4 Pine needle types of fire emissions. *111*
Figure 5. Activity fuels types of fire emissions. *112*
Figure 6. Sagebrush types of fire emissions. *113*
Figure 7. Temporal profiles for Acetic Acid and Methanol. *114*
Figure 8. The modified combustion efficiency versus time for two fires. *115*
Figure 9. Tracking not observed in a heterogeneous fuel bed. *116*
Figure 10. Emissions estimates for oxygenated organic compounds. *117*
Figure 11. Pathways for secondary acid production in biomass burning plumes. *118*
Figure 12. Comparison of NH_3 and HCN emissions for fire #11. ..... *119*
Figure 13. Illustration of the dependence of measured N emissions on fuel type. *120*
Figure 14. NH_3/NO_x as a function of modified combustion efficiency. *121*
Figure 15. Spectrum in the C-H stretch region presumably due to terpenes. *122*
Figure 16. Comparison of lab and field measurements. *123*

DATA TABLES FOR PART 3 ..... **124**

APPENDIX 3.1 ..... **137**

SOURCES OF UNCERTAINTY IN GLOBAL EMISSIONS ESTIMATES. 137
SOME ABOVE-GROUND BIOMASS DENSITY AND COMBUSTION FACTOR MEASUREMENTS IN TROPICAL ECOSYSTEMS. 140

SELECTED REFERENCES FOR APPENDIX 1 ..... **144**

APPENDIX 3.2 ..... **145**

FOREST MANAGEMENT IMPLICATIONS 145
Phosphorus Loss from Tropical Soils. *145*
Fire-fighter Exposure to Toxic Compounds in Smoke. *146*
Figure P3A3.2.1. Formaldehyde to CO ratio. *147*
Management implications for local impacts. *148*

Implications from the global perspective. *148*
Smoke effects on plant growth. *149*
Some Future Research Needs. *150*

SELECTED REFERENCES FOR APPENDIX 3.2 ..... **153**

APPENDIX 3.3 ..... **154**

MISCELLANEOUS EXPERIMENTAL NOTES. 154
H_2O *154*
CH_3OH *154*
HCHO *155*
HCOOH *156*
C_2H_2 ..... *157*
C_2H_6 ..... *157*
C_2H_4 ..... *157*
Implications of the lack of features due to some compounds. *158*
Field-sampling methodology of other workers summarized. *158*
Mass Balance. *159*
NO_X Partitioning. *161*
Fuel H balance. *161*
Percentage of heat released absorbed in convection column. *162*
Effects of Volatile Constituents. *162*
Preliminary assessment of effects of green fuels. *162*

PART 4. CHARACTERISTICS OF THE NEW SYSTEM **164**

S/N IMPROVEMENTS INCORPORATED INTO THE NEW SYSTEM **165**

Faster scan speed allowing more signal averaging. *165*
Longer path length. *165*
Optical Configuration. *165*
Combined effect of improvements. *165*

EXPERIMENTAL IMPROVEMENTS **165**

IMPLEMENTATION SCHEDULE FOR NEW SYSTEM **166**

FIGURE 4.1. SIMULATION OF DATA FROM NEW SYSTEM 168

PART 5. CO2, CO AND HYDROCARBONS EMITTED FROM SAVANNA FIRES IN AFRICA DURING 1992 AND 1993 177

Part 1. An Evaluation of Some Trace Gas Measurement Strategies for Biomass Burning and the Resulting Recommendations.

Introduction and scope of project.

The Fire Chemistry Group at the Intermountain Fire Sciences Laboratory (IFSL) operates an analytical laboratory for the analysis of trace gas emissions from biomass fires. The instrumentation at the IFSL includes: a gas correlation cell for measuring CO_2 and H_2O in real time; and chemiluminescence detectors for real-time measurement of O_3, NO_x, Total Hydrocarbons, and CO. Gas Chromatography is used to analyze canister samples for N_2O, CO_2, CO, CH_4, C_2 - C_8 hydrocarbons, and halogenated hydrocarbons. GC/MS is available through a cooperative agreement with the University of Montana, and it is being used to quantify the release of oxygenated hydrocarbons from smoldering combustion of forest fuels.

There are many other compounds produced during the pyrolysis and oxidation resulting from fires in forest fuels. These need to be measured to more fully characterize the composition of the smoke. Because of the need for improved estimates of what is in smoke and how much is produced, a survey was completed of the literature on air pollution, atmospheric chemistry, combustion chemistry, instrumental development, biomass burning, and related fields to assess new technology which might be usefully applied in the study of biomass smoke.

Biomass smoke presents a considerable measurement challenge. The large number of compounds gives rise to a very large potential for interference. (Appendix I contains an estimate of the concentrations of some representative components of smoke from biomass fires.) The analytes of interest are present in an extremely broad range of concentrations; from the hydroxyl radical at parts per quintillion to CO_2 at parts per hundred; a dynamic range of more than 12 orders of magnitude. The smoke also presents a harsh chemical and thermal environment. In order to meet the goals and challenges outlined above the evaluation process stressed the following criteria:

- Sensitivity to a broad range of important compounds especially reactive trace gases.

- Sensitivity to some trace gases which can be measured by our current instruments as a complementary technique.

- Resistance to "chemical noise" or interfering signals from compounds other than the one being measured.

- Time response for the measurement of one or many gases.

- Adaptability to use in both the combustion laboratory and the field (factors considered in this category include weight; "ruggedness" with respect to temperature, mechanical shock, and chemical attack; and the speed and complexity of deployment).

- Cost versus benefits of technique. (Benefits are defined here, primarily, as new information regarding the release of reactive gases, air toxics, and greenhouse gases.)

- Maturity of the technology and the timescale for reliable implementation. (Questions considered here include: Is a reliable version of the instrument commercially available? If not, what is the likely development time? Are methods available for analyzing the output from the instrument?)

- Compatibility with the complementary measurements which are necessary for scientific insight into the processes of interest. For example, can the instrument be deployed in a configuration which will not preclude making other necessary measurements?

Survey results.

Table I lists some of the broad range of techniques considered. For each of these techniques, the successful applications and chief limitations are also shown in Table I. For example, LIDAR is very expensive, measures only a few gases, and only one gas at a time. (Furthermore, LIDAR is only suited for field deployment.) The potential for relevant progress, within the next several years, was also assessed for each of these techniques. Three of the techniques surveyed were judged attractive enough to justify a complete evaluation. These techniques, ranked in order, were Fourier Transform Infrared Spectroscopy (FTIR), Room Temperature Diode Laser Long Path Absorption, and Atmospheric Pressure Chemical Ionization Mass Spectrometry (APCIMS).

Table 1

Key to Symbols:

sc = scattering of probe t = technology immature c = complex

e = expensive se = sensitivity limited l = limited # compounds

i = interference s = sampling problems

Technique and Reference	Limitations	Sample Applications
LIDAR (Light Detection and Ranging) (ref 1 - 3)	c l	O_3, SO_2, NO, NO_2, ambient air. particles, velocity, T°
Photoacoustic Spectroscopy (ref 4)	c e l	hydrocarbons, alcohols aromatics. ambient air auto exhaust.
Laser Induced Fluorescence (ref 5 - 7)	c e l s	OH, O_2, H_2O. flame. OH, NH, CN, NCO. flame. NO, NO_2. troposphere.

Table 1 (cont.)

Technique and Reference	Limitations	Sample Applications
GC/MS	l e	OH, DMS. air.
(ref 8 and 9)		
Multiphoton Ionization Mass Spec.	c e	numerous compounds
(ref 10 and 11)		stack
Electrospray Mass Spec	c e	numerous compounds
(ref 12)		liquids
Atmospheric Pressure Chemical Ionization	c e	numerous compounds
(ref 13 - 16)		ambient air.
Coherent Anti-Stokes Raman Scattering	c e l s	N_2, H_2, H_2O, CO_2.
(ref 17)		flame.

Table 1 (cont.)

Technique and Reference	Limitations	Sample Applications
Ionization Detected Stimulated Raman Scattering (ref 18)	c e l s	NO, benzene (cell) H_2, N_2, O_2 ?
Optogalvanic Spectroscopy (ref 19 and 20)	c e l s	NO, OH, O, H, all trace metals, many ions. flames
Flame Photometry (ref 21)	i l	sulfur compounds flames
Differential Optical Absorption (DOAS) (ref 22 - 24)	i l sc	many important compounds polluted air, but not thick smoke.

Table 1 (cont.)

Technique and Reference	Limitations	Sample Applications
Correlation Spectroscopy (ref 25)	i l se sc	SO_2, and NO_2 in air
Gas Cell Correlation Spectroscopy (ref 26 and 27)	i l	CO_2, H_2O we have CO, CH_4, C_2H_6. air, exhaust.
Chemiluminescence (ref 28)	have	NO_x, O_3, air.
Electrolytic Conductivity (ref 21)	i l	SO_2 air.
Coulometry (electrochemical cells) (ref 21)	have	NO, CO, CO2 air.
Secondary Ionization Mass Spectrometry (ref 54)	c e	Na, K, nitrates, chlorides, surfaces bromides, iodides.

Table 1 (cont.)

Technique and Reference	Limitations	Sample Applications
Membrane Introduction Mass Spectroscopy	c e	numerous organics
(ref 55)		aqueous solutions.
Laser Long Path Techniques.		
Tunable Lead Salt Diode Lasers (ref 29 - 32)	c	NO_2, HNO_3, NO, O_3, CH_4, H_2O, CH_4, HCl, N_2O_5, N_2O, air
Optical Parametric Oscillators	c e se	many gases in cell.
(ref 33)		limited sensitivity.
Excimer or Dye Lasers (uv or visible light)	e sc	OH air.
(ref 34)		
Neutral Gas Lasers (ref 35)	l i	CH_4, N_2O, NO, HCN, CO, HCHO, CH_3OH, air.

(continued next page)

Table 1 (cont.)

Technique and Reference	Limitations	Sample Applications
Room Temperature Diode Lasers (RTDL):		
Visible Diode Laser	sc l	NO_3 cell
(ref 36)		
Near IR Diode Laser (ref 37 - 39)	t	CO_2, CO, NO_2, HCl, H_2S, HBr, NH_3, H_2O, C_2H_2, HCN, air
Wavelength extended RTDL "blue"	t sc i	NO_2 to be tested
(ref 37)		
WEX mid IR	t	numerous compounds
(ref 40)		testing beginning.
Fiber Lasers	t c	acetylene
(ref 52)		other possibilities
Degenerate Four-Wave Mixing	c e	numerous compounds
(ref 53)		flames

A summary description of the most promising techniques.

Fourier transform infrared spectroscopy (FTIR).

Molecules absorb infrared radiation (IR) at characteristic frequencies. The frequency range from 400 cm^{-1} to 4000 cm^{-1} allows detection of the vast majority of molecules and has been termed the "fingerprint region". With a fourier transform infrared spectrometer (FTIR) one can measure molecular absorbance throughout this range of frequencies, simultaneously, and in a very sensitive fashion. (A complete description of a FTIR is beyond the scope of this review and the reader is referred to the text of Griffiths[41] for this information.) I will briefly describe the function of the major components of a FTIR. (See also Figure 1.)

As shown in Figure 1, the main components of an FTIR are the source, mirrors, beamsplitter, and detector. The source emits stable, intense, infrared radiation (IR) throughout the fingerprint region. The source radiation is passed through the interferometer and the sample, and then focused onto the detector. The interferometer consists of a beamsplitter and two mirrors. The beamsplitter directs one half of the incoming IR to a fixed mirror and the other half to a moving mirror. The IR which is returned from these mirrors is recombined by the beamsplitter and directed to the detector. The detector measures the infrared intensity as a function of the position of the moving mirror. This data is called the "interferogram". The fourier transform of the interferogram is the infrared intensity as a function of frequency.

Because of its design, a FTIR can complete measurements where high resolution, high sensitivity, and broad spectral coverage are required, at least a thousand times faster than a conventional IR spectrometer. It should also be noted that there have been dramatic improvements in FTIR technology in recent years. This is especially true in the areas of data analysis routines, reference spectra generation, detectors, beamsplitters, IR sources, coherent signal averaging technology, analog to digital converters, mirror coatings, filters, and sampling methodology. Up to date recommendations for some accessories appear in appendix II. Some attractive options for purchase of a FTIR appear in Appendix III.

An important trend in FTIR-based field measurements in recent years involves instrumental resolution. The atmospheric pressure-broadened linewidths of most species of interest are about 0.2 cm^{-1} (FWHM). Therefore an instrumental resolution of 0.1 cm^{-1}

gives the best S/N and "resistance" to interference. However, experience has shown that most compounds (with N_2O and NO being notable exceptions) can be measured, "adequately", with 1.0 cm^{-1} resolution. Under-resolved spectra do cause lowered sensitivity and more nonlinearity for the measurement of some compounds. However, the smaller data files can be analyzed faster and there is a tremendous savings in the cost of the instrument. Obviously a key part of the consideration of FTIR technology is for the user to analyze the tradeoffs involved in instrument cost and instrument resolution. It is the feeling of most experienced FTIR users, at this time, that it is easiest to justify the cost of a lower resolution instrument if measurements of NO and N_2O are not required.

Room temperature diode laser long path absorption.

Laser long path absorption measurements are accomplished as follows. Light from a tunable laser source passes through a long atmospheric path and then onto a detector. As the laser frequency is scanned through a molecular absorption feature the delivered intensity at the detector changes in a way that can be rigorously related to the average concentration of the molecule over the absorbing path. Many variations of this experiment exist, but will not be discussed here.

Most laser long path absorption studies have utilized dye lasers or lead salt diode lasers as the light source. Dye lasers require a precisely aligned pump laser with the two lasers costing in excess of $100,000. Lead salt diode lasers are inexpensive, but operate at liquid helium temperatures so that the apparatus required for a measurement is complex and expensive. Diode lasers are now available that operate at room temperature. Wavelength extension techniques, applied to these lasers have enabled straightforward production of inexpensive laser light from the IR to the UV. This laser light can be efficiently captured and transferred by optical fibers which offers some advantages for remote deployments.

Atmospheric pressure chemical ionization mass spectrometry (APCIMS).

A mass spectrometer (MS) has four basic regions. Region one is where some fraction of the analyte is converted to ions. This region is typically called the source. In region two (the "ion optics") the ions are efficiently collected by electric fields and directed towards region three. Region three contains a method for sorting the ions based on their mass to charge ratio. Some common mass-sorting techniques are based on magnetic deflection, time-of-flight, or the quadrapole filter. The sorted ions then enter region 4 and are

detected as a function of mass. A single ion is readily detectable by a variety of methods. Traditional mass spectrometry, if applied to the atmosphere, loses sensitivity in two major ways:

1) The spectrometer must be operated at low pressure ($< 10^{-5}$ torr) to avoid electrical discharges from the required high fields. Thus, there is a pressure drop between the sample and the ion source which corresponds to a sample dilution of many orders of magnitude.

2) Only a small fraction of the analyte can be converted to ions when using conventional means of ionization.

In APCIMS an ambient air sample can be directly ionized at atmospheric pressure by a controlled discharge. Alternatively, the incoming air can be mixed with another gaseous flow containing excess "reagent ions" which then impart their charge to the desired fraction of the analyte. In both of these cases, the ions are directed towards the mass sorting region by virtue of the fact that they are constrained to travel along stable lines dictated by the laminar flow of the gas. A small portion of the laminar flow, which contains the highest density of ions, is admitted, by a specially designed pinhole, to the mass sorting region. The APCIMS design has increased sensitivity because of the high ionization efficiency and the fact that there is not a large sample dilution factor. APCIMS has achieved the most sensitive field measurements made to date. By scanning the mass filter a variety of compounds can be measured within a few seconds.

Justification for the initial decision to purchase a FTIR.

In principle, FTIR is capable of measuring, simultaneously, hundreds of compounds of interest. (See Table II) A large number of compounds measured by our GC's and all the compounds measured by our chemiluminescence instruments are on this list. The FTIR can measure all these compounds, in situ, simultaneously, in a matter of seconds. It is beneficial to have more than one way to measure a compound as this guards against possible systematic errors in the implementation of a single technique. A number of useful intercomparisons between the path integrated measurements of FTIR and point sampling techniques have been made.[42] FTIR has been successfully used to measure trace gases in polluted atmospheres and in flames. The IFSL was involved in a feasibility study (see ref.

48) which showed the great value of FTIR for measuring components of biomass smoke. (In this study HCN, CH_4, HCHO, CO, CO_2, NO, NO_2, N_2O, and NH_3 were measured.) FTIR's have been deployed on balloons; vans; airplanes; and on US Army, "Blackhawk" helicopters. At least two dozen manufacturers offer FTIR models "ready to take data".

In comparison to diode lasers, FTIR offers a more mature technology and the capacity to measure compounds simultaneously. While diode lasers offer greater sensitivity for selected compounds than FTIR, interference, rather than sensitivity, is often the most serious problem in biomass smoke. The only way to detect interference with diode lasers is through distortion of the lineshape of the analyte transition. On the other hand, a FTIR can yield the entire spectrum of lines for the analyte and the interfering species. This usually allows far more powerful analysis. In addition, exploratory work with a FTIR can guide the eventual choice of the best lines to use for future diode laser work. The result is that FTIR is the technology of choice now with diode lasers being an attractive alternative in the near future; especially for N_2O and NO for which the suitable FTIR is considerably more expensive.

The main advantage of FTIR over APCIMS is cost. A FTIR can be deployed for as little as $50,000. For APCIMS one has a purchase price for the basic instrument of $450,000 and considerable, additional costs for deployment. The APCIMS is also considerably more complex to deploy, although this has been achieved nicely by several groups. At this time, I recommend developing a strong collaboration with another group which currently has the expertise and funding to deploy APCIMS. A pilot-scale study should be pursued.

Details of the deployment strategy for a FTIR and a related assessment of the best model to buy.

Hardware configuration.

There are a number of potential hardware configurations for FTIR. In our case, we must use the option which allows discrimination against emission and turbulence by source modulation. The light from the IR source passes through the interferometer, which modulates its intensity at high frequency, before it passes through the sample and is focused on the detector. Only the high frequency component of the light incident on the

detector is amplified, thus the slower variation in light intensity due to gas turbulence and emission from hot gases adds little noise to the data.

Projected sampling locations.

Laboratory.

Initially, the ideal location for the FTIR is on the sampling platform in the IFSL controlled environment combustion facility (CL). (See Figure 1 (part 3).) Many operational aspects of using the technique can be perfected while performing an extensive series of carefully controlled experiments. Because some of the more reactive compounds may be effected by the walls of the stack in the CL, it will be necessary to move the FTIR to locations below the stack entrance for some tests. In addition, field tests are envisioned to verify results found through CL research. The laboratory deployment is the focus of this report and is discussed in more detail in many of the following sections.

Field.

Unlike the situation in the CL, where it is easy to measure well-mixed smoke which is representative of the total fire emissions, the field measurements present a deployment challenge. Except in unique topographic situations, an FTIR and source which are deployed at ground level (for instance on tripods) will not be able to effectively sample the rapidly rising emissions which represent the bulk of the smoke. In order to sample "representative smoke", it is necessary to situate the optical absorbing path in the well integrated convection column above the fire. For this reason we are examining the option of a tower based deployment of the FTIR. This could conceivably work in one of two ways.

1) The FTIR, permanently aligned with the optical path, is mounted on a tower at a "safe" height.

2) The FTIR is buried, under the ground, near a tower on which the optical path is mounted. This option is safer for the instrument, but creates two difficult experimental problems. The light must be transferred through a nonabsorbing medium ("light pipe") to the path and achievement of a stable alignment of the widely separated components is necessary for each deployment.

At this time, I prefer the first option, but the actual field deployment is still in the future.

The length of the absorbing path in smoke.

The choice of optical path is very important. In theory, optimum sensitivity is achieved for each compound by choosing a pathlength such that 70% of the light is absorbed in the wavelength region of interest. In practice, this would dictate a different path length for each gas measured. A reasonable, standard pathlength must be adopted. A 100 meter path through smoke will give strong enough absorption and strong enough transmission, of the IR radiation, to yield the best measurement for most compounds.

External optics.

There are two "leading" alternatives for the type of external optics used to create the absorbing path.

Multipass cell

In a multipass cell (see figure 1) the light is refocused many times so that the IR energy delivered to the detector depends on the sample absorbance and the mirror absorbance. The second effect is small and stable. An open path, multipass cell could directly sample smoke with few wall effects, but the optics and mounts must be able to withstand the harsh smoke environment. This compatibility is achievable to temperatures of about 150° C. There are a number of cell designs which can achieve a 100 meter path with a 1.5 meter (or less) base path length. The temperature and humidity can be measured at the cell independently. A multipass cell can weigh as little as 15 pounds and can be mounted on a Invar baseplate in permanent alignment with the FTIR. This makes an attractive option for a tower deployment. Even small fires can fill the whole optical path with smoke. In the combustion lab, the multipass option is the only way to get a long path and the resulting high sensitivity.

Telescope-retroreflector.

A widely used type of optical path for FTIR deployments is based on the following hardware configuration. The IR radiation passes through the interferometer, external beamsplitter, collimating telescope, and the sample; then it is retroreflected through the

sample again, back into the same telescope (for collection), off the external beamsplitter, and then it is focused onto the detector. In this arrangement there are less reflections and less absorption by the mirrors. However, because of the external beamsplitter and beam divergence a much smaller fraction of the source energy is transmitted to the detector. This causes a decrease in sensitivity of several orders of magnitude. (S/N is proportional to the square root of the number of transmitted photons.) Furthermore, the optics must be realigned with each use. There are some advantages to this approach. The optics and the instrument do not need to be exposed to the smoke and there is no chance for wall effects to cause systematic error. However, because of the long, "unfolded" path; a very inhomogeneous thermal environment might be sampled which considerably complicates the data analysis. Also the whole absorption path does not sample smoke which compromises attempts at absolute, or even relative, measurements.

At this time, the optimum choice for the CL deployment is the multipass cell and this also seems to be the best choice of external optics for any future field deployment.

Determination of the most suitable model of FTIR.

As stated earlier, there are at least two dozen models of FTIR commercially available. For our application, described more below, there are three leading candidates. Bomem makes a permanently aligned 1.0 cm^{-1} resolution interferometer which has a long history of successful field deployment. Midac manufactures a 0.5 cm^{-1} resolution, plane mirror interferometer for about the same price, but with one sixth the weight. (The low weight is attractive when considering tower deployment.) Idealab sells a 0.1 cm^{-1} interferometer for the same price as the lower resolution models of Bomem and Midac, but they do not yet offer the necessary software and hardware interfaces. Unless we determine soon that the interfaces for the Idealab product can be acquired trivially, a logical choice for a first instrument is the Midac. Midac offers several rental options for which I have the details. I have not yet ruled out the Bomem; and they sometimes have "trade-ins" available for 50% off list. Notes, and details on the cost of the various options for a new system are given in appendix III.

Analytical method development for the FTIR.

There are numerous approaches to retrieving concentrations from FTIR spectra. In the simplest situation, where the temperature and pressure in the region of the sample is known, the detector is perfectly linear, there is a single component to be measured whose pressure broadened and self broadened linewidth is much greater than the instrumental resolution, and the sample is not "optically thick", the concentration and peak height (A) are related by equation (1)

(1) $A\ (\text{peak wavelength}) = s(T, P, l, c) \times c \times l$

where l is the pathlength and s has been precisely determined for the exact wavelength and temperature, as well as degree of pressure broadening and self broadening. A is defined by Beer's law as $-\log_e(i/i_o)$. Here, i/i_o is the reduction in light intensity due only to the presence of the sample. Alternatively, one can determine concentration directly from the transmission data where transmission is measured directly and is related to absorbance by equation (2).

(2) $T = e^{-A}$

This is our approach since the data analysis is computerized and it is difficult to measure a meaningful background spectrum for a biomass fire. We can retrieve concentrations by analyzing a series of differential transmission features occurring on a single spectrum. Measurements of s as detailed above are sparse because it is often difficult to acquire spectra for a precisely known amount of a pure compound under precisely known conditions. The measurements have inaccuracies which reflect the difficulty of the measurement and furthermore they can be made for only a few of the conditions and millions of spectral lines that are important. As an alternative, an extremely detailed application of advanced quantum mechanical principles can usually achieve an effective parameterization of the shape of the whole spectrum, once certain portions are very carefully measured at very high resolution. This then allows calculation of a reference spectrum for a wide variety of conditions. Recently this practice has been called into question in the case of O_3, but it is believed to be accurate for many compounds to within a few percent.

In practice, with a low resolution instrument, nonlinear effects are introduced and the concentration of a gas in a sample is retrieved in a variety of ways. As in the case of a

high resolution instrument, reference spectra can be experimentally measured for a wide variety of concentrations and under the appropriate conditions. In this way, any nonlinear effects are directly measured for the compound of interest. Because of the difficulty in experimentally measuring reference spectra, noted above, it is now more common for the reference spectra to be calculated. As stated previously, this requires a highly accurate parameterization of the molecular spectra (which is an active research area for many molecules) and, for a low resolution instrument, a very accurate parameterization of the instrumental effects. This is especially true if a nonlinear detector is used. (Nonlinear detectors are often used because they have greater sensitivity.) This second parameterization is normally accomplished by using the low resolution instrument, under well controlled conditions of the operators choice, to experimentally measure a spectrum for a known amount of a compound (such as water) which is relatively easy to handle and whose high resolution spectrum is well studied. Then, the transformation is determined which will degrade the "true" spectrum (i. e. the spectrum calculated from the molecular parameters assuming the same concentration and conditions or the spectrum measured at the same concentration and conditions with a high resolution spectrometer") into the spectrum measured with the low resolution instrument. This is a complex transformation as nonlinear effects and resolution are not equal across the spectrum. Once this transformation is known, the molecular parameterization, in tandem with the instrument transformation, can be used to calculate the reference spectra for many compounds under a variety of conditions.

The reference spectra are used in two main ways to arrive at sample, trace gas concentrations. In one method, the sample spectra is bracketed by a set of reference spectra and interpolation is used to arrive at the sample concentration. As an alternative the concentration can be obtained through a least squares fit of the appropriate portion of the sample spectrum to a properly manipulated reference spectrum.

One must also deal with the presence of multiple absorbers. This is usually done in one of two ways.

(1) Use an isolated line to determine the concentration of one component of a mixture and then subtract the appropriate reference spectrum from the composite sample spectrum and proceed to analyze the "residual".

(2) A more complex, but often more accurate approach is to generate reference spectra of all the suspected components of a mixture, for a variety of assumed concentrations, and then incorporate all these spectra simultaneously in a global, classical least squares fit to the experimental, composite-sample spectrum. This approach may fail when the wrong components are assumed for the mixture.

I hope to implement approach number (2) above, with approach number (1) as an option, in tandem with reference spectra calculated from the HITRAN[43] data base. Dave Griffith has developed a version of approach (2) and validated it over the last several years. He has offered to share his software with us. I will learn this approach, revalidate it, and hopefully extend it to more species and also to higher temperatures. Currently, the HITRAN data base is incomplete in the area of higher temperatures. This can be overcome by referral to the literature, experimental work at high temperature, and by use of the quantum mechanical description of the molecular structure to calculate the high temperature spectrum of the molecule. The Hitran data base is also incomplete in the area of environmentally significant molecules. The 1994 version will have 31 molecules which I have listed in Table III, Appendix IV. We can get useful information, from our spectra, on the concentrations of gases not listed in the HITRAN data base, but a future project will involve construction of a larger data base in order to allow rigorous analysis of more molecules.

A good deal of thought will go into the spectral regions used to retrieve concentrations. A choice of certain lines or regions can minimize nonlinearities and interferences, although sometimes at the expense of sensitivity. The best regions have been determined for numerous compounds under a variety of atmospheric conditions. Some of this work can be used to guide the analysis of smoke spectra, but the high temperatures can introduce complications that prevent blind adoption of "time-honored" procedures. The "experience base" is more limited for smoke analysis and I will have to actively develop some optimized procedures.

Examples of experimental protocols.

For CL fires, continuous measurement of trace gases by the FTIR, can be carried out with temporal resolution on the order of seconds. Simultaneous, well placed measurements of the vertical velocity in the stack will allow characterization and quantification of the flow;

thus enabling conversion of the measured concentrations into trace gas fluxes. Another useful measurement may be the time-resolved particle concentration and carbon content. The change in fuel weight can be monitored simultaneously as well. After the fire, the weight of the unburned fuel, charcoal, and ash, as well as the carbon content of the ash must be measured so that carbon mass balance can be used to check the gas fluxes.

The combination of all these measurements will allow extremely reliable determinations of suitably integrated emission ratios and emission factors for the various trace gases. Emission factors (and useful descriptions of the correlations among the emission factors for various compounds) have been published, but these efforts have largely been for field fires where precise measurements are more difficult. These studies will help "fine tune" previous observations because of the opportunity to acquire a more complete database. Also, some existing work may be beneficially reanalyzed using the results of the proposed experiments in at least two ways.

1) We can carry out a double blind test of the fuels inventory approach versus measured change in weight to test the reliability of the former approach to quantification of biomass burned.

2) The indications from the wood chemistry laboratory work are that the condensable compounds, which currently cannot be explicitly included in CE or EF calculations, may be important. Because FTIR can measure methane and some of the condensable compounds simultaneously, an independent check can be made of the relative importance of the condensable compounds.

In general, once this approach is perfected for one fuel type, the effects of varying the nature of the fuel on combustion efficiency and trace gas emissions can be investigated.

I would also like to propose another valuable approach to the study of fuel effects on biomass burning emissions. I will call this approach " differential experimental burning" (DEB) and it allows suppression of some of the formidable problems in FTIR data analysis. A typical DEB experiment could proceed as follows.

1) A stable "background" fire is established and a spectrum is taken.

2) With care taken to achieve minimal disruption of the flow, small amounts of additional substance are added and "sample" spectra are acquired.

A strength of this approach is that differential analysis of the sample and background spectra should allow the changes in spectral features due to changes in trace gas emissions (which are in turn related to the change in the fuel) to stand out clearly. This is accomplished because the analysis suppresses the interfering spectral features due to the gases which change little in concentration. (The features of the interfering gases cannot be eliminated entirely in one step, but they can be reduced.) Quantification of changes in concentration can be achieved for most of the compounds for which the spectrum is well resolved and optically thin. This will include a lot of important, especially larger, molecules. There is no shortage of interesting substances to add to the "background fire". A partial list includes; NaCl; acetic acid; lignin; cellulose; green branches; red needle branches; gently dispersed, dried, grass clippings; and different sized sticks of known fuel moisture. These experiments might actually represent a useful way to "get started" and guide the associated quantitative measurements described above.

SUMMARY

This work will result in a more complete description of biomass smoke; thus enhancing predictions of global emissions and plume chemistry modeling. The quantitative description will not only enhance our understanding of the likely atmospheric effects, but also allow us to estimate the relative contributions of pyrolysis, condensation, radical-radical kinetics, heterogeneous processes, and the various types of oxidation reactions that occur during fuel consumption. This work will provide expanded knowledge of air toxics emitted from biomass burning and can thus guide the design of mitigation strategies. In short, our work will increase the quantitative understanding of some important aspects of biomass burning, and facilitate insights into other important processes.

Appendix 1.1

An Estimate of Probable Concentrations of Trace Gases in Biomass Smoke and an Estimate of the FTIR Detection Limits for Selected Compounds.

How the concentration estimates were derived:

A complete description of all the compounds in wood smoke is beyond the scope of this work. (More than 400 compounds have been detected in auto exhaust, where the fuel is relatively simple.) Even a complete list of compounds in wood smoke that could be detected by FTIR is beyond the scope of this work. One study alone, reported detection by FTIR, of more than 40 of the 189 molecules listed as hazardous air pollutants in the Clean Air Act Amendments of 1990.[44] Another source lists 174 ambient air molecules detected by FTIR.[45] I will present a necessarily, rough estimate of the "smoke" concentrations for some representative molecules which is based on existing experimental results.

Using the standard, approximate, chemical formula for biomass fuel, one can write the equation for complete combustion of $C_6H_9O_4$ (with air as the source of O_2) as in equation (3).

(3) $$4C_6H_9O_4 + 25O_2 + 100N_2 \rightarrow 24CO_2 + 18H_2O + 100N_2$$

One then, very roughly, expects "pure smoke" to contain about 17% or less CO_2. In the combustion lab studies of Lobert *et al*,[46] a maximum of 6 - 10 percent CO_2 was observed. These authors also list values for the concentration of a number of other compounds. Unfortunately, these results are reported as a range of maximum values. I took the middle of this range as a guess at the average maximum value. In the IFSL CL, the average, maximum, observed value for CO_2 is about 3000 ppm: a factor of 30 lower than in the work of Lobert *et al*. These differences are probably due to varying degrees of dilution by background air. Ideally, the detection limit of our instruments would be below the level present in background air. This would ensure that the emissions released could be followed for the entire course of the fire. Background levels for some of these compounds are either unknown or highly variable. Alternatively, consideration of the real time data of Lobert *et al* and Sussot *et al* (ref. 51), suggests that during most of the fire the concentration of a trace gas is within 0.1 of its maximum value. The convention used in compiling Table II was to list the maximum expected

concentration under conditions similar to those used by Lobert et al. Under these conditions, detection limits would have to be at least a factor of 10 lower than the entry in column 4, in order to follow the temporal profile of the emission for most of the fire. Under conditions similar to those currently used in the IFSL CL, the detection limit would have to be a factor of 300 lower. These are the entries in column 5. A useful, early experiment will be to determine the optimum configuration of the CL. Operating with no dilution at all may allow excessive temperatures in the stack and damage the multipass cell. Operating with too much dilution may complicate the analysis or bar detection of important compounds. It should be a fairly simple matter to optimize the CL configuration, but even if this is not attempted the FTIR should still "see" many compounds during most of the fire. Lobert *et al* list the range of maximum values for these flaming stage compounds CO_2, NO_x, N_2O, SO_2, and C_2H_2. These authors also list analogous results for the following flaming stage compounds CO, CH_4, C_2H_4, C_2H_6, NH_3, HCN, and CH_3CN. All these values are listed in Table II. Furthermore, these authors list emission ratios for some compounds as a percentage of CO. Table II lists concentrations for HNO_3 and CH_3Cl derived by multiplying the appropriate emission ratios by the reported CO concentration.

At least two other authors have attempted to divide the NO_x into NO_2 and NO. The aircraft study of Andrea *et al*[47] gives the ratio of NO_x/NO as 4:1. In contrast, the study of Griffith *et al* [48] measured smoke closer to the fire where the reaction of NO and O_3 would have had less impact. Griffith *et al* report a NO/NO_2 ratio of 2:1. Furthermore, Griffith *et al* report a NO_x/CH_4 ratio of .1 as opposed to .66 reported by Lobert *et al*. These differences may reflect the fact that the study of Griffith *et al* was biased towards the smoldering stage *and* sampled ambient air in addition to smoke. I derived a minimum "average maximum" for NO and NO_2 by using the NO_x/CH_4 and NO/NO_2 ratios of Griffith *et al* and the actual reported concentrations of Lobert *et al*.

Measurements on smoldering fires in the Wood Chemistry Lab[49] can be analyzed for the ratio of a number of condensable compounds relative to methane. (FTIR can provide an important check on these ratios.) The reported ratios in this study and the reported concentrations for CH_4 of Lobert *et al* are used to estimate smoke concentrations for methanol, acetic acid, vinyl acetate, pyruvic acid, and formic acid.

Griffith *et al* reported measurements for NH_3 and Formaldehyde relative to carbon dioxide. Using Griffith's emission ratio to CO_2 and Lobert's $\langle[CO_2]_{max}\rangle$ one gets very high values for

these two compounds. Lower values (by a factor of 5) are obtained by noting that Griffith *et al* report ratios of Formaldehyde and Ammonia to Methane of 20 and 75 percent respectively and using these values with the measured methane concentrations of Lobert *et al.*

An estimate for CH_3Br is based on the fact that brominated compounds are normally about 2 orders of magnitude less common than the chlorinated analog. An estimate of the ethyl chloride concentration is derived based on the apparent correlations for homologous series. Lobert *et al* and the wood chemistry group report CH_4/C_2H_6 ratios of 13.4 and 7.5 respectively. The ratio of emission ratios in the study of Lobert *et al* for methylamine/ethylamine and acetonitrile/proprionitrile are 8 and 12.5. These trends suggest that the ethylchloride concentration might be about one tenth of the methyl chloride concentration. This could well be a low estimate as the reaction of OH and ethane is 37 times faster than the reaction of OH and methane. (One FTIR-based combustion study detected more than 20 chlorinated organic molecules.)[50]

Lobert *et al* list emission ratios, relative to CO, of 0.21, 0.12, and 0.05 percent for benzene, toluene, and xylenes respectively which compares to 9.11% for methane. Thus aromatics are estimated to be 4% of methane and mono-chlorinated aromatics are estimated at 4% of methyl chloride.

The work of Sussot *et al*[51] with the FASS system shows average maximum CO_2 concentrations a factor of 7 lower than in the work of Lobert *et al.* This factor may useful to keep in mind for any future, tower-based, field deployments.

How the detection limits were estimated.

The detection limits are based on equation (1) with an assumed pathlength of 100 meters, 0.5 cm^{-1} resolution, and an ability to resolve an absorption of 10^{-4} with a S/N of 1.0. These are not assumptions requiring heroic efforts, but it should be remembered that a S/N of 10.0 has roughly 10% relative accuracy. It is also possible that chemical noise will raise the detection limits for some species.

Table 2. Some Compounds Important in Biomass Smoke That Can be Measured By FTIR.

Chemical Name or Formula	Hitran Database?	Minimum Detectable Level	Estimated Concentrations	
			Lobert *et al* (max)	Sussot *et al* (min) ppb
CO	Y	0.6 ppb	1500 - 3000 ppm	5000 - 10000
CH_4	Y	0.6 ppb	43 - 350 ppm	100 - 1200
C_2H_2	Y	0.03 ppb	4 - 36 ppm	13 - 120
C_2H_4	Y	0.3 ppb	11- 46 ppm	37 - 153
C_2H_6	Y	2.0 ppb	5 - 36 ppm	17 - 120
HCN	Y	* ppb	4 - 30 ppm	13 - 100
CH_3CN	Y	30.0 ppb	2 - 10 ppm	7 - 33
HNO_3	Y	0.3 ppb	4 -8 ppm	13 - 26
methyl nitrate	N	0.2 ppb	1.7 - 3.4 ppm	6 - 12
SO_2	Y	0.4 ppb	20 -30 ppm	67 - 100
O_3	Y	0.6 ppb	50 - 100 ppb	0.2 - 0.3
NH_3	Y	0.2 ppb	4 -148 ppm	13 - 493

Table 2. Some Compounds Important in Biomass Smoke That Can be Measured By FTIR. (cont.)

Chemical Name or Formula	Hitran Database?	Minimum Detectable Level	Estimated Concentrations	
			Lobert *et al* (max)	Sussot *et al* (min) ppb
HCHO	Y	0.6 ppb	39 ppm	130
pyruvic aldehyde	N	sufficient	46 ppm	153
NO_x	-	not measured	100 - 160 ppm	333 - 533
NO	Y	2.0 ppb	12 ppm	40
NO_2	Y	0.2 ppb	6 ppm	20
N_2O	Y	* ppb	2 - 19 ppm	7 - 63
CH_3OH	N	0.25 ppb	138 ppm	460
CHOOH	N	0.7 ppb	59 ppm	197
acetic acid	N	1.0 ppb	99 ppm	329
vinyl acetate	N	0.1 ppb	67 ppm	22
CH_3Cl	Y	1.8 ppb	2 -5 ppm	7 - 17
ethyl chloride	N	2.0 ppb	0.25 - 0.5 ppm	0.8 - 1.6
methyl bromide	N	6.4 ppb	24 -48 ppb	0.08 - 0.16

Table 2. Some Compounds Important in Biomass Smoke That Can be Measured By FTIR. (cont.)

Chemical Name or Formula	Hitran Database?	Minimum Detectable Level	Estimated Concentrations	
			Lobert *et al* (max)	Sussot *et al* (min) ppb
benzene	N	1.0 ppb	4 ppm	13
chloro-benzene	N	0.3 ppb	0.05 - 0.1 ppm	0.2 - 0.3
H_2O_2	Y	0.6 ppb	-	
OCS	Y	2.8 ppb	-	
HOCl	Y	1.0 ppb	150 - 300 ppb	0.5 - 1.0
ClON	N	-	" "	" "

highly resolution dependent

Appendix 1.2

Some Recommendations on Accessories.

Detectors.

A wide-band, linearized MCT detector costs about $16,000. A more common choice is to buy a InSb and a "narrow-band" MCT detector to cover the same spectral range for about $8,000. The combination gives more sensitivity and at a lower price, but requires frequent switching.

Beamsplitters.

The ideal beamsplitter has T = R = 50% for the entire spectral range of interest. This has never been achieved. A self-compensating KBr beamsplitter has the best throughput and should be specified.

Windows.

Depending on the type of multipass cell purchased, we would need 1 or 2 windows for the interferometer. ZnSe is very corrosion resistant, but only transmits 50% of the light. A less expensive window with higher transmission could be used if it is purged during use and cleaned daily.

Mirror coatings.

Ceramic-protected silver has the highest R value, but must be cared for as above or it will be rapidly destroyed.

IR source, ADC, Scan Speed.

The combination of an intense, stable source and a fast scan speed gives the least noise. A more intense source could eventually be employed to enhance sensitivity, but care must be taken that the ADC will not then saturate at the fastest scan speed.

Resolution.

Resolution has been discussed previously. The highest S/N is achieved when the resolution is just below the natural linewidth. One wavenumber is sufficient for the vast majority of compounds.

Filters.

Filters can reduce the unwanted light more than the needed light and thus increase S/N. I will probably want to invest in a few filters as the measurements proceed.

Dedicated Computer.

Most of the vendors charge about $5,000 dollars for the required, dedicated computer, but are willing to let us save money here by getting this on our own.

Manpower.

Given the amount of data that will be generated and the complexity of the analysis, the full benefits of the FTIR could best be utilized by getting some graduate students or technicians involved.

Appendix 1.3

Some Cost Estimates for Specific Systems:

Bomem

1.0 cm^{-1} interferometer and source	20,000
Software Driver	2,000
Hardware Coprocessor	2,000
Two Detectors	10,000
Computer	5,000
Multipass Cell	10,000
Total	**49,000**

Notes:

purgeable

permanently aligned

weight 120 pounds (can be reduced to 60 or 70)

industry standard

add approximately $80,000 for 0.1 cm-1 resolution (Total = $129,000)

Midac

0.5 cm^{-1} interferometer and source	26,000
Software Driver	2,000
Detectors, Computer, Cell	25,000
Total	**53,000**

Notes:

not purgeable

not permanently aligned

weight < 17 lbs

can measure NO, which the 1.0 cm^{-1} Bomem can not do.

Idealab

0.1 cm^{-1} interferometer and source	27,000
Software Driver Program and Board	5,000
Technician (?) Salary to write driver	12,000 - 20,000*
Detectors, Computer, Cell	25,000
Total	**69,000 - 77,000**

Notes:

*This charge may disappear in a year or two, or if I can get a "donated" driver.

permanently aligned

we build case

weight 45 pounds with no walls or top

Can measure NO, N_2O, and has the most potential to allow analysis of complex mixtures.

Appendix 1.4

List of Molecules on the HITRAN Data Base.

Molecule	Isotopes	# of Bands	# of Lines
H_2O	4	134	48 523
CO_2	8	592	60 790
O_3	3	76	168 881
N_2O	5	140	24 125
CO	5	31	3 600
CH_4	3	48	47 415
O_2	3	18	2 254
NO	3	13	7 385
SO_2	2	7	26 225
NO_2	1	9	55 468
NH_3	2	9	5 817
HNO_3	1	13	143 021
OH	3	27	8 676
HF	1	6	107
HCl	2	17	371
HBr	2	16	398
HI	1	9	237
ClO	2	8	6 020
OCS	4	6	737
H_2CO	3	10	2 702
HOCl	2	6	15 565
N_2	1	1	120
HCN	3	8	772
CH_3Cl	2	6	6 687
H_2O_2	1	2	5 444
C_2H_2	2	9	1 258
C_2H_6	1	2	4 749
PH_3	1	2	2 886
COF_2	1	7	46 894
SF_6	1	1	11 520
H_2S	1	1	661

Selected references.

1. H. Kolsch, ed., special issue, *Appl. Phys.* **B55**, 1 - 158, 1992.

2. M. Beniston et al, *J. Geophys. Res.*, **95**, 9879, 1990.

3. A. Waggoner, P. Hobbs, and J. Nance, in: Proceedings Pacific Northwest International Section of the Air and Waste Management Association Annual Meeting 11- 13 November 1992, Bellevue WA.

4. P. Meyer, and M. Sigrist, *Rev. Sci. Instrum.*, **61**, 1779, 1990.

5. P. Andresen et al, *Appl. Opt.*, **27**, 365, 1988.

6. J. Jeffries, R. Copeland, G. Smith, and D. Crosley, in: *Twenty-first Symposium on Combustion*, 1709, 1986.

7. S. Sandholm, J. Bradshaw, K. Dorris, M. Rodgers, and D. Davis, *J. Geophys. Res.*, **95**, 10155, 1990.

8. F. Eisele, and D. Tanner, *J. Geophys. Res.*, **96**, 9295, 1991.

9. F. Eisele, and H. Berresheim, *Analyt. Chem.*, **64**, 283, 1992.

10. B. Williams, T. Tanada, and T. Cool,in: *Twenty-fourth Symposium on Combustion*, 1587, 1992.

11. J. Syage, J. Pollard, and R. Cohen, *Appl. Opt.*, **26**, 3516, 1987.

12. J. Fenn et al, *Science*, **246**, 64, 1989.

13. T. Kelly and D. Kenny, *Atmospheric Environment*, **25A**, 2155, 1991.

14. M. Dearth, C. Gierczak, and W. Siegl, *Environ. Sci. Technol.*, **26**, 1573, 1992.

15. J. French et al, *in: Mass Spectrometry in Environmental Sciences*, Plenum, New York, 1984.

16. D. Kenny, C. Spicer, G. Sverdrup, K. Busness, and R. Hannigan, in: *Proceedings 85th Annual Meeting and Exhibition of the Air and Waste Management Association* 21 - 26 June 1992, Kansas City MO.

17. R. Hall and A. Eckbreth, *Optical Engineering*, **20**, 494, 1981.

18. P. Esherick and A. Owyoung, *Chem. Phys. Lett.*, **103**, 235, 1983.

19. P. Schenck and J. Hastie, *Optical Engineering*, **20**, 522, 1981.

20. J. Goldsmith, *Journal de Physique*, **44 - C7,** C7-277, 1983.

21. D. Adams, in: *Air Pollution*, Academic, New York, 1976.

22. U. Platt and D. Perner, *J. Geophys. Res.*, **85**, 7453, 1980.

23. G. Mount, S. Solomon, R. Sanders, R. Jakoubek, and A. Schmeltekopf, *Science*, **242**, 555, 1988.

24. R. Stevens, R. Drago, and Y. Mamane, *Atmospheric Environment*, **27B**, 231, 1993.

25. R. Varey, in *Handbook of Air Pollution Analysis*, Chapman and Hall, London, 1986.

26. H, Wallio et al, *Appl. Opt.*, **22**, 749, 1983

27. D. Lawson, P. Groblicki, D. Stedman, G. Bishop, and P. Guenther, *J. Air Waste Manage. Assoc.*, **40**, 1096, 1990.

28. F. Fehsenfeld et al, *J. Geophys. Res.*, **95**, 3579, 1990.

29. C. Webster and R. May, *J. Geophys. Res.*, **92**, 11931, 1987.

30. R. May and C. Webster, *J. Geophys. Res.*, **94**, 16343, 1989.

31. H. Schiff, D. Karecki, and G. Harris, *J. Geophys. Res.*, **95**, 10147, 1990.

32. C. Webster and R. May, *J. Geophys. Res.*, **95**, 13851, 1990.

33. R. Eckhardt et al, in: *Laser Spectroscopy VIII*, Springer, Berlin, 1987.

34. George Mount, private communication.

35. Aerodyne Corporation, private communication.

36. R. Yokelson, to be submitted, *Journal of Physical Chemistry*.

37. R. Fox, in press, *Spectrochimica Acta Rev*.

38. D. Cooper and R. Martinelli, *Laser Focus World*, November, pp 133, 1992.

39. K. Uehara and H. Tai, *Appl. Opt.*, **31**, 809, 1992.

40. U. Simon, Z. Benko, R. Curl, and F. Tittel, *Appl. Phys. B*, in press.

41. P. Griffiths, *Transform Techniques in Chemistry*, Plenum Press, New York, 1978.

42. D. Grosjean, E. Tuazon, and E. Fujita, *Environ. Sci. Technol.*, **24**, 144, 1990.

43. L. Rothman (and 13 others), *J. Quant. Spectrosc. Radiat. Trans.*, **48**, 469, 1992.

44. W. Grant, R. Kagann, and W. McClenny, *J. Air Waste Manage. Assoc.*, **42**, 18, 1992.

45. P. Hanst and S. Hanst, *Gas Analysis Manual for Analytical Chemists*, Infrared Analysis Inc., Anaheim, 1994.

46. J. Lobert (and 6 others), *in: Global Biomass Burning*, MIT Press, Cambridge, Massachusetts, 1991.

47. M. O. Andrea (and 13 others), *J. Geophys. Res.*, **93**, 1509, 1988,

48. D. Griffith, W. Mankin, M. Coffey, D. Ward, and A. Riebau, *in: Global Biomass Burning*, MIT Press, Cambridge, Massachusetts, 1991.

49. Lisa McKenzie, University of Montana, private communication.

50. M. Hall, D. Lucas, and C. Koshland, *Environ. Sci. Technol.*, **25**, 260, 1991.

51. R. Sussot, D. Ward, R. Rabbitt, and D. Latham, *in: Global Biomass Burning*, MIT Press, Cambridge, Massachusetts, 1991.

52. Sarah Gilbert, NIST, ongoing work, private communication.

53. Patrick H. Vaccaro, Yale University, private communication.

54. A. D. Appelhans, D. A. Dahl, and J. E. Delmore, *Anal. Chem.*, **62**, 1679, 1990.

55. F. R. Lauritsen, T. K. Choudhury, L. E. Dejarme, and R. G. Cooks, *Analytical Chimica Acta*, **266**, 1, 1992.

Part 2. Specifications for the Design of a FTIR System Optimized For Combustion Emissions Measurements

Summary of Research Goals and Experimental Approach

1.1 Scope of Contract.

The contractor shall furnish all materials, labor, supervision, transportation, associated services, and incidental supplies necessary to design, construct, and supply an infrared spectrometer detection and analysis system. The system shall be capable of determining, through passive sampling techniques, the concentrations of trace gases emitted from the combustion of biomass fuels. The system shall be supplied in accordance with the attached specifications and shall incorporate the capability to provide computerized results. The system shall include, but is not restricted to, the following components: Fourier Transform Infrared Spectrometer (FTIR); open, heatable, multipass cell; baseplate; computer; detector; and infrared energy source. Additionally, the system shall incorporate the capability to establish permanent alignment; and the contractor shall include all applicable software and appropriate training for one operator.

1.2 Research goals.

Wildland fires in the United States burn about 7 million acres annually, with more than half of this area burned intentionally to meet land management objectives. There is a need to know more about the composition of the smoke that is released by these fires. The Fire Chemistry Research Work Unit has established research goals that require the simultaneous quantification of the numerous reactive, and stable, trace gases in the harsh (chemical and thermal) environment of smoke plumes measuring 1 - 2 meters in diameter above laboratory and field fires burning in biomass fuels. The measurements will be related to the environmental and fuel properties that determine the mix of combustion products so that models can be developed. A partial list of the chemicals that must be measured includes HCHO, NH_3, CH_4, CO, CO_2, NO, NO_2, N_2O, O_3, HNO_3, and CH_3OH. The required detection limits are generally single digit ppbv in tandem with time resolution on the order of several seconds. (See Table I, Part 1.3.3.j for more details.) The technique must be extremely resistant to interference from other trace gases a problem which is extreme in this application.

1.3 Introduction to experimental approach.

A technical investigation has led to the conclusion that no existing system is optimized for the above goals. We have determined that a modified version of an existing apparatus will

constitute a system which *is* capable of the above goals. Bids are being solicited for the construction of this adapted system or the design and construction of an equivalent (or better) system at comparable cost.

1.3.2 Derivation of technical approach adopted for system design.

A "special order" system has been designed to meet our measurement needs. A useful way to explain the need for this novel system is to review the limitations of existing systems.

1.3.2.a Limitations of extractive sampling.

We wish to determine the total fire emissions of trace gases and are therefore pursuing measurement techniques that operate on a larger spatial scale than extractive sampling. Extractive sampling techniques involve drawing sample through a transfer line to the instrument or a collection/storage device. The initial sample is drawn from a "point" approximately the i.d. of the transfer line and this point may or may not accurately reflect the composition of the whole smoke plume. Furthermore, production or loss of trace gases can occur in the transfer lines, instruments, and/or storage containers. Some of these problems have been suppressed, for a few reactive trace gases by use of a wide, short, sample transfer line and powerful pumps (which add to the expense and power requirements) in tandem with real-time gas monitors. This solution is not available for all the reactive gases we need to measure and the group already employs those instruments of this type that are suited to our needs.

1.3.2.b Limitations of optical remote sensing "fenceline monitoring" systems.

Optical remote sensing (ORS) technology is available that might seem to address the goals outlined above. These systems are manufactured primarily for fenceline monitoring of industrial facilities and usually consist of a fourier transform infrared spectrometer (FTIR) with a collimating/collection telescope and a retroreflector. These systems require a large separation (100 meters) between the retro and the rest of the system in order to achieve the required sensitivity. This makes the spatial scale of the sampling inappropriate for our needs. A 100 meter path would not fit in any lab (which is the only place where important data such as the fuel bed weight can be monitored during fires). Also, it would not be possible to establish a stable 100 meter optical path in the field that would be completely filled with smoke from the

rapidly rising convection plume above a moving fire. It is probable that this approach would result in sampling the fire and the background at the same time. The inhomogeneous sample would unacceptably complicate analysis.

1.3.2.c Justification for using optical techniques with a "folded", open optical path.

Optical remote sensing is the only way to completely avoid sampling artifacts with reactive gases. Only broadband optical techniques can measure many species simultaneously. Of the two broadband techniques uv broadband techniques are subject to excessive scattering of the probe light by the smoke particles. Therefore a broadband ORS technique in the IR is the only realistic option for meeting our measurement needs. Scanning monochrometer spectrometers operating in the IR have low throughput (which translates to low sensitivity) and scan speeds that are too slow to follow the fire in real time. Interferometer-based infrared spectrometers (FTIR) can scan the spectral range we are interested in within a second and with increased IR throughput, which translates to more sensitivity. Very developed instrumentation of this type, which can be adapted to our needs, is readily available.

With a folded optical path a long optical path can be fit in the total space of approximately a meter. This matches the spatial scale of our fires. Furthermore, the optical path will be characterized by higher IR throughput since beam divergence and external beamsplitters are eliminated. Finally, the spectrometer and the "folded path can be mounted on the same baseplate, in permanent, stable alignment and then deployed in a variety of locations (tower-based: field, stack-based: laboratory). This approach does not require a "heat resistant" telescope. This approach features an open optical path. The smoke passes freely between the mirrors and no pumps are required. There is no opportunity for significant surface processing of smoke constituents to occur.

1.3.2.d The need for a custom design for the open, folded optical path.

Folded optical paths, also known as multipass cells, are commercially available. Many of these cells can withstand heating to 200°C. However, with one exception, the vendors have designed these cells for extractive sampling. These cells have walls which provide a reactive surface for many trace gases and furthermore they require transfer optics (which lead to light loss and lower sensitivity) and pumps (which add expense, weight, and increased power requirements). Some of these cells can be rejected because the optical design accommodates lasers and not broadband light sources. Finally, these cells often have a pathlength which gives

insufficient sensitivity. A Long path, "open", multipass cell; which is "heatable" and permanently aligned with a FTIR spectrometer is not currently available "off the shelf". However, it has been confirmed that minor modifications to existing products will result in a design that meets our criteria for alignment stability being resistant to thermal distortion; the lack of reactive walls; and passive, representative sampling on the correct spatial scale.

Specifications for Gas Analysis System for Fire Chemistry Project.

2.1 Summary of crucial elements of proposed system.

The system proposed contains a base plate and an open multipass cell which resists thermal distortion. The system is assembled by mounting the FTIR and the multipass cell on the baseplate in permanent optical alignment with each other. The FTIR must be thermally isolated from the ambient environment. The open multipass cell "end" of the system is "inserted" in the smoke plume when taking data. The system must be able to resolve a one part in 10,000 difference in optical transmission without the need for a background spectrum. Some definitions are adopted for the purpose of this document.

2.2 Definitions.

1) *Baseplate*: The super-invar girders and the super-invar plates which are directly attached to the girders. The cell components and the FTIR are attached to the baseplate.

2) *Cell*: The mirrors, the mirror mounts, mirror adjustments, and that part of the baseplate to which the optics are attached or that lies between the optics. I.E. not the part of the baseplate to which the FTIR is attached.

3) *FTIR*: The IR source, interferometer, detector, driver board, controlling computer, etc...

2.3 Detailed system specifications.

Some aspects of the system design are open for the bidder to define. This section is intended to describe those requirements which are absolute and provide enough detail to potential bidders to propose a system which will meet our goals. In some cases, a preferred alternative is outlined and the choice made by the vendor will be weighed on its technical merit. The potential bidder is encouraged to refer to the figures as an aid to this discussion.

2.3.2.a Total size of system.

It is anticipated that the system will have an overall "T" shape. The shorter moiety of the "T will be the baseplate to which the FTIR is attached and should simply be large enough for this

purpose. The FTIR baseplate is rigidly attached to girders on which plates are mounted for attaching the multipass cell optics. The total size of the multipass cell portion of the system cannot exceed 1.25 meters in length and 0.3556 meters in width so that it will fit in the stack of our combustion laboratory. The 0.3556 meter (14") width is intended to accommodate two 0.1524 meter (6") mirrors, thus allowing 19 spots and 40 passes through the cell. The system will have a 1.25 meter optical base pathlength, so that 40 passes will give a total pathlength of 50 meters. A shorter path length will not have enough sensitivity.

2.3.2.b Overall configuration of system components.

The relative order of optical elements must be as follows. IR energy will pass from the source, through the interferometer, through the sample, and then onto the detector. This is the most efficient way to achieve source modulation and phase sensitive detection which is needed to discriminate against noise from both atmospheric turbulence and emission from hot gases.

2.3.2.c Cell: general aspects.

The cell must be a refocusing device to prevent divergence and throughput loss and it must be an imaging device so that the interferometer fringes will be faithfully projected on the detector. The input and output beams should be separated so that a beamsplitter is not required to do this. Mirror coatings must be protected silver because of the high reflectance. Aluminum is not acceptable. The optics will be purged with N_2 during use and it must be possible to easily and effectively clean the mirror surfaces, after each use, to prolong their life.

The design of the cell and the baseplate are interactive as they share some common components. Temperature could potentially effect the optical configuration through effects on the baseplate or through effects on the mirror mounts and mirror adjustments. The overall goal is stability of the optical alignment. Crucial optical dimensions and adjustments are:

1) The base path length must be 1.250 meters and not change by more than ± 0.00007 meters *due to temperature*. This is primarily achieved by specifying low thermal expansion for the girders in the system baseplate.

2) The mirror diameter must be 0.1524 meters (6"). All three mirrors must have the same nominal radius of curvature.

3) The horizontal and rotation (w.r.t. vert. axis) adjustment of mirrors A and A' must be such that the system is received so that there are 40 passes of the IR energy. This setting must be unaffected by vibration (including during shipping) and by use at up to 150°C.

4) It must be possible to purposely change the number of passes as required by the operator.

5) Mirror mount stability must be sufficient to ensure that the output beam alignment is insensitive to rapid temperature changes, high temperatures (150°C) and thermal gradients. A temperature change of 20°C to 150°C within 30 seconds would be encountered in normal use. For this reason we prefer the use of Zerodur-M, or Corning ULE, as the mirror substrate as these are the optical substrates least effected by rapid temperature changes. An alternate substrate could be used if it does not complicate operation and suitable performance can be demonstrated. In addition, during the hottest part of the fire, we don't want the output beam to "walk" off the detector.

6) The reflectivity and image quality of the optics must not be degraded by the thermal variables mentioned in item 5). The thermal distortion coefficient (defined as the thermal expansion coefficient divided by the thermal conductivity) of materials must be low enough to prevent optical distortion. The bid should include a complete listing of materials and a demonstration of performance under the expected experimental conditions can be used to justify a choice of material.

7) The differential thermal expansion of various materials must not lead to stresses that result in damaged components.

We anticipate that these items require high quality of the mirrors, mirror mounts, and mirror adjustments, and a properly constructed baseplate.

2.3.2.d Detectors: speed, amount, sensitivity, and linearity.

The detectors must have a 3 Decibel bandwidth at least 10 times faster than the fastest interferometric modulation frequency at the fastest scan speed. The combination of an MCT and InSb detector gives the best sensitivity over the operating range (600 - 3300 cm^{-1}). It is preferred that these detectors be supplied and that a convenient scheme for switching between

the detectors within seconds be supplied. This might involve mounting both detectors kinematically or a kinematically mounted mirror. Alternately a single wide band, "linearized" MCT detector is acceptable if it provides at least 70% of the D^* value achieved by the pair and if the linearity meets the specifications given in part 1.3.3.g item 2.

2.3.2.e Interferometer: attributes.

1) Resolution and accuracy: A minimum of resolution 1.0 cm^{-1} is necessary. Resolution of 0.5 cm^{-1} may be preferable with 0.1 cm^{-1} resolution being ideal. A demonstrated detection limit of 10 ppb for NO is more important than a stated nominal resolution. The absolute frequency accuracy should be no less than 0.1 cm^{-1}.

2) Alignment: A permanently aligned interferometer is desirable. A non-permanently aligned interferometer is acceptable under the following conditions.

a) The alignment procedure is only necessary at most once per day and the alignment procedure requires less than 15 minutes to achieve 95% of the maximum possible energy delivered to the detector.

b) The user-alignment of the interferometer does not have the potential to decrease the number of passes, throughput, or IR energy delivered to the detector.

3) Beamsplitter and window: The interferometer should have a corrosion resistant, ZnSe window (AR coated for high throughout (>90%)). If there is no window to protect the interferometer from the environment then the beamsplitter should be ZnSe and there must be a warranty of several years on the interferometer mirrors and drive mechanism. We prefer a self-compensating beamsplitter because of the higher throughput.

4) Fringe type compatibility: The source collimation optics, and interferometer mirror type (i.e. plane or corner cube) must be specifically chosen to be compatible with the optical design of the multipass cell so as to avoid unwanted fringes.

5) Vibration: The laboratory where the deployment is planned is subject to vibration of the intensity approximately equal to that experienced on the fifth floor of most buildings. The

system should not produce "ghost lines" caused by nonlinear mirror drive due to these vibrations.

2.3.2.f Source: attributes.

1) Intensity and stability: The intensity and stability of the IR source should be equal to or better than that of a Nernst glower constructed of compressed zirconium and yttrium oxides. The source should be capable of continuous operation for several years.

2) Collimation with respect to interferometer and cell: As stated above source collimation must be compatible with the other optical components in terms of preventing unwanted fringes. The divergence should be less than 5 mrads to optimize the throughput.

2.3.2.g Overall system attributes:

1) Sensitivity: The system should be capable of resolving a spectral feature whose depth corresponds to a change in transmission of 10^{-4} or less within several seconds of signal averaging with a S/N of 2.0 (where the noise is the 2s variation in the base line).

2) Linearity: Overall nonlinear response of absorption to concentration (deviations from Beers Law) due to underresolved lines *and* detector nonlinearity should be small (i. e. < 15%) at absorbances less than 0.7. These nonlinearities should be fairly constant throughout the spectral range of interest (600 - 3300 cm^{-1}) and easily modeled. The instrument lineshape (i.e. the output for a delta function input) should be constant and also easily modeled. The overall goal is that a computerized data analysis program should be capable of rapidly retrieving concentrations for the chemicals in the smoke with instrument artifacts contributing at most a few percent error.

3) Normal operating environment: It is possible that at times the whole system would be exposed to the smoke plume for several hours. This would constitute an environment characterized by approximately 30% water, 15% carbon dioxide, gas phase acids and bases, and temperatures up to 150°C. It is anticipated that a ZnSe window will be necessary to protect the interferometer and that the thermal isolation of the FTIR be capable of maintaining a 120°C temperature differential for up to two hours.

4) Weight Limit: Ideally one person should be able to manipulate the instrument which implies a weight limit of approximately 70 pounds. A system weighing as much as 200 pounds could be considered only if there were significant (as judged by the panel) performance advantages gained.

5) Power requirements: The best solution is for the system to be capable of operation using a common 12V source (automobile battery) or something equally portable. A system requiring a generator for field operation will be considered if there are significant performance advantages.

2.3.2.h Baseplate: attributes.

1) *Notes on materials and machining*: The baseplate girders and the three mounting plates consist of super-invar to provide the necessary thermal stability. The super-invar must be annealed after machining according to the manufacturers specifications to preserve its thermal properties. (As stated above, the optical mounts must also allow for thermal effects and protect both the components and the alignment.) Fasteners for the super-invar parts need not be super-invar provided allowance is made that the thermal expansion will not degrade the rigidity of the baseplate and optical mounts.

2) *Notes on thermal isolation of the FTIR*: The FTIR must be mounted to the baseplate in such a way that 1" of ceramic thermally isolates the instrument from the high temperatures of the baseplate. The FTIR must be stably mounted, but not by bolts that directly connect it to the baseplate and allow thermal conduction. The system must be designed so that the FTIR is unaffected by high temperature operation. The electronic components of the FTIR must be capable of operation when exposed to temperatures up to 45°C for two hours.

3) *Reactivity*: The system must be designed so that the smoke passes "freely" (without the need for a pumping system) through the optical path and without the chance for significant surface processing of the chemicals in the smoke to occur. Specifically, rigidity should not be achieved through the addition of structural elements that "see" the smoke before the probe energy does. If necessary, any baseplate component which is subject to chemical attack will be appropriately coated so that a long system lifetime can be expected despite deployment in a corrosive environment.

4) *Size*: The spatial scale of sampling must be such that the system will return the average concentration of a chemical over an area of space approximately 1.25 meters long and .3 meters wide. Specifically, we are not interested in a system where the optical base pathlength is significantly shorter than 1.25 meters, even if the overall pathlength is still 50 meters.

2.3.2.i Computerized data acquisition and analysis.

The system must be delivered ready to operate with computerized data acquisition and analysis and storage. This must include the Grams 386 and Lab Calc software, with the CLS add-on, or their equivalent. The software should be capable of fast fourier transforms; real time data display; multicomponent, multivariate least squares statistical analysis; center of gravity peak location, and any other features found in the above named software packages. The data acquisition board must be compatible with the ISA, or other standard, slot of a 60 MHz, 64 bit internal bus, "pentium" style computer. Unless the system is controlled by a "notebook" style computer it must be operable with an interface cable 50 meters in length.

2.3.2.j Measurement capabilities.

The sensitivity listed below is required and must be demonstrably achieved using a five second measuring time, for simultaneous measurements of the listed compounds in smoke samples. Sensitivity must be achieved at temperatures up to 150°C and not require an experimental "background" spectrum. In other words these are the detection limits for concentrations retrieved directly from transmission data and not from ratioed spectra.

Table of Detection Limits

Compound	Detection Limit
O_3	3.0 ppb
CO	3.0 ppb
CH_4	3.0 ppb

Table of Detection Limits (cont.)

Compound	Detection Limit
HCHO	3.0 ppb
CH_2O_2	4.0 ppb
CH_3OH	2.0 ppb
CH_3Cl	7.0 ppb
NO	10.0 ppb
N_2O	7.0 ppb
NO_2	1.0 ppb
NH_3	1.0 ppb
HNO_3	2.0 ppb

2.3.3. Service, warranty and delivery schedule specifications.

2.3.3.a Delivery schedule.

The successful vendor must be able to deliver a system warranted to give unconditional satisfaction within six months of the receipt of the order. The delivery schedule will have the following phases:

1) Award

2) Detailed design by contractor and preproduction review by customer (with up to 2 weeks allowed for review).

3) Final design approval.

4) Complete production.

5) Demonstration of performance for all specifications (site open).

6) Training (site open).

7) Delivery.

8) Inspection.

9) Installation in combustion lab. (Note: items 7, 8, and 9 may proceed item 5).

10) Demonstration of performance to specifications on site.

11) Payment.

2.3.3.b Service: attributes.

1) System downtime should be less than 6 days per quarter.

2) A complete list of recommended maintenance procedures, spare parts and prices should accompany the bid.

3) A service manual with schematics must accompany the system.

4) Extensive telephone service support, including troubleshooting and repair guidance, must be available during "normal working hours".

5) In the event that a service call is necessary, response time should be within 48 hours.

6) The bid should include complete details on the cost of service calls, including details on travel expenses, lodging, hourly rates etc.

2.3.3.c Warranty: minimum 1 year parts and labor.

Terms: Unconditional satisfaction guaranteed.

Schematics of Gas Analysis System for Fire Chemistry Project.

3.1 Schematic of the Optical Configuration of the FTIR and the Cell.

(not to scale)

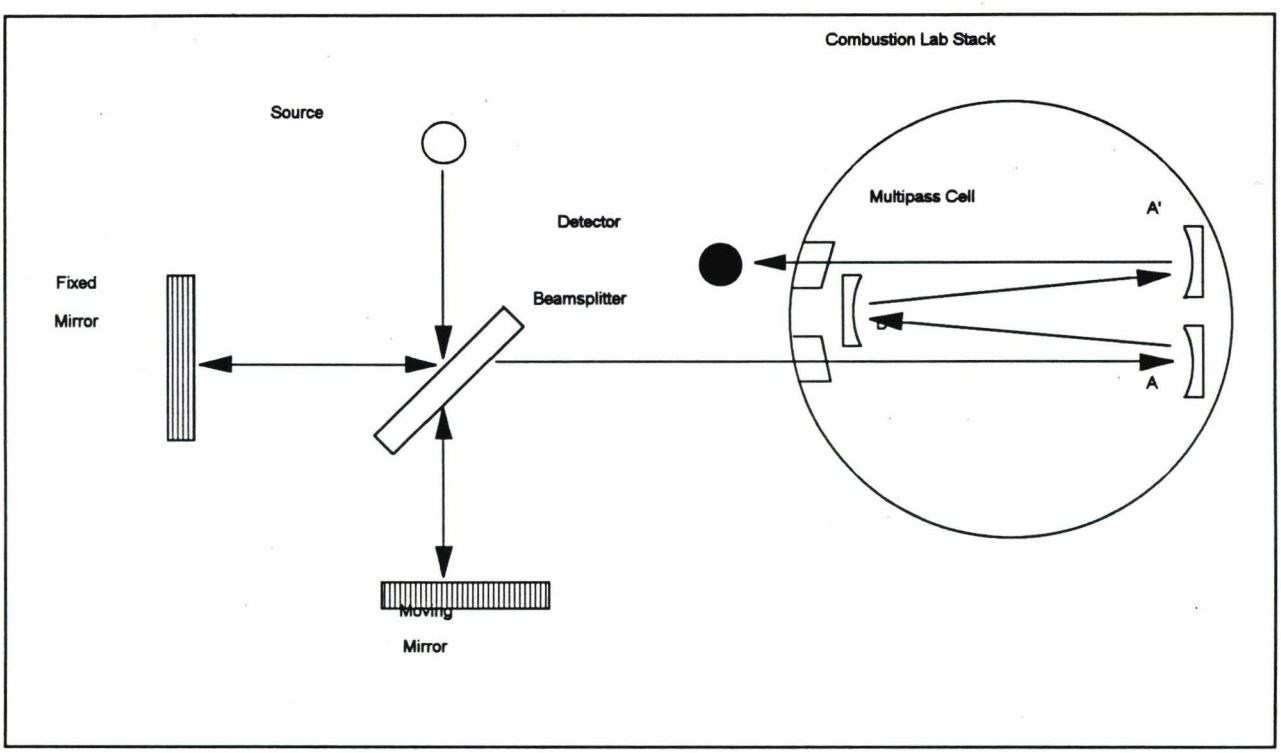

3.2 Diagram of the Baseplate.

(not to scale)

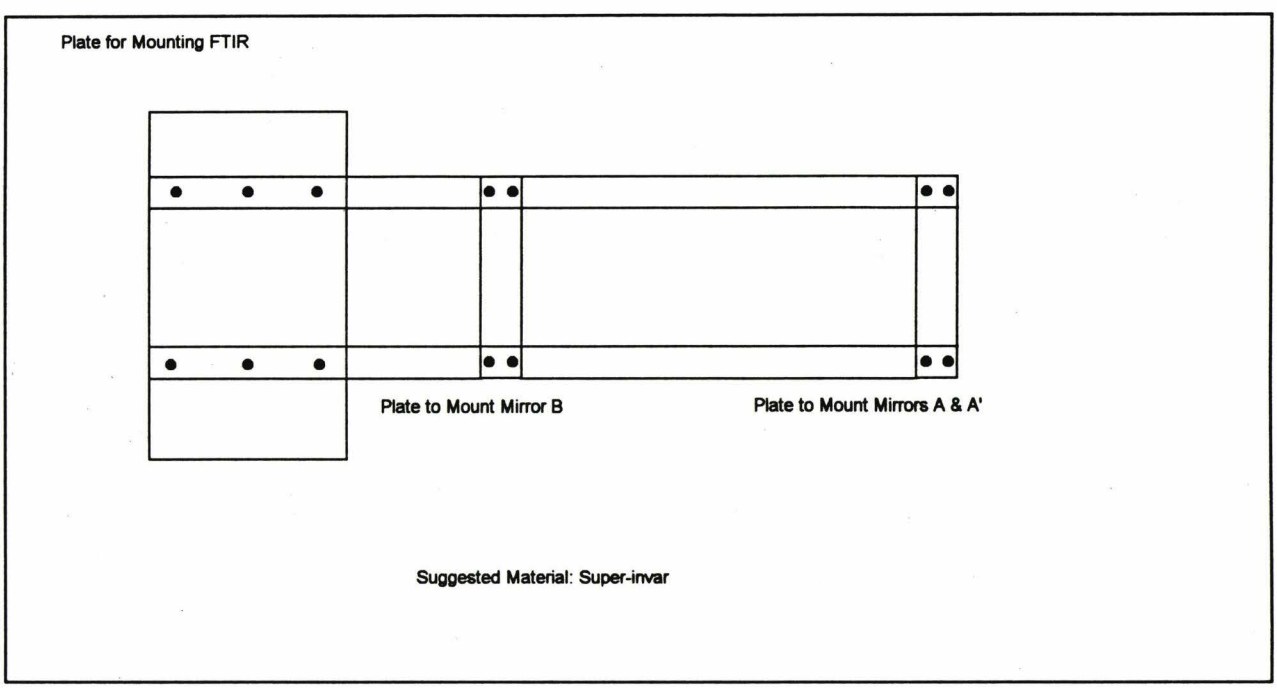

3.3 Diagram of a Deployment Option.

(not to scale)

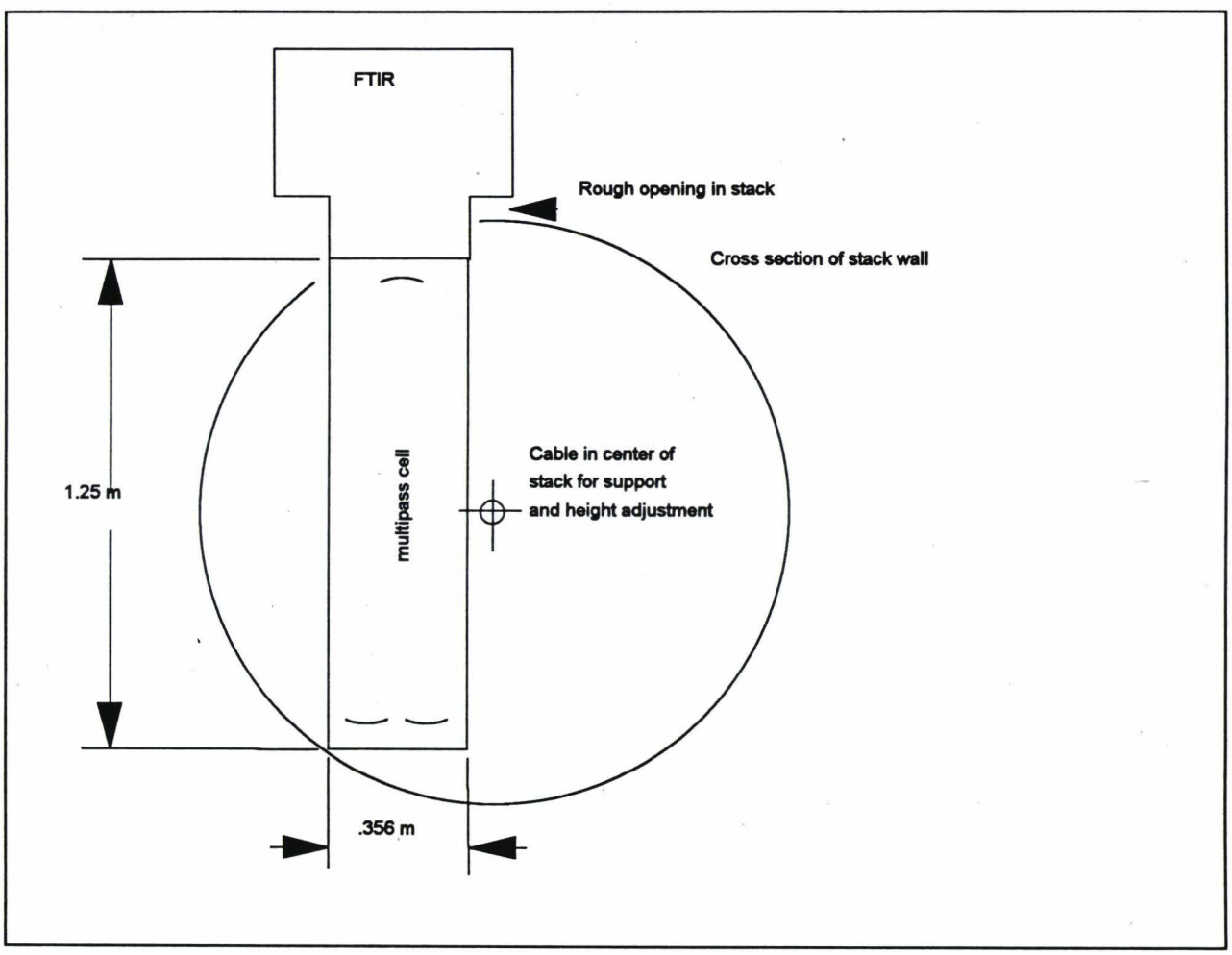

Selection Criteria for the Gas Analysis System for the Fire Chemistry Project.

A technical panel will review all bids and consider the following factors in making a selection.

1) Performance. The system must be judged as capable of performance in accordance with the specifications outlined in Part 1.

2) Contractors plan for demonstration of performance for this system. The panel will take into account the bidders proposal for demonstration that the system will perform according to specs

3) Contractors past performance and related experience. The panel will judge past performance in successful implementation of related technology and likelihood of success in this project.

4) Delivery Schedule. The delivery schedule outlined in the specifications must be completed with the phases indicated.

5) Reliability. Warranty, service response time, quality of service contract if available, and other items in part 2.3.3.b.

6) Simplicity of operation (the least adjustment and maintenance).

7) Cost.

Relevant Information for Staff in Ogden: Not to be included in Bid.

Bid Evaluation Panel Membership

We request that Dr. Darold Ward be included in the evaluation panel.

Government estimate of cost

No more than $75,000 for the complete system including the FTIR, cell, baseplate, computer, detector, source, permanent alignment, installation, training, and software.

Itemized breakdown follows.

Item	Cost Estimate
Interferometer:(mounted and enclosed and with	
anti-reflection coated ZnSe windows)	25000
Source	2000
Detectors	15000
Computer	3000
Software:	
data acquisition drivers	2000
data analysis	5000
Multipass Cell and Baseplate:	
materials	7000

design	7000
construction	7000
training	1000
Total	**74000**

(note that costs associated with installation and operation are not included here)

Notes on some vendors contacted regarding project.

These vendors have demonstrated expertise in cell design, construction, and system integration.

1) Advanced Fuels Research

PO Box 380379

East Hartford, CT 06138-0379

They are developing an extractive sampling/closed cell design system since they are not interested in reactive gases. Their system also has a maximum pathlength of 25 meters. They have not expressed an interest in modifying their design.

2) Aerodyne Research, Inc.

45 Manning Road

Billerica, MA 01821-3976

They market a multipass cell known as a Herriott Cell. It has Al mirrors with low reflectivity and the cell requires an external beamsplitter which causes the sensitivity to drop by a factor of 7 compared to the same pathlength Whites Cell. In addition, it is not yet clear that the cell optical design will work with the diffuse IR sources used in FTIR spectrometers.

3) Axiom Analytical, Inc.

18103-C Sky Park South

Irvine, CA 92714

They market a FTIR system which involves extractive sampling into a cell with reactive metal walls. They have not indicated an interest in modifying there product.

4) Bomem: (See list of prospective bidders for address.)

This company has a long reputation of manufacturing top quality and very rugged (but also very heavy) FTIR instrumentation. They manufacture a system which is similar to our design, but features a 7M pathlength which is too short for the sensitivity we need. They are interested in modifying their product. They would buy a longer path cell from IR analysis and interface it to a lower weight version of their FTIR.

5) Infrared Analysis: (See list of prospective bidders for address.)

This company is widely acknowledged as the experienced industry leader in the design of high temperature or open path multipass cells and in interfacing multipass cells with FTIR. (Multipass cells require a specific source-collimation/interferometer configuration in order to avoid fringes.) This company has expressed a great deal of interest in working with us to adapt their product to our needs.

6) Midac: (See list of prospective bidders for address.)

This company makes the lightest weight interferometer and their product has proven performance in the field on Army Blackhawk Helicopters.

List of Interested Prospective Bidders

The following prospective bidders have asked that we send them a copy of the advertisement. They want to submit a bid, but do not normally read the CBD. I indicated to these people that I would fax them a copy of the advertisement when it appeared, but I will be out of the country and I understand that the Ogden office can forward the advertisement to interested parties.

1) Contact Person: Steven Hanst

Telephone: 8-714-236-8900 Fax: 8-714-236-8909

Address: Infrared Analysis Inc., 1334 North Knollwood Circle, Anaheim, CA 92801

2) Contact Person: Raymond Roberge

Telephone: 9-1-418-877-2944 Fax: 9-1-418-877-2834

Address: Bomem Inc., 450 St. Jean-Baptiste, Quebec, Quebec J2E5S5

3) Contact Person: Jerry Auth

Telephone: 8-714-660-8558 Fax: 8-714-660-9334

Address: Midac Inc., 17911 Fitch Avenue, Irvine, CA 92714

Acknowledgements.

The design of this custom system was greatly facilitated by extensive consultation with experts in various fields. Among the helpful corporations or individuals are the following:

Advanced Fuels Research; Aerodyne; Axiom; Bomem; Burkholder, Dr. James; Burliegh; Cincinnati; Coherent; Corning; Data Translation; Galactic; Galilleo; Graseby; Green Bay Supply; Griffith, Dr. David; Griffiths, Dr. Peter; Hall, Dr. Donald; Ideal Lab; Infrared Analysis; Jones, Dr. Nicholas; Killinger, Dr. Dennis; Koshland, Dr. Kathy; Maxwell, Dr. Jonathan; McLaren, Dr. Scott; MDA; Melles Griot; Midac; Murcray, Dr. Frank; Newport; Nicolet; Ontar; PCI; Precision Lapping; Radiant; Schott; Scientific Alloys; Stedman, Dr. Donald; and Vukobratovich, Dr. Daniel.

Part 3. Results From Use of a FTIR System With a Design Similar to the Proposed System

Open-path FTIR Studies of Large-Scale Laboratory Biomass Fires

David W. T. Griffith[a], Robert J. Yokelson[b], and Darold E. Ward[c]

a) Department of Chemistry, University of Wollongong, Wollongong NSW 2522, Australia

b) Department of Chemistry, University of Montana, Missoula, MT 59812

c) USDA Forest Service, Intermountain Research Station, PO Box 8089, Missoula, MT 59807

Abstract

A series of 9 large-scale, open fires was burned in the Intermountain Fire Sciences Laboratory (IFSL) controlled environment combustion facility. The fuels were pure pine needles or sagebrush, and a series of fire type simulations of forest-floor, ground fire; crown fire; broadcast burn; and slash pile burn. Open path FTIR measurements of the mid-infrared spectrum of the smoke were acquired at 0.12 cm^{-1} resolution over a 3 meter cross-stack pathlength and analyzed to yield simultaneous concentrations of up to 16 compounds. Simultaneous measurements were made of fuel mass loss, stack gas temperature, total mass flow, and replicate CO_2 and CO by NDIR, and NO and NO_x by chemiluminescence.

The products detected are classified by the type of process that dominates in producing them. Carbon dioxide is the dominant emission of (and primarily produced by) flaming combustion from which we also measure nitric oxide, nitrogen dioxide, sulfur dioxide, and most of the water vapor from combustion and fuel moisture. Carbon monoxide is the dominant emission formed primarily by smoldering combustion from which we also measure carbon dioxide, methane, ammonia, and ethane. A significant fraction of the total emissions is evidently formed primarily as unreacted pyrolysis or distillation products; such as methanol, formaldehyde, acetic and formic acid, ethene, acetylene, hydrogen cyanide, terpenes and other higher hydrocarbons. Few previous data exist for these compounds and they are likely to have an important, but as yet poorly understood, role in plume chemistry. Large differences in emissions occur from different fire and fuel types, and the observed temporal behavior of the emissions is found to depend strongly on the fuel bed and product type.

The FTIR technique is proving to be a valuable diagnostic tool for continuous, real-time analyses of many gases in smoke, and is providing an improved understanding of smoke composition and chemistry, fire behavior, carbon and nitrogen cycles, and biomass burning impacts on atmospheric chemistry.

Introduction

Biomass burning has important effects on the atmosphere, soil, biosphere, and the hydrosphere. The prompt effects of biomass burning include injection of significant amounts of trace gases and particles to the atmosphere on a global scale and significant air pollution on a regional scale. This paper applies a new technique, open-path Fourier transform infrared (FTIR) spectroscopy, for simultaneous analysis of many gaseous components in smoke and adds substantially to our understanding of the combustion chemistry of biomass.

Quantification of representative emissions from fires is difficult, and many different configurations of analysis techniques and sampling platforms have been utilized. Aircraft can probe a large area of well-mixed, integrated emissions, investigate secondary chemistry, and provide details on transport [*Andreae et al.*, 1988]. However airborne sampling is expensive, it is difficult to monitor a single fire continuously from beginning to end, and specific knowledge of the fuels and fire types are difficult to correlate with measurements. Ground based measurements provide the opportunity for more detail on the fire and fuels [*Delmas et al.*, 1991 and *Ward et al.*, 1992], but may tend to underestimate the emissions in the convection column above the fire [*Andreae et al.*, 1988]. Tower-based measurements have been implemented as a means of more representative ground-based sampling [*Ward et al.*, this issue]. Altogether a large body of field work on biomass fires has produced many details on the primary emissions, secondary chemistry, transport, and cloud processing of smoke [*Radke et al.*, 1990 and *Andreae et al.*, 1988]. Correlations have been developed between the constituents of smoke, in particular those identified with flaming and smoldering combustion [*Lobert et al.*, 1991].

The companion work to the study described here was the first application of open-path FTIR spectroscopy to the analysis of smoke from biomass burning, and focused on prescribed fires in sagebrush and forestry operations in the western United States [*Griffith et al.*, 1991]. This study extends that work to large-scale, open biomass fires in a controlled environment laboratory (IFSL). There are a number of advantages in studying biomass fires in the laboratory. Laboratory studies allow burning under controlled conditions where the chemical and physical properties of the fuel and environment are known in detail. Since all the smoke can be captured for the entire course of the fire, emission factors for any measurable airborne species can be determined accurately. These

advantages facilitate our understanding of the fundamentals of combustion chemistry and fire behavior for biomass fuels, which leads to improved regional and global emissions estimates and may ultimately contribute to the design of effective mitigation strategies. The laboratory characterization of the products of biomass burning began with work to assess the contribution of forest fires in the southeastern US to regional air pollution [*Ryan and McMahon,* 1976] and the emissions due to burning agricultural waste [*Darley et al.,* 1966] or wood for heat [*Dasch,* 1982]. This early work often distinguished between flaming and smoldering combustion, distillation and pyrolysis, and normally featured detection of CO_2, CO, and NO_x. Formic acid and acetic acid were later added to the range of products detected in laboratory fires [*Talbot et al.,* 1988]. The laboratory experimental fires of *Lobert et al.* [1991] were the first to characterize a wide variety of emission products of particular importance to atmospheric chemistry.

In addition to the challenges presented by the need to sample fires representatively, there is the additional challenge of identifying instrumental techniques that can cope with hot, reactive samples where the potential for chemical interference and the dynamic range of concentrations is very high. *Griffith et al.* [1991] demonstrated the advantages of an FTIR-based study of biomass fires:

- Simultaneous measurements can be made of a wide variety of species with good selectivity over a wide range of concentrations.

- Measurements can be made in real time so that dynamic processes can be followed.

- Measurements can be pseudo-continuous for any desired amount of time so that there is no need to determine the appropriate time to take a representative sample, if indeed there is such a time.

- There is no need to take samples and no possibility of sampling- or storage-related artifacts so that reactive gases can be quantified.

- The measurement is path integrated, averaging over small-scale, local variations. It is thus relatively immune to spatial variation compared with point sampling.

The study reported here represents the first application of FTIR spectroscopic analysis to large-scale open biomass fires in the laboratory. It features extensive time-resolved product characterization of up to 16 species from 9 biomass fires. The potential of the laboratory technique is demonstrated and significant insights into biomass fires are also achieved.

Methods

Fire & fuel types.

The data were collected in late October of 1989 in the Intermountain Fire Sciences Laboratory large-scale, controlled environment, open combustion facility (IFSL). Table 1 summarizes the fuels burnt in each fire. The fuels were selected for the fires with several objectives in mind. There were two fires each of brown ponderosa pine needles (fires 3 & 5) and freshly cut sagebrush (fires 8 & 12), which offered the opportunity to measure separately the products of important components of fuel in western US land management fires, to investigate the reproducibility or natural variation in nominally identical fires, and, especially from the pine needles, to investigate the temporal behavior of fire emissions in a relatively simple fuel bed.

Many important biomass fires burn in an inhomogeneous mixture of several fuels [*Kauffman et al.*, 1994 and *Seavoy*, 1973]. We therefore included simulations of widely occurring natural and anthropogenic fire types. Two of the fuel beds (fires 9 & 10) contained litter and "duff" (partially decomposed organic matter) and represent initial attempts to simulate a typical forest floor ground fire in a coniferous forest. A further common type of wildfire is the crown fire which, along with the ground fuels, consumes the foliage of live, mature trees. This was simulated by fire 11, which contained a top layer of green pine needles and twigs over litter, dry needles and small woody fuel. Finally, the two main fire types used to dispose of "activity fuels" (logging waste or harvesting residues also termed "slash") were also simulated. Unpiled, scattered fuels were burned in fire 6, a broadcast burn simulation, and fire 7 simulated burning piled, woody logging waste.

C:H:N elemental analysis of the fuel was carried out only for the relatively homogeneous brown pine needles, with total carbon 50.7% and nitrogen 0.31% in dry matter (See Table 1). For the other fires the C:H:N could only be estimated based on the results of a limited set of subsamples. These subsamples ranged from 43 to 47 percent carbon and an average value of 45% is adopted for all fuels other than pine needles. [*Dave, Darold says these numbers need to be updated or justified on the basis of their literature dominance.*]

Experimental.

The experimental configuration and FTIR spectrometer have been described previously [*Griffith et al.*, 1991]. The experimental configuration is shown in Figure 1. The fuel is burned on a ca. 1 x 2 m continuously weighed fuel bed, and the smoke captured by a 1.5 meter diameter stack with a 3.6 meter inverted funnel opening just above the fuel bed. A sampling platform surrounds the stack 15 meters above the fuel bed. The IR source was collimated and transmitted twice across the stack through the smoke for a total smoke absorption path of 3 m, then focused and re-collimated into an EOCOM interferometer and InSb/MCT sandwich detector. Spectra were continuously recorded by, alternately, the InSb (1800-3900 cm^{-1}) and MCT (700-1900 cm^{-1}) detectors. Resolution was 0.12cm^{-1}, which is approximately the pressure-broadened full width at half height of individual spectral lines. The spectra recorded before the fire were used to determine background levels of H_2O, CO_2, CO and CH_4, and to serve as reference spectra to create absorbance spectra from spectra collected during the fire where required. Normally 5-20 scans were coadded over 0.5 to 2 minutes for each spectrum, with higher time resolution used near the beginning of the fire. Fires typically burnt for about 1 hour, resulting in 25-40 individual spectra per fire.

Auxiliary data included measurement of flow by a mass flow meter (Kurz, Model 455), temperature by thermocouple gauge, CO and CO_2 by NDIR (Horiba PIR-2000), and NO and NO_x by chemiluminesence (Thermoelectron Model 42). These measurements were logged every 5 s. Samples for simultaneous gas measurements were drawn from the center of the stack near the FTIR beam through ca. 30m of .25" teflon tube. The fuel bed mass was recorded every 30 s. Particulates were sampled with teflon or glass fiber filters (with a cyclone in the filter prehousing to exclude particles with an effective diameter greater than 2.5 micrometers) to give a fire-averaged particulate concentration. The stack gas flow was driven by convection without additional fan-forcing. Normal atmospheric

pressure at the IFSL is 909hPa . Temperatures in the stack gas absorption path 15 m above the fuel bed ranged from 300 to 420 K.

Spectrum analysis.

Three different procedures were followed to compute trace gas concentrations from spectra. For most gases, classic least-squares (CLS) fitting of calculated calibration spectra to the measured spectra in selected spectral regions was the method of choice. For species where this was not applicable, either interactive spectral subtraction or peak-height-based analyses using reference spectra were used.

MALT/CLS based retrievals.

The MALT/CLS method is described in detail elsewhere [*Griffith*, 1995]. Briefly, a set of calibration spectra is calculated using the computer program MALT, such that the calculated spectra closely match real experimental spectra over a range of gas concentrations. These spectra are then used as a calibration set for conventional CLS quantitative analysis [*Haaland*, 1990]. For each trace gas species a small spectral region is optimally selected for the gas or gases of interest. The regions used for each gas are listed in Table 2. For each region, a set of calibration spectra was calculated at 10 K intervals from 290 to 420 K and the analyses of measured spectra were carried out at the temperature nearest the measured temperature at the time the spectrum was recorded. Figure 2 shows examples of the MALT/CLS fits to the experimental data.

Spectral subtraction and peak-height based retrievals.

For species for which line parameters are not available, MALT/CLS cannot be used and more traditional methods are required. This was the case for CH_3OH, C_2H_4, CH_3COOH and terpenes. For CH_3OH, a prominent Q-branch feature appears near 1033 cm^{-1}, along with single lines of NH_3. A calibrated laboratory spectrum of 36.1 ppmv CH_3OH in 1 atm N_2 was recorded in a 5.6 m White's cell on a Bomem DA3 FTIR spectrometer at 0.12cm^{-1} resolution and used as a reference for interactive spectral subtraction. The spectrum was assumed to be temperature independent. Each measured spectrum was ratioed to a background spectrum collected before the fire to form an absorbance spectrum. A MALT-calculated NH_3 spectrum at the correct temperature was then subtracted from the measured spectrum, followed by interactive subtraction of the

reference CH_3OH spectrum. The scaling factor of the CH_3OH spectrum required to strip the CH_3OH feature from the measured spectrum provided the equivalent CH_3OH concentration.

For C_2H_4, CH_3COOH, and terpenes the concentrations were based on hard copies of published reference spectra at appropriate resolution [*Hanst and Hanst*, 1994]. Peak absorption coefficients were determined from the published spectra and applied to peak heights in the measured spectra to retrieve concentrations according to the Beer-Lambert Law. For CH_3COOH and the higher hydrocarbons the spectral features are very broad but their characteristic shapes and positions provide unambiguous identification.

Auxiliary data.

The CO_2, CO, NO and NO_x analyzers were calibrated by standard methods using NIST traceable standards. The flow meter and thermocouple gauge relied on manufacturer's calibrations. The collection time and volume flow rates were noted for the particulate filters which were subsequently re-weighed.

A cubic spline interpolation was used to reduce all data to a common one-minute time base.

Accuracy & precision of results.

For gas concentrations from FTIR spectra, signal:noise ratio (S:N) in the spectra determines detection limits and a lower limit to precision. This is around 1 ppmv for most species analyzed by MALT/CLS, and for spectral subtraction or peak-height analyses. In good quality laboratory spectra (S:N > 1000), precision is normally better than 1% and absolute accuracy better than 2% [*Griffith*, 1995] whereas for the spectra here the S:N is typically around 100. Based on replicate measurements, actual relative precision for most species is estimated at 5% (1σ). In addition, the MALT/CLS analysis has a sensitivity of ca. 1% K^{-1} to assumed temperature. Thus rounding of the analysis temperature to the nearest 10 K (and variation in temperature across the stack of the same order) introduces an additional maximum error of ca. 5%, which may be greater when temperature is changing rapidly at the start of a fire. In summary, we conservatively estimate total error in single gas concentration measurements of ca. 7% (1σ) or 1 ppmv, whichever is higher.

For the specific case of H_2O, a significant part of the total absorption is due to H_2O at room temperature in the optical path outside the stack. To avoid large errors due to temperature-dependence, the water analysis used lines in the spectral window near 3010 cm^{-1} which were found to be only weakly temperature-dependent.

For some species, independent measures of precision are possible. Comparisons of FTIR and NDIR measurements of CO_2 show good relative agreement but with FTIR measurements ca. 7% higher than NDIR. Similar comparison of NO by FTIR and chemiluminescence show agreement within 10%. Analyses of several species from two or more independent spectral regions (e.g. CO_2, CH_4, NH_3, C_2H_2) agree to within 5% at concentrations well above the detection limit.

Measurement of total mass flow in the stack by the hot-wire flowmeter is subject to uncertain calibration and considerable error. The flowmeter functioned only for fires 3-8, for which its output showed fluctuations (± 20-30%), possibly due to turbulence and temperature changes in the stack. The flow measurements must therefore be used with caution, as discussed in more detail below. The errors in mass and temperature measurement are assumed to be negligible relative to those in concentrations and flow.

Derived quantities.

The raw data from each fire consist of time series of concentrations, fuel mass, temperature and stack gas flow. A number of derived quantities are of use in discussing these results:

Emission ratio is the ratio of (molar) concentrations of two species, normally as the excess concentrations above background.

Emission factor is the ratio of the amount of a species emitted to the amount of fuel burned in g/kg or mol/kg. (*Molar emission factor* is the ratio of the amount of a particular element in a species emitted to the amount of that element in the fuel burnt, in units of mol/mol). Emission factors are integrated over time and may be defined for the whole fire or for separate fire processes such as flaming and smoldering. Calculation of emission factors from the experimental data is described below.

Combustion efficiency (CE) is the molar ratio of CO_2 emitted to the carbon burnt, and should be 1.0 for complete combustion. For practical purposes we use *modified combustion efficiency (MCE)* as the ratio of measured emitted CO_2 to the sum of emitted CO_2 + CO:

$$MCE = [CO_2] / [CO_2 + CO]$$

on the grounds that $[CO_2 + CO]$ correlates well with the total carbon burnt [*Ward and Radke*, 1993]. MCE can be calculated on an instantaneous or time-integrated basis. From the definition, the emission factor of CO_2 is approximately equal to MCE, and the emission factor for CO is approximately (1-MCE). The commonly-quoted CO/CO_2 emission ratio is then approximately equal to (1-MCE)/MCE.

Combustion factor is the fraction of the total fuel load exposed to the fire which is actually burnt.

Calculation of emission factors.

The molar emission factor for species X relative to carbon is determined as the molar flow of X up the stack, Flow(X), divided by the molar flow of C in all carbon-containing species up the stack, Flow(C):

$$\text{Molar EF(X)} = \text{Flow(X)} / \text{Flow(C)}$$

The molar emission factor relative to fuel mass (grams dry matter), EF(X), requires the fuel carbon mass fraction, C(fuel):

$$EF(X) = \text{Molar EF(X)} \times C(\text{fuel}) / 12$$

Flow(X) is the product of the total molar flow (determined by the flow meter) times the mixing ratio of X (determined by FTIR). For Flow(C), we take the sum of flows of all measured C-containing species as a close approximation to total C. The molar emission factor for species X times the molecular weight of species X gives the emission factor on a mass ratio basis.

This method provides the most reliable result because any absolute error in the flowmeter calibration cancels and it is only important that the shape of the flow vs time profile be correct. In principle the total carbon stack flow can also be determined from the measured total fuel mass loss if the fuel composition is known. For fires 9-12 the flowmeter malfunctioned and the data were discarded, and for fires 3-7 no fuel mass data were collected during the fire. For fire 8 the mass loss and stack flow were available and thus allow a consistency check. Figure 2 shows plots of the integrated carbon loss, as calculated from both Flow(C) and the mass loss, against time for fire 8 (assuming fuel composition of 45%C and 6%H). The FTIR H_2O measurements then constrain the fuel moisture (which was unmeasured) to be 50% of dry matter, which is reasonable for the recently cut sagebrush fuel. The integrated carbon loss for the whole fire were forced to agreement by scaling the flowmeter calibration by 0.76. For fires 9-12 the flows implied by the measured fuel mass loss were therefore calculated assuming 45%C and 6%H and used in place of actual flow measurements in all subsequent emission factor calculations. It was confirmed that the flow profile calculated for these "fire-driven burns, from the mass loss, tightly correlates with excess CO_2, H_2O, and temperature.

Results and Discussion

Time series of concentrations of fourteen species could be determined simultaneously for most of each fire. These species were carbon dioxide, carbon monoxide, methane, ethane, ethene, ethyne, formaldehyde, methanol, acetic acid, volatile higher hydrocarbons (terpenes), water, nitric oxide, nitrogen dioxide, ammonia and sulfur dioxide. Three others, formic acid, hydrogen cyanide and carbonyl sulfide, were measurable only during periods of peak emissions for some fires. Emission factors and modified combustion efficiency for each fire are summarized in Table 3, which also includes these quantities further divided by fire process as described in the ensuing discussion.

The following discussion is divided into five sections:

1) We explain observations of the time-resolved emissions of various species from different fires in a consistent interpretive model involving flaming, smoldering and pyrolysis/distillation products. We present and interpret results for a fire in the simplest type of fuel bed, then describe and interpret complications in the temporal profiles caused by more complex fuel beds.

2) We address the production of oxygenated organic compounds and some reactive nitrogen-containing compounds which are measured in this work but have been difficult to measure in the past by other techniques. Some of these compounds may be produced more abundantly than previously assumed and some implications of this to sampling programs and plume chemistry are discussed.

3) We present observations on the effects of fire type and fuel parameters on fire emissions and behavior.

4) We examine the degree to which these laboratory results should reflect the situation in field fires.

5) We briefly present observations on sulfur compounds.

Temporal Behavior of Fire Emissions.

Earlier laboratory studies of *Lobert et al.* [1991] were carried out in homogeneous, well-characterized fuels. That work demonstrated that some compounds can be attributed to flaming or smoldering combustion based on a linear correlation with CO_2 or CO, similarity of the normalized temporal profile with CO_2 or CO, and degree of oxidation.

Our results confirm some of these observations. The normalized temporal profiles for selected flaming and smoldering compounds can be seen in Figures 4- 6 (a) and (b) for fires burning in dry brown pine needles, sage brush, and a homogeneous mixture of forest residues.

We also measure significant amounts of compounds that do not correlate linearly with either CO_2 or CO and show markedly different normalized temporal profiles. The temporal profiles for some of these compounds can be seen in Figures 4 - 6. These compounds are principally unburned pyrolysis and distillation products originating from heating of the primary fuel [*DeGroot et al.*, 1988, *Evans et al.*, 1986, *Shafizadeh et al.*, 1976, and *Overend et al.*, 1985]. Compounds of this type that we measure are acetic and formic acid, methanol, formaldehyde, light unsaturated hydrocarbons, and terpenes. In studies limited to the emissions from smoldering combustion, the entrainment of unburned pyrosynthesized compounds in the smoke naturally falls within the definition of smoldering

combustion [*McKenzie et al.*, 1995]. However, in this work, these compounds also occur in the emissions during times dominated by flaming combustion. (See Figures 4 - 6.) For this reason, and because production of these compounds exhibits poor temporal correlation with both CO and CO_2 and further because they may primarily be formed by thermal "cracking" of biomass and without the reaction of an atmospheric oxidant with the fuel, we adopt an operational definition of smoldering combustion that excludes these compounds and we invoke one further category of compounds: the "distillation and pyrolysis" category. We recognize that the construct of a category or class of compounds is a simplification and that there may be some overlap. For example, most of the CO_2 is produced by flaming combustion, but CO_2 is also the major product of smoldering combustion. The smoldering compounds correlate well with CO which can be produced by direct pyrolysis of biomass, by gassification of char, or by incomplete oxidation of other emissions in flames. Formation of methane is a high temperature pyrolysis process, and formaldehyde can be formed pyrolytically or from the partial oxidation of methanol or methane.

The pyrolysis compounds do not always track with each other or with any single tracer species because they often originate from different precursors or in different thermal or moisture regimes and because heat production and combustion efficiency vary throughout a fire. On the other hand, correlations among pyrolysis compounds may identify common precursors or thermal regimes. An example is shown in Figure 7 where two pyrolysis compounds, methanol and acetic acid, are highly correlated in nearly a 1:1 ratio for three different fires, but with the peak in emissions occurring at markedly different times in the three fires. The 1:1 production is also in contrast to the 1:2 production observed for brown pine needles (Figure 4c). Consideration of the temporal profiles and production ratios suggests that methanol and acetic acid may be produced from biomass in similar thermal regimes (relatively low temperature), but from different precursors.

Interpretative model.

From the perspective of being able to monitor total fire emissions for many species continuously, we find that the concept of fire *stages* or *phases* separated in time is less useful than the more general concept of fire *processes*, which may coexist in time. These processes are summarized in the following paragraphs. Figure 8 presents a plot of modified combustion efficiency vs time for two fires which is useful in interpreting the different processes.

For a homogeneous or well-mixed fuel bed a typical fire behaves as follows:

1. Upon ignition, a flame front with an associated pyrolysis/distillation zone begins to move through the fuel bed and the emissions are dominated by the products of flaming combustion with a comparably minor contribution from unmodified pyrolysis products. During this time the fire burns with high (typically 99%) combustion efficiency. This behavior corresponds to the first 10 minutes in Figure 8a.

2. As the flame zone propagates across the fuel bed the combustion processes behind the continuous flame front tend to shift towards intermittent pockets of smaller flames mixed with glowing combustion and gasification of char which are part of "smoldering" combustion. Chemisorption of O_2 on char is exothermic and drives glowing combustion which provides heat to pyrolyze and "distill" adjacent fuel which, in turn, contributes to more char formation. CO_2, CO and hydrocarbons are released from the char. With less flames, a larger fraction of distilled and pyrolytically formed compounds can be entrained in the smoke unoxidized. If the flame front propagates across the fuel bed at a constant rate then the combustion efficiency drops in a ca. linear fashion with respect to time as the ratio of smoldering to flaming increases. This behavior is illustrated in the midsection of Figure 8a. During these intermediate times of the fire, especially, the emissions are the products of all three processes.

3. After the flame front has passed completely over the fuel bed the products are dominated by smoldering, but still with an important contribution to emissions from pyrolysis. During this time the combustion efficiency was observed to range from 80 to 88% until the fire ceases to burn. This second sustained level of combustion efficiency is seen at the end of the fires in Figure 8.

Emissions from flaming and smoldering peak with the maxima in flaming and smoldering combustion, but peaks in the production of pyrolysis products are more variable. The higher heat release rate associated with flaming combustion pyrolyzes more fuel and there is often a peak in the measured pyrolysis products either before, during, or shortly after

the peak in flaming products. However, the majority of the initial pyrolysis products would normally be oxidized in the presence of vigorous flaming. Therefore, in all fires, the quantity of pyrolysis products detected *per unit fuel consumption* is always higher during times dominated by smoldering combustion. During smoldering combustion the pyrolysis products are made at a lower absolute rate, but they have a higher probability of escaping the fire to be detected in the smoke. For a specific, homogeneous fuel the flaming and smoldering processes tend to produce smoke that is approximately of fixed relative composition, so that the ratio of highly oxidized compounds to CO_2 is more or less constant from flaming combustion, and the ratio of certain incompletely oxidized compounds to CO is roughly constant for smoldering combustion for a specific fire type. (See Figures 4a, b - 6a, b) This is the basis for the observation of "tracking", in which the normalized concentration profiles for flaming or smoldering compounds show a high degree of correlation with the other compounds in the same class. In fires that exhibit tracking it is meaningful to report the ratio of the concentrations, obtained from a spot measurement and for two compounds from the same class, as an approximate emission ratio for the fire as a whole. This is useful because it allows reliance on data which is not fire-integrated to derive emission ratios. Thus, in such fires the emission ratio for two compounds that are either both from flaming or both from smoldering can be measured at nearly any time. However, even for a homogeneous fuel bed, where tracking occurs for flaming and smoldering compounds, the pyrolysis products *do not track* a single tracer species well. This implies that an integrated sample or (preferably) real-time, continuous sampling of the emissions and the smoke velocity is necessary to obtain good emission ratios for these compounds.

When spotty or layered (inhomogeneous) fuel beds are burned, tracking is not observed even for flaming or smoldering compounds. As different fuels dominate fuel consumption during the course of the fire, the tracking may go away. An example of this type of temporal behavior is shown in Figure 9 which shows the ratio of some smoldering compounds to each other during the crown fire simulation. During this fire the ratio CH_4/CO changes by a factor of five from an initial value of 0.2 which is characteristic of pine needles to a value of 0.04 which is characteristic of woody material. At the same time the value of NH_3/CH_4 increases by a factor of about 7. In practice, virtually all real fires run in such complex fuel beds, the one possible exception being pure grassland fires. A general approach to quantifying fire emissions is thus preferred, in which time-resolved concentrations and flow are measured and integrated to obtain total emissions.

Relative fuel consumption by various combustion processes.

Because the three major fire processes produce different products it is of use to be able to estimate the fuel consumption by process. Flaming and smoldering would normally account for most emissions by mass, but pyrolysis is important from an emissions standpoint as the sum of its products is similar to total methane emission. Essentially 90 - 99 % of the fuel carbon is converted to either CO_2 or CO from flaming and smoldering. Therefore for the purposes of estimating fuel consumption by process we make the mathematical approximation that all the fuel consumption is due to flaming or smoldering combustion. During the initial stages of a fire emissions are dominated by flaming combustion and we may measure the emissions of nearly pure flaming combustion. For many fires it is also true that near the end of the fire the emissions are dominated by smoldering combustion and we can measure the products of this process. For each fire that featured time periods dominated by pure flaming or smoldering combustion we have computed the emissions per unit amount of fuel for those pure processes. By also quantifying the average emissions per unit amount of fuel for the whole fire we can then determine the relative importance of each process in consuming fuel in an accurate manner following *Ward and Radke* [1993]:

$$\%S = [EF(flame) - EF(total)] / [EF(flame) - EF(smolder)] \times 100$$

and

$$\%F = 100 - \%S$$

We can calculate the percentage fuel consumption by smoldering combustion (%S) for each species individually. For CO_2 and CO, which are measured with excellent S/N throughout the entire fire the agreement is within 1%. For other flaming or smoldering emissions there is also normally good agreement. However if the emitted species is a distillation or pyrolysis product, for example, methanol, formaldehyde, acetic or formic acid, good agreement is not normally found using such an analysis based on only flaming and smoldering.

Emission factors and combustion efficiencies for examples of nearly pure flaming and smoldering processes, and the percent fuel consumption by smoldering combustion determined as above, are included in Table 3 for all applicable fires. For the compounds

listed as in the pyrolysis/distillation category the total emission factors are more accurate than the process emission factors.

We can contrast our process approach to that of Lobert et al., which distinguishes flaming and smoldering phases in time. In Lobert's work, CO is considered a tracer for smoldering combustion and the time of maximum rate of increase of CO emission is taken as the beginning of the smoldering stage. The results from the two approaches are compared for each fire as entries in Table 3. We find that the calculated fuel consumption for a "smoldering phase" is larger than the calculated fuel consumption by a smoldering process. The agreement between the two approaches is best when the fire makes a rapid transition between periods dominated by the two types of combustion; as in fire three (See Figure 8b). The difference between these approaches is more significant to understanding the combustion chemistry than it is in emissions estimates. In emissions estimates, the fuel consumption by a smoldering "phase" may be overestimated, but in these cases the emission factor for a smoldering "phase" will be underestimated and the resulting emissions estimate should be nearly the same.

Production of Oxygenated Organic Compounds.

Which compounds and how much.

The oxygenated organic compounds measured in this work are formaldehyde, methanol, and acetic acid (with one fire giving good data for formic acid). Our data on individual and total oxygenated organics is included in Table 3. The dominant species varies by fire as discussed in more detail below. To date, relatively little information has been available on the direct fire emissions of these difficult to measure compounds, but it is possible to make a limited comparison between our measurements and results obtained earlier. *Cooper et al.*, [1980] report a range from 1 to 5 X 10^{-4} moles *total aldehyde* production per mole C burnt in their woodstove study with formaldehyde accounting for most of this. In our 6 most comparable fires, in which most of the fuel consumption was due to flaming combustion, we report an average value of 4.0 X 10^{-4} ± 1.2 X 10^{-4} (1σ) moles *formaldehyde* per mole C burnt. *Hurst et al.*, [1994*a*] sampled Australian savanna fires from aircraft followed by laboratory MI-FTIR analysis. These authors report ratios to CO_2 which can be approximately converted to the units used above to yield 1.9 X 10^{-4} ± 1.4 X 10^{-4} moles *formaldehyde* per mole C burnt and 2.8 X 10^{-4} ± 2.2 X 10^{-4} moles *acetaldehyde* per mole C burnt. The field study of *Griffith et al.*, [1991] primarily probed

smoldering combustion and thus reports much higher levels of HCHO with their value of $HCHO/CO_2$ being 2.2×10^{-3}. Our study featured two fires dominated by smoldering combustion and for these fires our average value of $HCHO/CO_2$ was 2.3×10^{-3}. This work and the study of *Griffith et al.*, [1991] use remote sensing techniques and do not report evidence of acetaldehyde.

Our measured production of methanol and acetic acid from coniferous fuels compares well with the data from the laboratory fires in coniferous fuels of [*McKenzie et al.*, 1995] if combustion efficiency is considered. (See table 4.) Two studies report the direct emission from biomass fires of excess acetic acid to excess carbon dioxide ($\Delta HAc/\Delta CO_2$). [*Talbot et al.*, 1988] report an average value of $\Delta HAc/\Delta CO_2$ of $6.9 \times 10^{-5} \pm 3.6 \times 10^{-5}$ for their laboratory fires with brush and hard wood fuels. [*Van Dinh et al.*, 1991]. report an average value of $\Delta HAc/\Delta CO_2$ of 5.8×10^{-4} from savannah fires. Our value of $\Delta HAc/\Delta CO_2 = 1.87 \times 10^{-3} \pm 1.54 \times 10^{-3}$ for coniferous fuels is somewhat higher than these values, but in our, perhaps, more comparable fires in sagebrush fuels acetic acid was below the detection limit. *Lacaux et al.*, [1994] measured a ratio of excess formic plus excess acetic acid to excess CO_2 of 2.0×10^{-3} from African charcoal making kilns. This implies an acetic acid to CO_2 ratio similar to ours as our work and the studies of *Talbot et al.* and *McKenzie et al.* find that formic acid emissions are less than 25% of acetic acid emissions.

We can make a preliminary estimate of the direct biomass fire production of some oxygenated organic compounds. These estimates are not intended to be taken as global source strengths as they do not include data from tropical fuels nor do they include secondary production and losses in biomass fire plumes. However, these estimates may be useful in assessing the initial impact of these compounds on plume chemistry. Figure 10 shows the fire integrated emissions per unit amount of fuel for HCHO, CH_3OH, and CH_3COOH as a function of fire integrated (modified) combustion efficiency. Qualitatively, in the fires studied in this work, these compounds are each emitted at levels about 20 to 25% of methane and the sum of the oxygenated organics is a large fraction of the methane emissions. This suggests that the emissions of these compounds and their effect on regional atmospheric chemistry should be better understood.

Potential effects of oxygenated organic compounds on plume chemistry.

The production of oxygenated organic compounds in fires is of potential atmospheric significance for several reasons: 1) Many of these compounds are reactive. 2) Organic acids contribute significantly to rain and cloud water acidity in remote regions [*Keene and Galloway*, 1984*a* and 1984*b*]. 3) Other oxygenated organics (e.g. HCHO) may serve as precursors (by oxidation) for organic acids and (by photolysis) for oxidants such as HO_2 and OH.

The atmospheric chemistry of oxygenated organics has been summarized elsewhere [*Finlayson-Pitts and Pitts*, 1986, pp 394-6 and 499-507]. We note that oxidation of methanol can be a formaldehyde source, that oxidation dominates photolysis as a formaldehyde sink in "moderately polluted conditions", and that oxidation of formaldehyde can produce formic acid. Thus we speculate, as have [*Andreae et al.*, 1988], that some emitted oxygenated organics may contribute to a secondary gas-phase formic acid source. In addition to this secondary source of formic acid could be the oxidation of the emitted alkenes [*Arnts and Gay*, 1979, *Finlayson-Pitts and Pitts*,1986]. Alkenes detected in this work include both ethene and terpenes. [*Helas et al.*, 1992] suggested that volatilized biogenic compounds from biomass burning may be a source of formic acid. We find spectroscopic evidence that the emission of these compounds may indeed be significant as discussed in more detail below. Figure 11 illustrates a few of the pathways which may contribute to secondary acid production.

Production of reactive nitrogen-containing compounds.

Which compounds are produced.

The C:H:N analysis was done for the pine needles burnt in fires 3 and 5 and on that basis the fraction of fuel N detected by the FTIR technique can be calculated. If we assume that all the burnt fuel carbon was volatilized and detected and that we properly measured the C:N ratio of the fuel than we can estimate the closure on the fuel N. For fires 3 and 5, we find that the sum of NH_3, NO, and NO_2 accounts for 53.4 and 54.3 % of the fuel nitrogen respectively for an average value of 54%. We observed N compounds, other than the three mentioned above, at significant levels only in the "crown fire" simulation, which showed HCN accounting for about 10% of the measured N emissions. (See Figure 12.) We also find that N_2O and CH_3CHN are below the detection limit and presumably account for a negligible fraction of the fuel nitrogen. These findings are in general

agreement with *Hurst et al.* [1994*a* and 1994*b*] who report high levels of NH_3, NO, and NO_2 but that N_2O, HCN, and CH_3CN each account for less than 1% of the fuel nitrogen.

If we accept the value of *Kuhlsbusch et al.* [1991] of 36 ± 13% for N_2, and a value for ash nitrogen of 10% [*Hurst et al.*, 1994*a* and 1994*b*, *Crutzen and Andreae*, 1990] than these values, added to our 54% as NH_3, NO, or NO_2, total to 100% of the fuel nitrogen: within our precision accounting for all the fuel N with 5 measurements.

Production levels and relative importance of nitrogen-containing compounds

We find that our total measured N depends more on the fuel type than the combustion efficiency which suggests a correlation with fuel N. (See Figure 13) The probable upper limit for fuel nitrogen in our fuels was 1%. Since nitrogen contents up to 2.66% have been reported for leaves and 3.5% for organic soils, we should extend our work to include these fuels.

Our data confirms the earlier observation of *Griffith et al.* [1991] that NO_x dominates the measurable nitrogen release during flaming combustion and that NH_3 is the dominant measured N product in smoldering combustion. Early estimates of NH_3 production from biomass burning project NH_3 production be about one-third of NO_x production [*Crutzen and Andreae*, 1990]. The laboratory studies of *Lobert et al.* [1991] yield an average value for NH_3/NO_x of 0.57. In our data we find that at fire-integrated combustion efficiencies below approximately 0.91 the molar ratio of NH_3/NO_x exceeds unity (See Figure 14). The field measurements of *Griffith et al.* [1991] yield an average NH_3/NO_x ratio of 3.7, although that experiment was not optimized to compare flaming and smoldering compounds. The data of *Hurst et al.* [1994*a* and 1994*b*], from aircraft sampling of Australian savannah fires, suggests a NH_3/NO_x estimate near 1.1. Thus our results and those of *Griffith et al.* and *Hurst et al.* suggest that biomass burning may be a more significant source of ammonia than has been generally recognized.

Potential effects of nitrogen-containing compounds on plume chemistry and sampling.

Except for N_2 and the nitrogen remaining in ash, most of the fuel nitrogen is emitted as a reactive compound. The atmospheric chemistry of ammonia is poorly understood, but it is important as the only common water-soluble base in the atmosphere and it could potentially interact with organic and inorganic acids in the plume (in the liquid or gas

phase). There are indications that a significant fraction of the emitted ammonia may be converted to ammonium ion [*Andreae et al.*, 1988*a*], but only a small fraction of the formic and acetic acid present in plumes appears to be converted to formate or acetate [*Talbot et al.*, 1988, *Andreae et al.*, 1988*b*]. NO and NO_2 can be precursors for regional ozone and nitric acid production. We find that fresh plumes contain reactive nitrogen compounds at a level one-half to four times the amount of methane. (See Table 3.) It may be possible that reactions involving these compounds could produce detectable levels of new species in sample containers that are not important in the field.

Dependence of measured emissions on fuel and fire type.

The crown fire simulation was successful in achieving visible flaming in green needles and twigs, but did not produce the explosive combustion witnessed in some crown fires. This and the other fire type simulations were not replicated in this pilot study. Our ability to quantify the effects of fire type and fuel type on emissions is limited by the precision of our data from nominally identical fires. Consideration of the pine needle and sagebrush fires that were replicated demonstrates the potential of the technique and allows some qualitative statements to be made.

The fires with green needles or with duff produced the highest levels of oxygenated organics. The broadcast burn simulation emitted more formaldehyde than the slash pile simulation which may have been due to the greater amount of duff in the fuel mixture. The sagebrush fires were the highest intensity fires and featured the most efficient oxidation of the fuel N and S. In both sagebrush fires methanol and organic acids were below the detection limit. This is in contrast to the high levels of these compounds measured from the brown pine needle fires which burned at nearly as high combustion efficiency. In the sagebrush fires HCHO was the dominant oxygenated organic compound and was the fourth most common carbon compound. The CH_4/CO ratio for sagebrush was only .2 of this ratio for brown or green pine needles. The most noticeable difference between the ground fire simulations and the crown fire simulation was the large increase in the peak presumably due to the terpenes in the smoke from green needles (vide infra). In general, with a larger number of fires and more supporting data, it should become possible to determine some of the underlying causes for the observed variation.

We observe a broad spectral feature in the C-H stretch region (near 2930 cm-1) that resembles the C-H stretch spectra for terpenes and is especially large in our spectra of

smoke from green needles. (See Figure 15) This feature is about three times smaller in smoke spectra from brown needles and even smaller in the ground fire simulations where brown needles are only a component of the fuel. Terpenes are unstable in stainless steel canisters [*Westberg*, 1981], but have been detected at high levels previously by GC/FID in campground smoke [*Rasmussen*, 1981]. Our preliminary upper limit on the concentration of terpenes in the smoke from green needles is quite high, peaking at 70% of the methane concentration. More work is underway to further quantify these concentrations and verify the compounds. If our preliminary identification and concentration estimates are verified and reproducible then these compounds may be significant in plume chemistry, as discussed earlier [*Arnts and Gay*, 1979], and as a precursor for particulate [*Ward*, 1979, and *Finlayson-Pitts and Pitts*,1986].

Variation in emission factors in comparison to other uncertainties.

For fire 11 (the crown fire simulation) we measure a fire integrated emission ratio of formic acid to carbon dioxide of 7.25×10^{-4} which is about two orders of magnitude higher than the average value of $6.9 \times 10^{-6} \pm 4.2 \times 10^{-6}$ reported by *Talbot et al.* [1988] in their laboratory study using brush for fuel. The fire 11 data, expressed as an emission factor (g/kg), is only slightly larger than values of *McKenzie et al.* [1995] for smoldering combustion of coniferous fuels. (Their study did not probe green fuels.) This example illustrates that for some trace gases the variation in emission factors from different types of biomass burning may be greater than the uncertainty in the amount of biomass burned [*Crutzen and Andreae*, 1990].

Comparison of Laboratory and Field Data

Comparison with FTIR field data.

The intercomparison between this study and the companion study in the field [*Griffith et al.*, [1991] for HCHO was described above for fires of similar combustion efficiency. A detailed comparison between the IFSL fires and field fires from the companion study that burned in nominally similar fuels (sagebrush) was also performed for CH_4, CO, HCHO, NH_3 and NO_x. The emissions for the IFSL fires were reported in the same way as they were reported for the field fires: i.e. the time average of the excess gas ratioed to excess CO_2 was calculated. These results are presented in Table 5. It can be seen that the

intercomparison of these nominally similar fires must be made with caution for several reasons.

1) A lack of details on what actually burned in the field fires. For instance the sage brush fires at the IFSL contained only sagebrush plants while in the field some grass and litter undoubtedly burned as well. Live fuel moisture can be highly variable and also subject to some decrease after cutting. The field fires burned at a lower air temperature and a higher relative humidity than the lab fires which may have reduced the combustion efficiency.

2) There was a difference in the effective sampling platform for the field and the lab which effected the relative amounts of flaming and smoldering sampled. For the field fires the concentration retrievals were by a different method than that used in the lab data. The data is limited to two fires in the field and two in the lab, so neither experiment is extensive enough to establish a trend line of use in projecting to the other experiment.

Examination of Table 5 illustrates the importance of both combustion efficiency and fuels in determining emissions. The smoldering process in fire 12, a lab fire in pure sagebrush, gives similar results for CO/CO_2 as the whole fire average for the field fires indicating that the products of smoldering combustion were predominantly sampled in the field. However the laboratory, smoldering process data shows markedly lower levels of methane, ammonia, and formaldehyde than the field fires. This may be due to the absence of litter and grass and duff in the lab sagebrush fires. To illustrate this Table 5 also includes data from lab fire #9 which burned with a MCE similar to the field sagebrush fires, but in coniferous litter and duff. While this fuel is not the same as the "missing fuel" in the lab sagebrush fires it does show levels of methane, ammonia, and formaldehyde that are similar to the field sagebrush fire data. This indicates that the lack of a ground fuel component may explain some of the difference between the laboratory and field results for "sagebrush."

Comparison with tower-based integrated canister sampling.

Tower-based sampling represents a field "point sampling" platform which is similar to our "fire integrated" laboratory platform in terms of vertical position relative to the fire. We compare the EF(CH_4) vs MCE from our simulated field fires in mixed coniferous fuels with the same quantity derived from tower-based canister samples of biomass burning in mixed coniferous fuels which were subsequently analyzed by GC/FID [*Ward and Hardy*, 1991]. Our plot has slope, intercept, and r-squared values of -48.8, 48.9, and 0.96; (See Figure 16a) compared to the field values of -45.0, 45.4, and 0.77.

Comparison with aircraft grab samples.

Aircraft sampling should probe a fire-driven plume similar to that in our lab work. These samples are not integrated over the fire, but may reflect contributions from a wide variety of simultaneous processes. Canisters were collected by the IFSL group from aircraft plume penetrations of wildfires burning in coniferous fuels in the Western US during the summer of 1994 [*Babbitt et al.*, 1995]. A comparison of the methane data from the aircraft campaign with our laboratory data is shown in figure 16b.

Emission of Sulfur compounds.

We consistently observe SO_2 emitted from flaming combustion with an average SO_2/CO_2 ratio of $7.3 \times 10^{-4} \pm 3.0 \times 10^{-4}$ (1σ precision). This ratio is lower than that reported by [*Crutzen and Andreae*, 1990] of $3.0 \times 10^{-3} \pm 1.5 \times 10^{-3}$. However, these values are not directly comparable without fuel S content. Low (<1 ppm) levels of OCS may be present in only one of our spectra. This is consistent with the findings of [*Crutzen et al.*, 1979, *Crutzen et al.*, 1985, and *Crutzen and Andreae*, 1990] as well as [*Ward et al.*, 1982] that OCS accounts for a very small fraction of fuel S. [*Bowen*, 1979] reports that plants contain from .1 to .9 percent S and [*Ward et al.*, 1982] measure that 48 to 74 percent of fuel S is volatilized. Thus, there are probably other significant S-containing emissions that went undetected in this study. Consideration of sulfur phytochemistry [*Richmond*, 1973, *Salisbury and Ross*, 1978] suggests that hydrogen sulfide, methyl mercaptan, and dimethyl sulfide are likely to be in this class, but they are very weak absorbers of IR radiation.

Conclusions

This work establishes the value of the FTIR laboratory technique for studying biomass fires and already provides a number of significant insights into the nature of these fires.

The observations in this study with the most relevance to projecting impacts on atmospheric chemistry are summarized below.

1) The concept of dividing a fire into two stages is insufficient to categorize the temporal behavior of the emissions. There are at least three "processes" that should be kept in mind. One consequence of this is that a representative sample cannot always be taken "at any time" during a fire. To measure oxygenated organics, or any compound from heterogeneous fuels, correctly requires continuous sampling, along with flow measurements or isokinetic integrated sampling.

2) Though a lot is known about the combustion chemistry of light alkanes, the gaseous fuel that supplies flaming combustion of biomass is likely to contain large amounts of volatile plant constituents and oxygenated organics. The combustion chemistry of these materials is less understood and will influence the emissions. The simplest example of this is that the smoke from biomass fires may contain levels of unburned oxygenated organics and volatilized biogenic compounds that are high enough to have a significant impact on local and regional atmospheric chemistry. The emission levels and their impacts deserve more attention than they have received to date.

3) There is increasing evidence that the fate of nearly all the fuel nitrogen may be determined with the measurement of 5 quantities and that of these quantities the NH_3 measurement is likely to be more significant than sometimes assumed, especially for low combustion efficiency fires.

Acknowledgements

The authors would like to thank Bill Mankin for the use of an FTIR, staff of the IFSL for support in measurements and informative discussions; Ron Sussot, Ron Rabbitt, Gerald Olbu, Patrick Boyd, and Lynn Weger, Andy McCann of Ontar corporation for assistance in blending databases, Aaron Goldman for providing molecular parameters for formic acid and ethene, and Bill Herget and Rei Rasmussen for informative discussions. This research was supported in part by the USFS RJVA93847.

References

Andreae, M. O., E. V. Browell, M. Garstang, G. L. Gregory, R. C. Harriss, G. F. Hill, D. J. Jacob, M. C. Pereira, G. W. Sachse, A. W. Setzer, P. L. Silva Dias, R. W. Talbot, A. L. Torres, and S. C. Wofsy. 1988a. Biomass-burning emissions and associated haze layers over Amazonia. *J. Geophys. Res.* 93, 1509-1527.

Andreae, M. O., R. W. Talbot, T. W. Andreae, and R. C. Harriss. 1988b. Formic and acetic acid over the central Amazon region, Brazil, 1, Dry season. *J. Geophys. Res.* 93, 1616-1624.

Arnts, R. R. and B. W. Gay, Jr. 1979. *Photochemistry of some naturally emitted hydrocarbons.* EPA-600/3-79-081. Research Triangle Park, NC: USEPA.

Babbitt, R. E., D. E. Ward, R. A. Sussot, W. M. Hao, and S. P. Baker. 1995. Smoke from western wildfires, 1994. Proceedings of the 1994 meeting of the Interior West Fire Council. Cour D'Alene, ID.

Bowen, H. J. M. 1979. *Environmental Chemistry of the Elements.* New York: Academic Press.

Cooper, J. A. 1980. Environmental impact of residential wood combustion emissions and its implications. *J. Air Pollut. Control Assoc.* 30, 855-861.

Crutzen, P. J., A. C. Delany, J. Greenberg, P. Haagenson, I. Heidt, R. Lueb, W. Pollock, W. Seiler, A. Wartburg, and P. Zimmerman. 1985. Tropospheric chemical composition measurements in Brazil during the dry season. *J. Atmos. Chem.* 2, 233-256.

Crutzen, P. J., L. E. Heidt, J. P. Krasnec, W. H. Pollock, and W. Seiler. 1979. Biomass burning as a source of atmospheric gases CO, H_2, N_2O, NO, CH_3Cl and COS. *Nature* 282, 253.

Crutzen, P. J., and M. O. Andreae. 1990. Biomass burning in the tropics: impact on atmospheric chemistry and biogeochemical cycles. *Science* 250, 1669.

Darley, E. F., F. R. Burleson, E. H. Mateer, J. T. Middleton, and V. P. Osterli. 1966. Contribution of burning of agricultural wastes to photochemical air pollution. *J. Air Pollut. Control Assoc.* 12, 685.

Dasch, J. M. 1982. Particulate and gaseous emissions from wood-burning fireplaces. *Environ. Sci. Technol.* 16, 639.

DeGroot, W. F., W. Pan, M. D. Rahman, and G. N. Richards. 1988. First chemical events in pyrolysis of wood. *J. Anal. Appl. Pyrolysis* 13, 221-231.

Delmas, R. A., A. Mareco, J. P. Tathy, B. Cros, and J. G. R. Baudet. 1991. Sources and sinks of methane in the African savanna, CH4 emissions from biomass burning. *J. Geophys. Res.* 96, 7287-7299.

Dinh, P. V., V. Yoboue, J. P. Lacaux, L. Schafer, and G. Helas. 1991. Organic acids from savannah fires experiment in Ivory Coast. *EOS* Oct 29, 1991 Supplement, 86.

Evans, R. J., T. A. Milne, and M. N. Soltys. 1986. Direct mass-spectrometric studies of the pyrolysis of carbonaceous fuels. III Primary pyrolysis of lignin. *J. Anal. Appl. Pyrolysis* 9, 207-236.

Finlayson-Pitts, B. J., and J. N. Pitts, Jr. 1986. *Atmospheric Chemistry: Fundamentals and Experimental Techniques*. New York: John Wiley.

Griffith, D. W. T., W. G. Mankin, M. T. Coffey, D. E. Ward, and A. Riebau. 1991. FTIR remote sensing of biomass burning emissions of CO_2, CO, CH_4, HCHO, NO, NO_2, NH_3 and N_2O. in Levine, J. S. ed. *Global Biomass Burning: Atmospheric, Climatic, and Biospheric Implications.* Cambridge: MIT Press.

Griffith, D. W. T. 1995. Synthetic calibration and quantitative analysis of gas-phase FTIR spectra. *in preparation.*

Haaland, D. M. 1990. Multivariate calibration methods applied to quantitative FT-IR analyses. in Ferraro, John R. and K. Krishnan eds. *Practical Fourier Transform Infrared Spectroscopy, Industrial and Laboratory Chemical Analysis.* San Diego: Academic Press.

Hanst, P. L. and S. T. Hanst. 1995. Gas Measurement in the Fundamental Infrared Region, an applications manual. Anaheim: Infrared Analysis, Inc.

Helas, G., H. Bingemer, and M. O. Andreae. 1992. Organic acids over equatorial Africa: results from DECAFE 88. *J. Geophys. Res.* 97, 6187-6193.

Hurst, D. F., D. W. T. Griffith, J. N. Carras, D. J. Williams, and P. J. Fraser. 1994a. Measurements of trace gases emitted by Australian savanna fires during the 1990 dry season. *J. Atmos. Chem.* 18, 33-56.

Hurst, D. F., D. W. T. Griffith, and G. D. Cook. 1994b. Trace gas emissions from biomass burning in tropical Australian savannas. *J. Geophys. Res.* 99, 16,441-16,456.

Kauffman, J. B., D. L. Cummings, and D. E. Ward. 1994. Relationships of fire, biomass and nutrient dynamics along a vegetation gradient in the Brazilian cerrado. *Journal of Ecology* 84, 519-531.

Keene, W. C. and J. N. Galloway. 1984a. A note on acid rain in an Amazon rain forest. *Tellus* 36B, 137-138.

Keene, W. C. and J. N. Galloway. 1984b. Organic acidity in precipitation of North America. *Atmos. Environ.* 18, 2491-2497.

Kuhlbusch, T. A., J. M. Lobert, P. J. Crutzen, and P. Warneck. 1991. Molecular nitrogen emissions from denitrification during biomass burning. *Nature* 351, 135-137.

Lacaux, J. P. D. Brocard, C. Lacaux, R. Delmas, A. Brou, V. Yoboue, and M. Koffi. 1994. Traditional charcoal making: an important source of atmospheric pollution in the African tropics. *Atmospheric Research* 35, 71-76.

Lobert, J. M., D. H. Scharffe, W. M. Hao, T. A. Kuhlbusch, R. Seuwen, P. Warneck, and P. J. Crutzen. 1991. Experimental evaluation of biomass burning emissions: Nitrogen and carbon containing compounds. in Levine, J. S. ed. *Global Biomass Burning: Atmospheric, Climatic, and Biospheric Implications* Cambridge, MA: MIT Press.

McKenzie, L. M., W. M. Hao, G. N. Richards, D. E. Ward. 1995. Measurement and modeling of air toxins from smoldering combustion of biomass. *Environ. Sci. Technol.* in press, and references therein.

Overend, R. P., T. A. Milne, and L. K. Mudge (eds). 1985. *Fundamentals of Thermochemical Biomass Conversion.* London: Elsevier.

Radke, L. F., J. H. Lyons, P. V. Hobbs, D. A. Hegg, D. V. Sandberg, D. E. Ward 1990. Airborne monitoring and smoke characterization of prescribed fires on forest lands in western Washington and Oregon. (General Technical Report; PNW-GTR-251 (USDA Forest Service Pacific Northwest Research Station).

Rasmussen, R. A. 1981. A review of the natural hydrocarbon issue. in Bufalini, J. J. and R. R. Arnts. eds. *Atmospheric Biogenic Hydrocarbons.* Ann Arbor, Michigan: Ann Arbor Science Publishers.

Richmond, D. V., 1973. Sulfur Compounds. in Miller, L. P. ed. *Phytochemistry: inorganic elements and special groups of chemicals*; v. III . New York: Van Nostrand Reinhold.

Ryan, P. W., C. K. McMahon. 1976. Some Chemical and Physical Characteristics of Emissions from Forest Fires. 69th Annual Meeting of the Air Pollution Control Association; June 27-July 1, Portland, OR.

Seavoy, Ronald E. 1973. The Shading Cycle in Shifting Cultivation. *Annals of the Association of American Geographers* 63, 522.

Shafizadeh, F., K. V. Sarkanen, and D. A. Tillman (eds). 1976. *Thermal Uses and Properties of Carbohydrates and Lignins.* New York: Academic.

Talbot, R. W., K. M. Beecher, R. C. Harriss, W. R. Cofer III. 1988. Atmospheric geochemistry of formic and acetic acids at a mid-latitude temperate site. *J. Geophys. Res.* 93, 1638-1652.

Ward, D. E. and L. F. Radke. 1993. Emissions measurements from vegetation fires: a comparative evaluation of methods and results. in Crutzen, P. J. and J. G. Goldammer eds *Fire in the Environment: The Ecological, Atmospheric and Climatic Importance of Vegetation Fires*. Chichester, England: John Wiley.

Ward, D. E., R. A. Susott, J. B. Kauffman, R. E. Babbitt, D. L. Cummings, B. Dias, B. N. Holben, Y. J. Kaufman, R. A. Rasmussen, and A. W. Setzer. Smoke and fire characteristics for cerrado and deforestation burns in Brazil: BASE-B Experiment. *J. Geophys. Res.* 97, 14,601-14,619.

Ward, D. E., C. K. McMahon, and D. F. Adams 1982. Laboratory measurements of carbonyl sulfide and total sulfur emissions from open burning of forest biomass. 75th Annual Meeting of the Air Pollution Control Association, June 20-24, New Orleans, LA.

Ward, D. E. 1979. Particulate matter and aromatic hydrocarbon emissions from the controlled combustion of alpha pinene. Ph.D. thesis, University of Washington, Seattle.

Ward, D. E. and C. C. Hardy. 1991. Smoke emissions from wildland fires. *Environment International* 17, 117-134.

Westberg, H. H. 1981. Biogenic hydrocarbon measurements. in Bufalini, J. J. and R. R. Arnts eds. *Atmospheric Biogenic Hydrocarbons*. Ann Arbor Michigan: Ann Arbor Science Publishers.

Figure 1. Experimental arrangement.

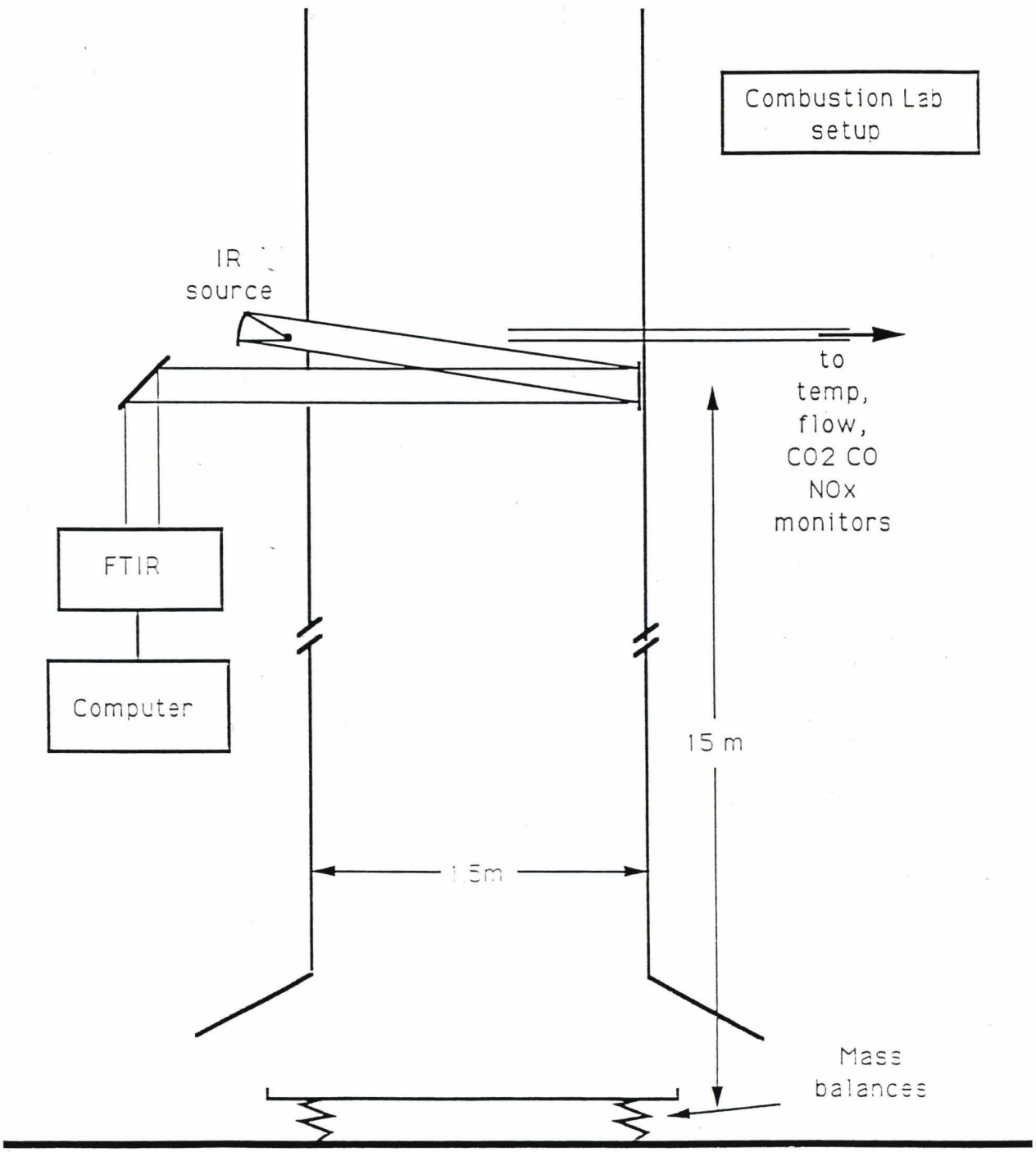

Figure 2. Examples of the fitted and measured spectra compared.

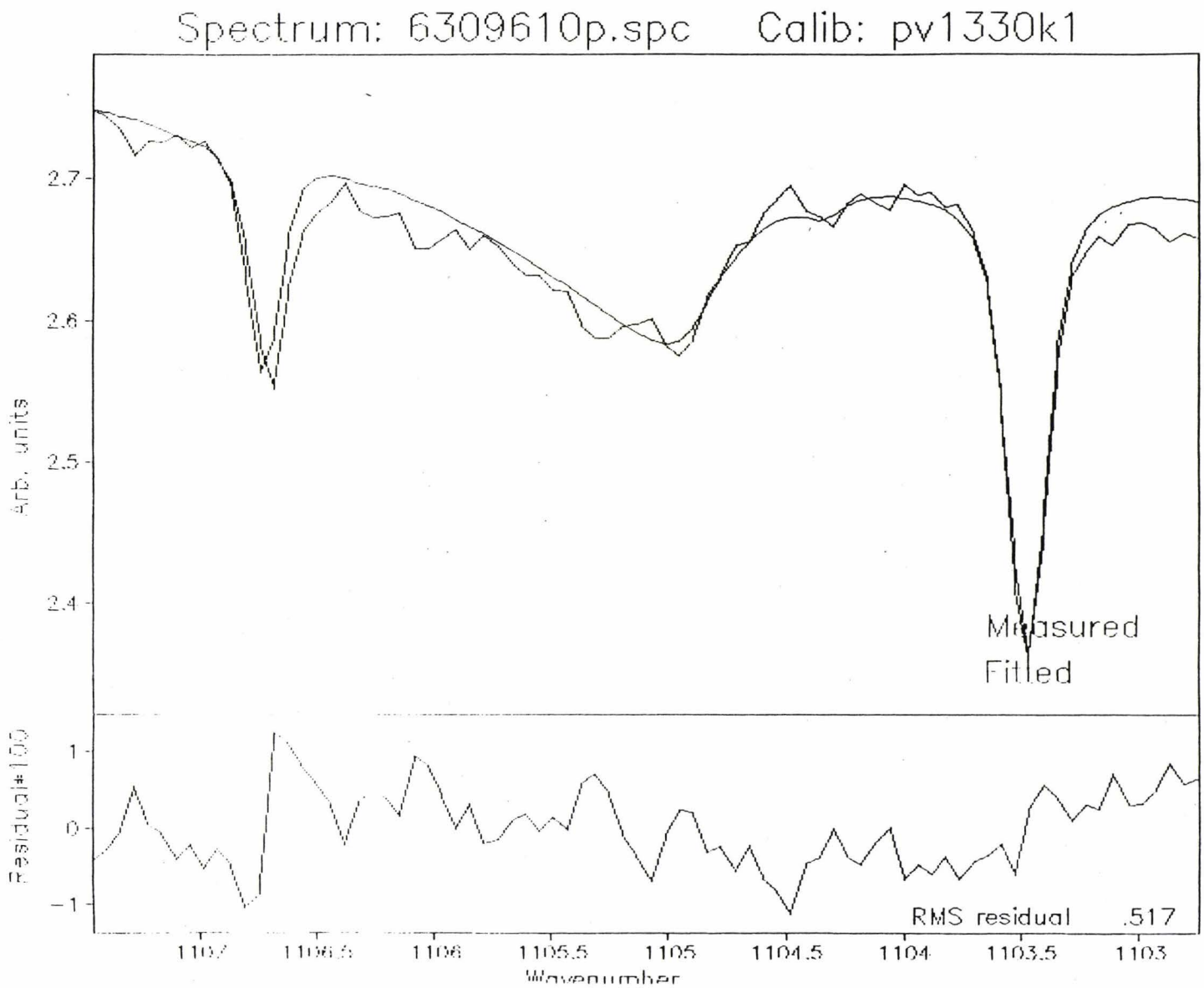

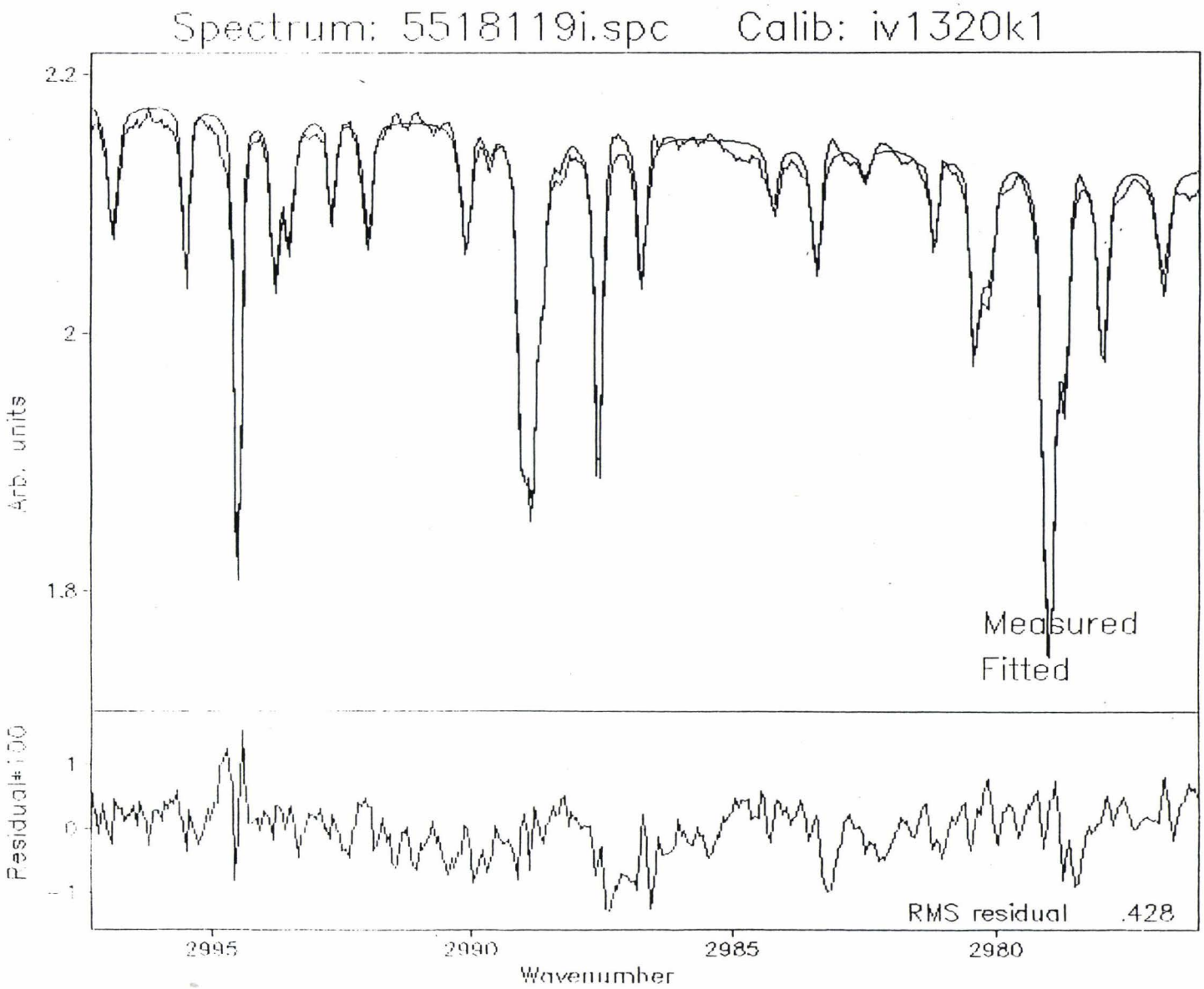
Spectrum: 5518119i.spc Calib: iv1320k1
2.2
2
1.8
Arb. units
Measured
Fitted
Residual*100
1
0
-1
RMS residual .428
2995
2990
2985
2980
Wavenumber

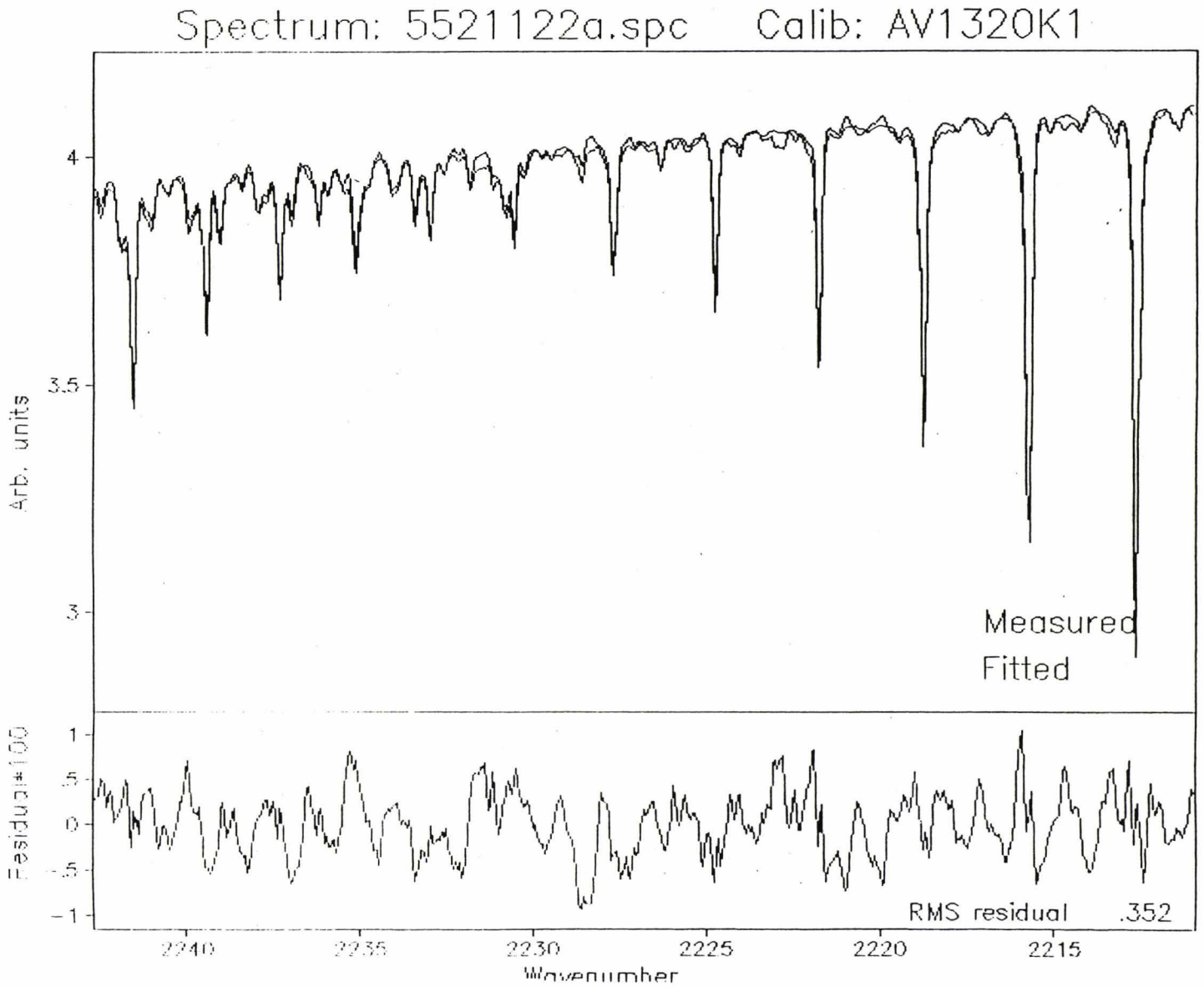
Spectrum: 5521122a.spc Calib: AV1320K1
Arb. units
4
3.5
3
Measured
Fitted
Residual*100
1
.5
0
-.5
-1
RMS residual .352
2240
2235
2230
2225
2220
2215
Wavenumber

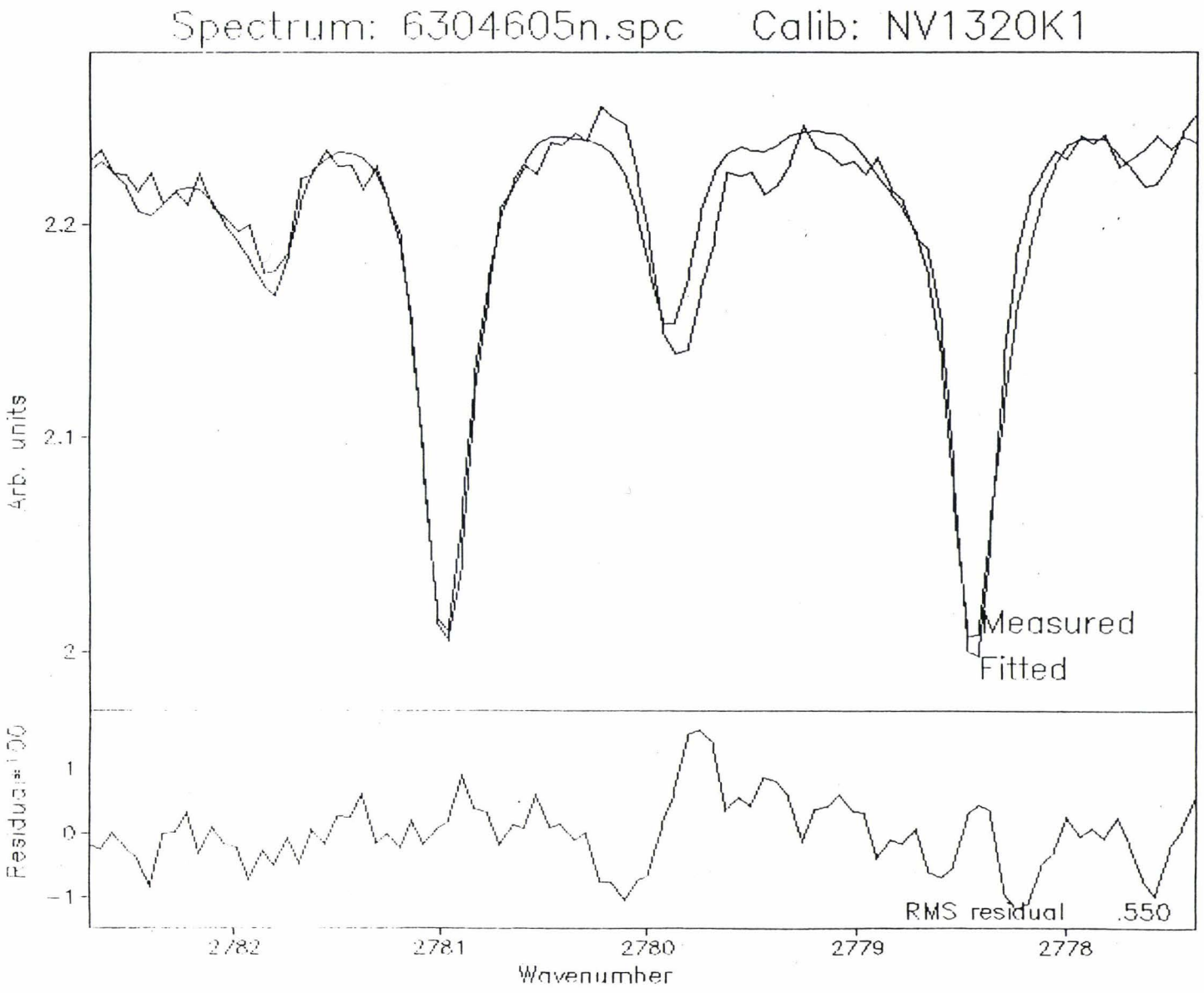
Spectrum: 6304605n.spc Calib: NV1320K1
2.2
2.1
2
Arb. units
Measured
Fitted
1
0
-1
Residual*100
RMS residual .550
2782
2781
2780
2779
2778
Wavenumber

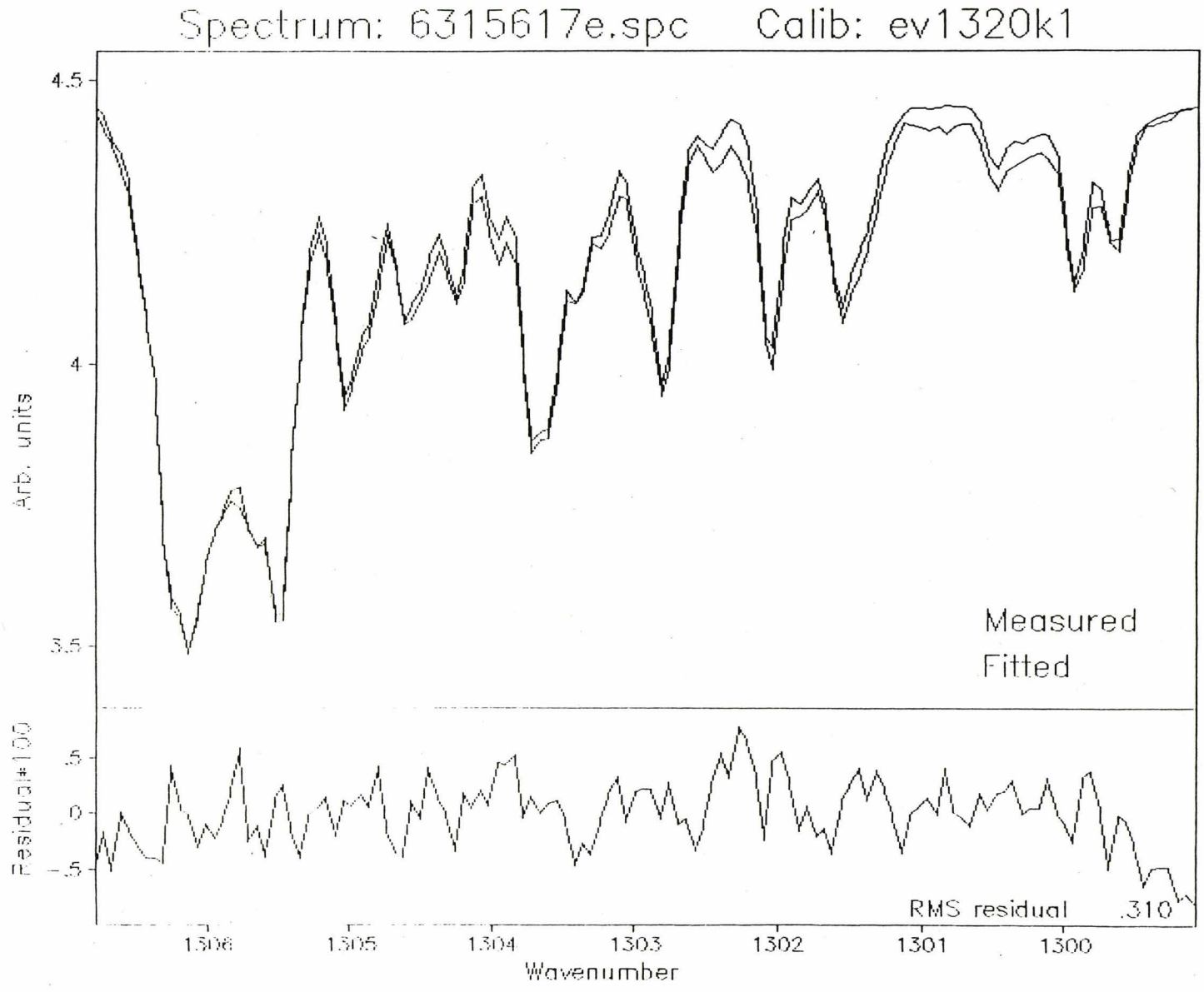
Spectrum: 6315617e.spc Calib: ev1320k1
4.5
4
3.5
Arb. units
Measured
Fitted
Residual*100
.5
0
-.5
RMS residual .310
1306
1305
1304
1303
1302
1301
1300
Wavenumber

Figure 3. Mass balance.

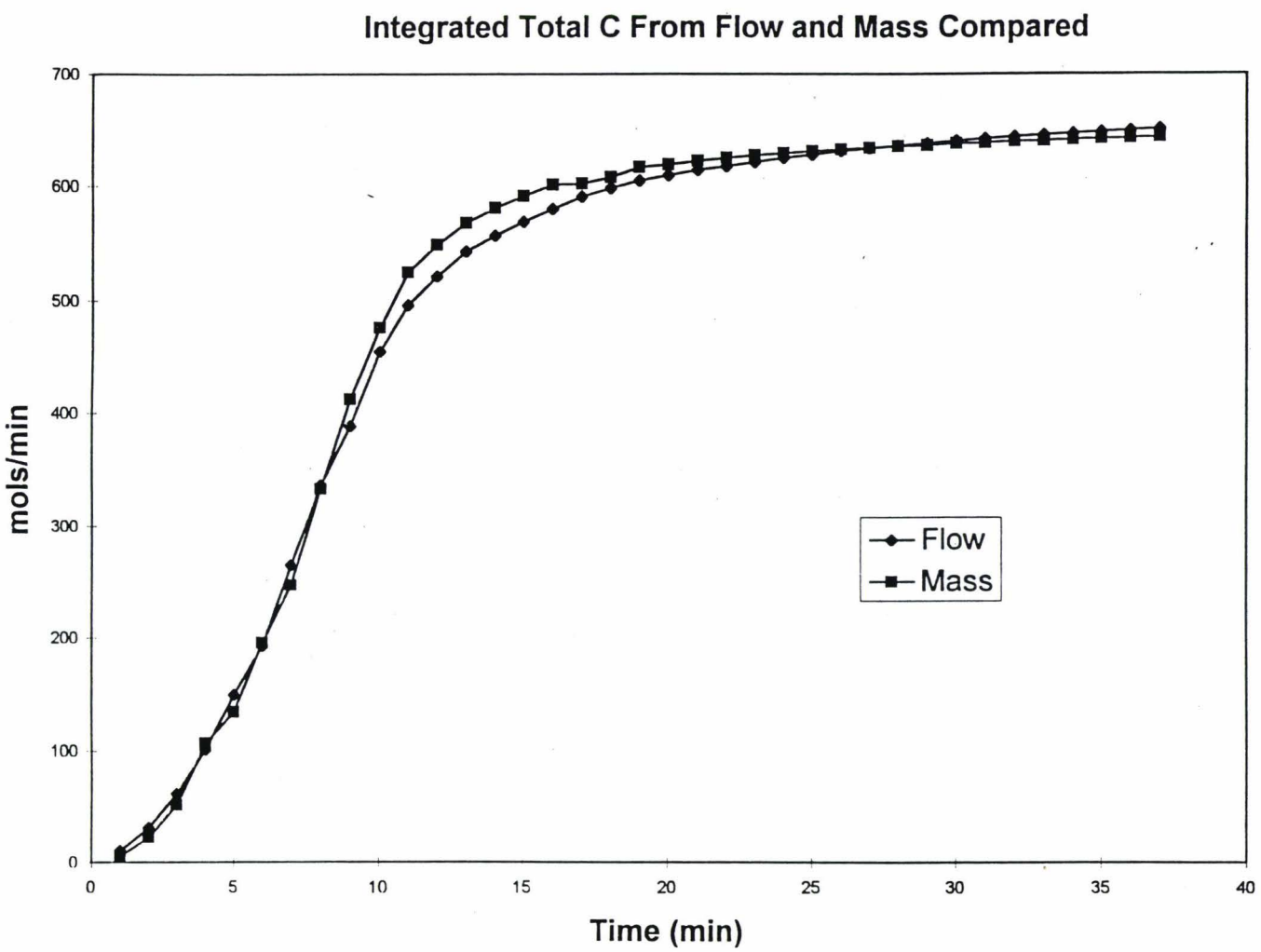

Figure 4 Pine needle types of fire emissions.

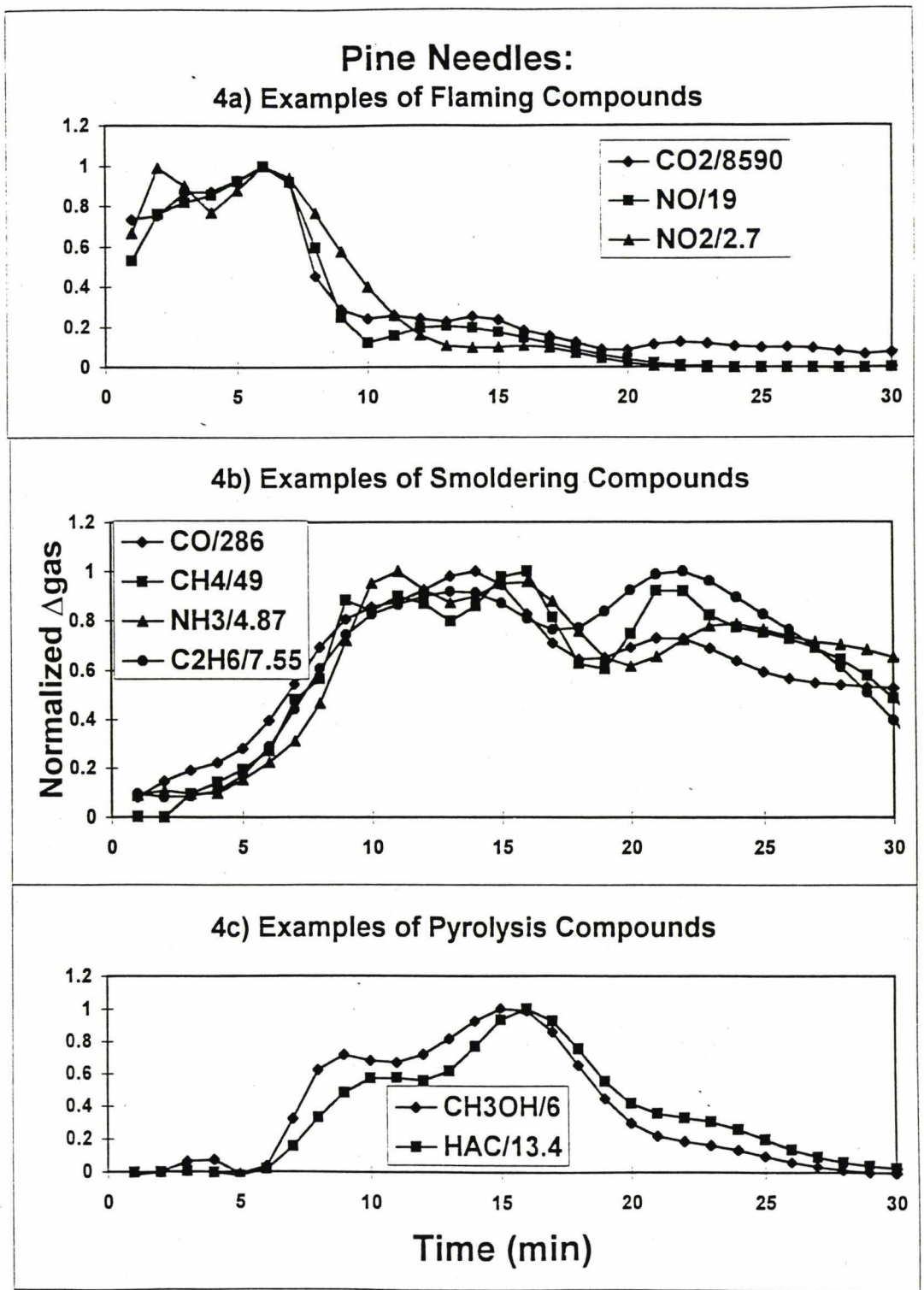

Figure 5. Activity fuels types of fire emissions.

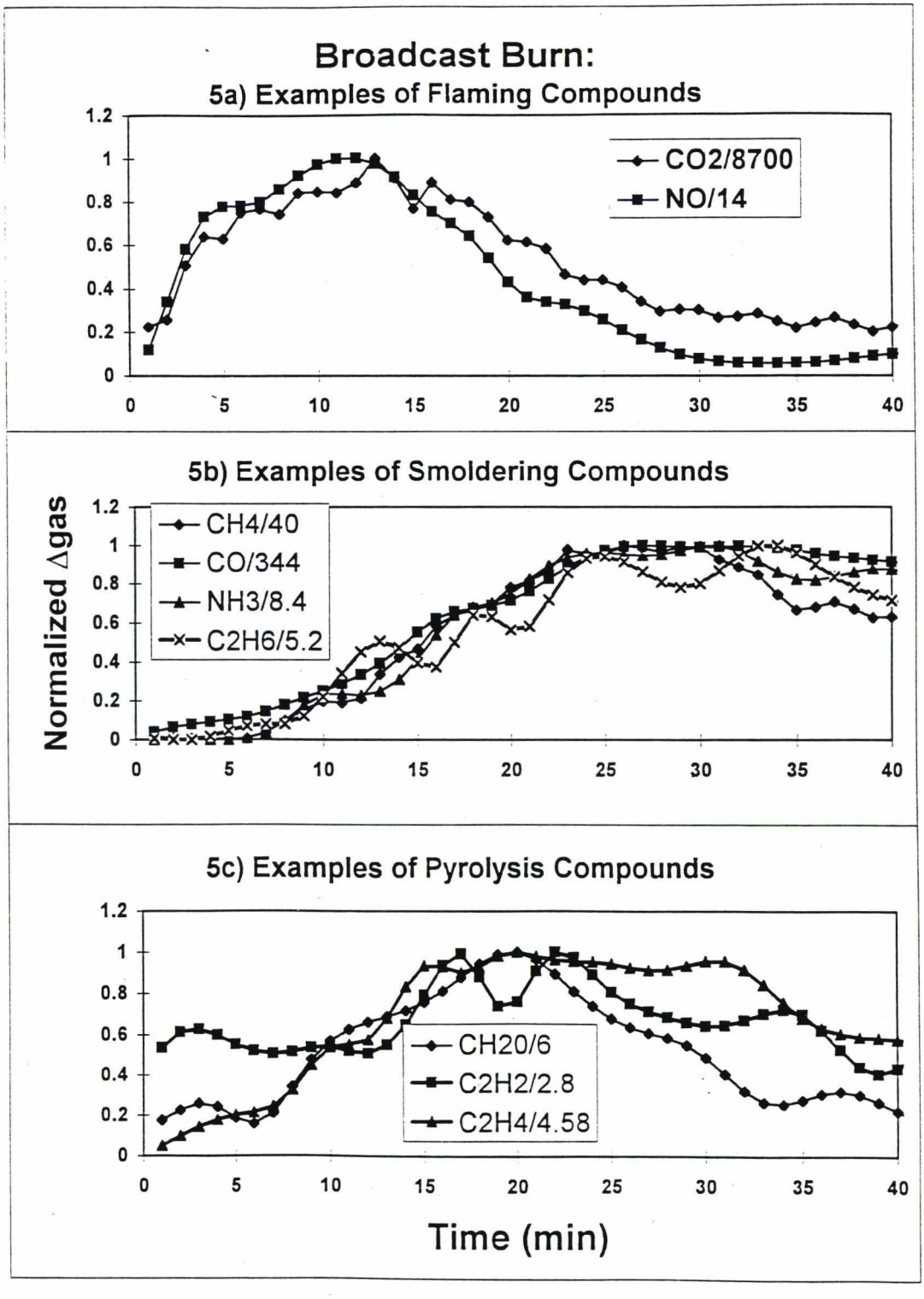

Figure 6. Sagebrush types of fire emissions.

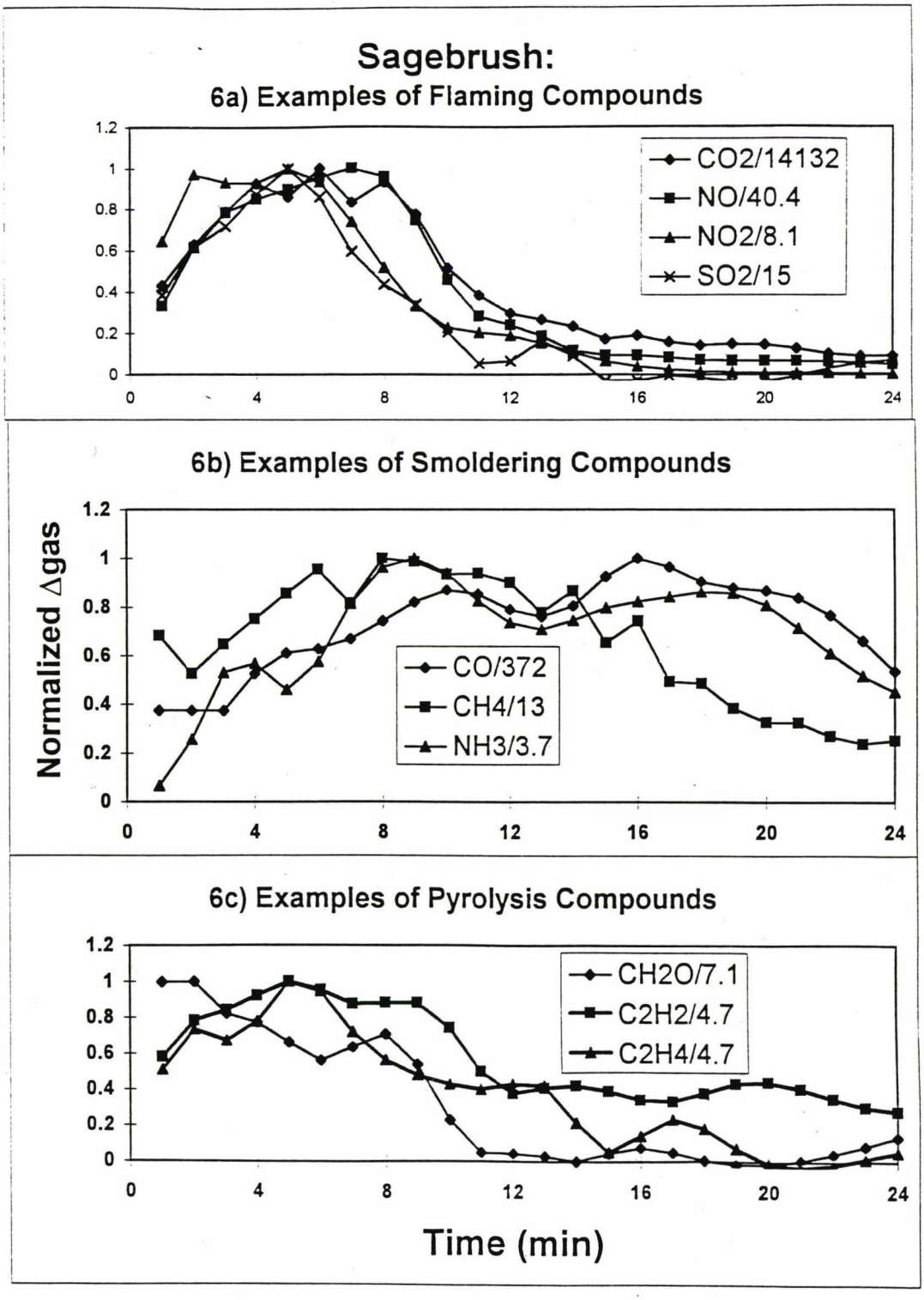

Figure 7. Temporal profiles for Acetic Acid and Methanol.

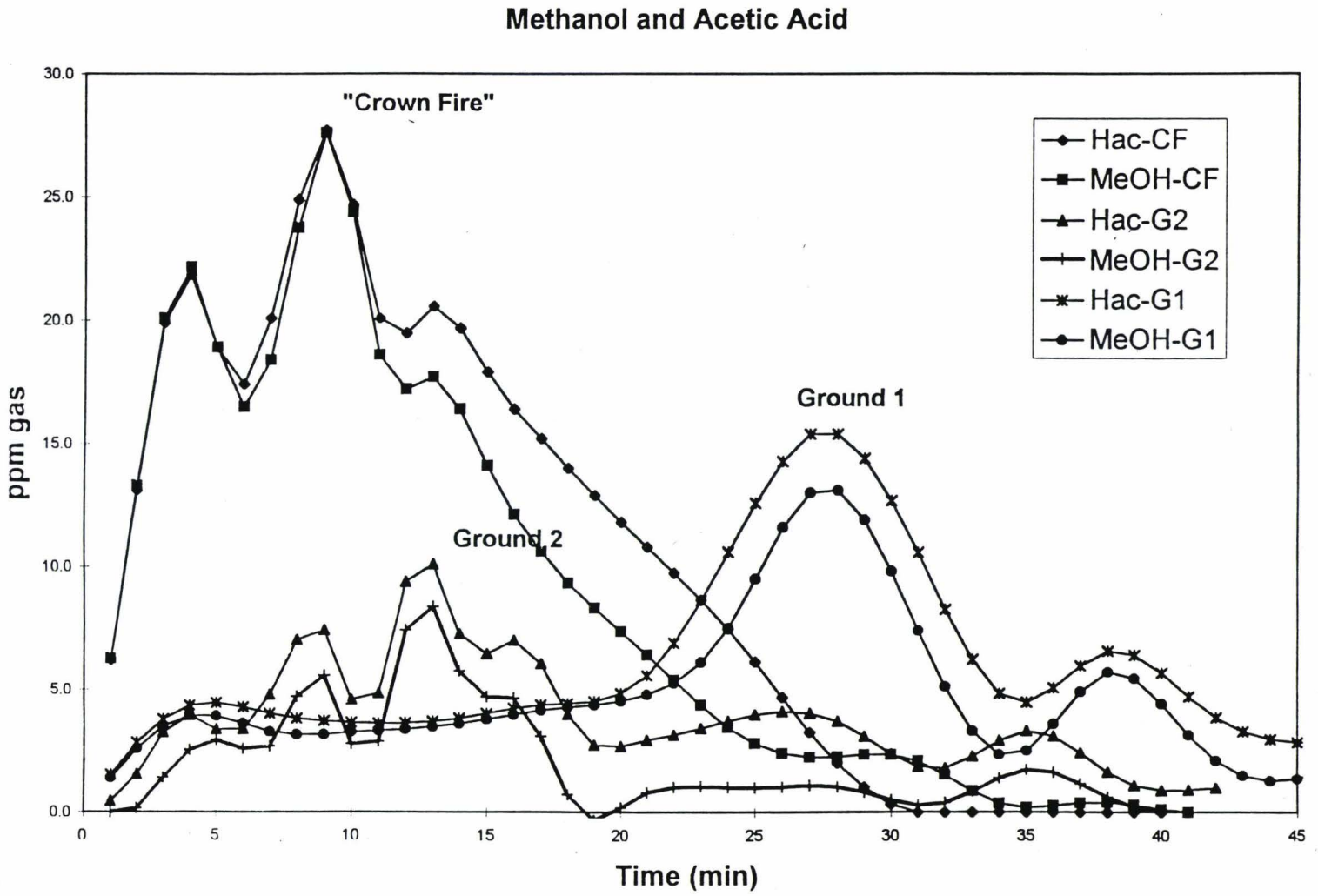

Figure 8. The modified combustion efficiency versus time for two fires.

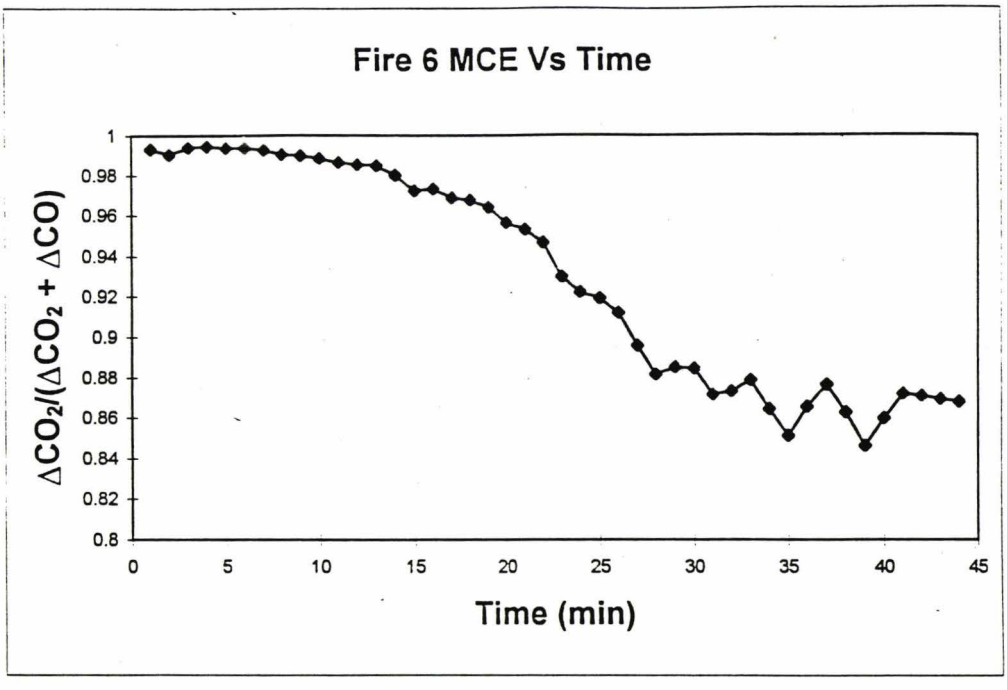

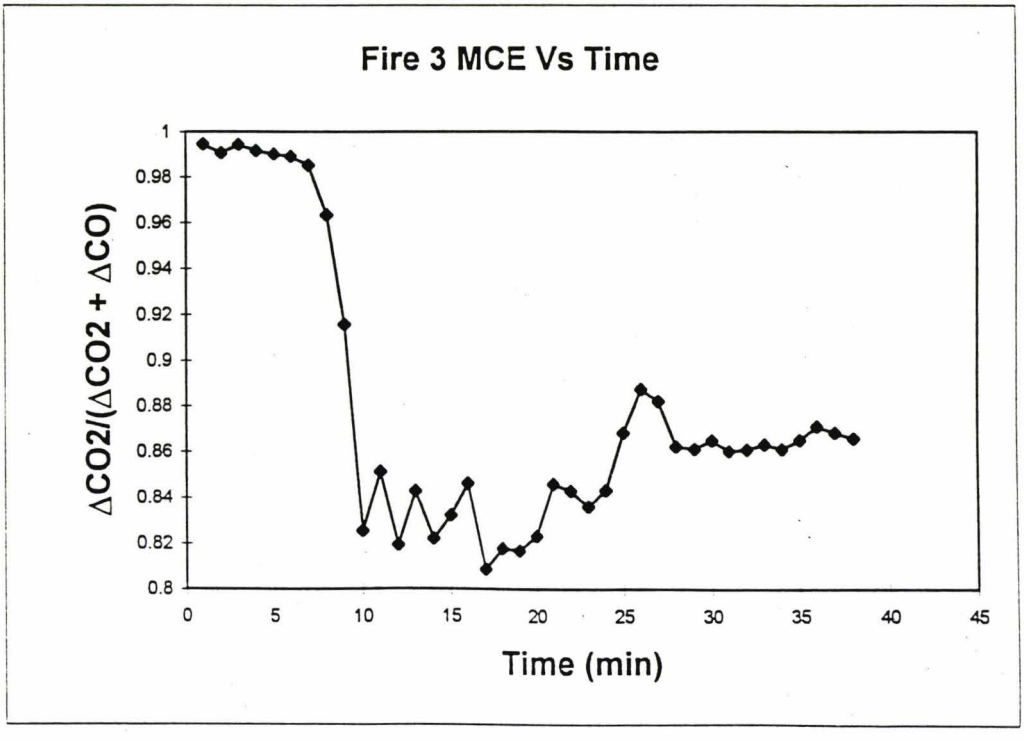

Figure 9. Tracking not observed in a heterogeneous fuel bed.

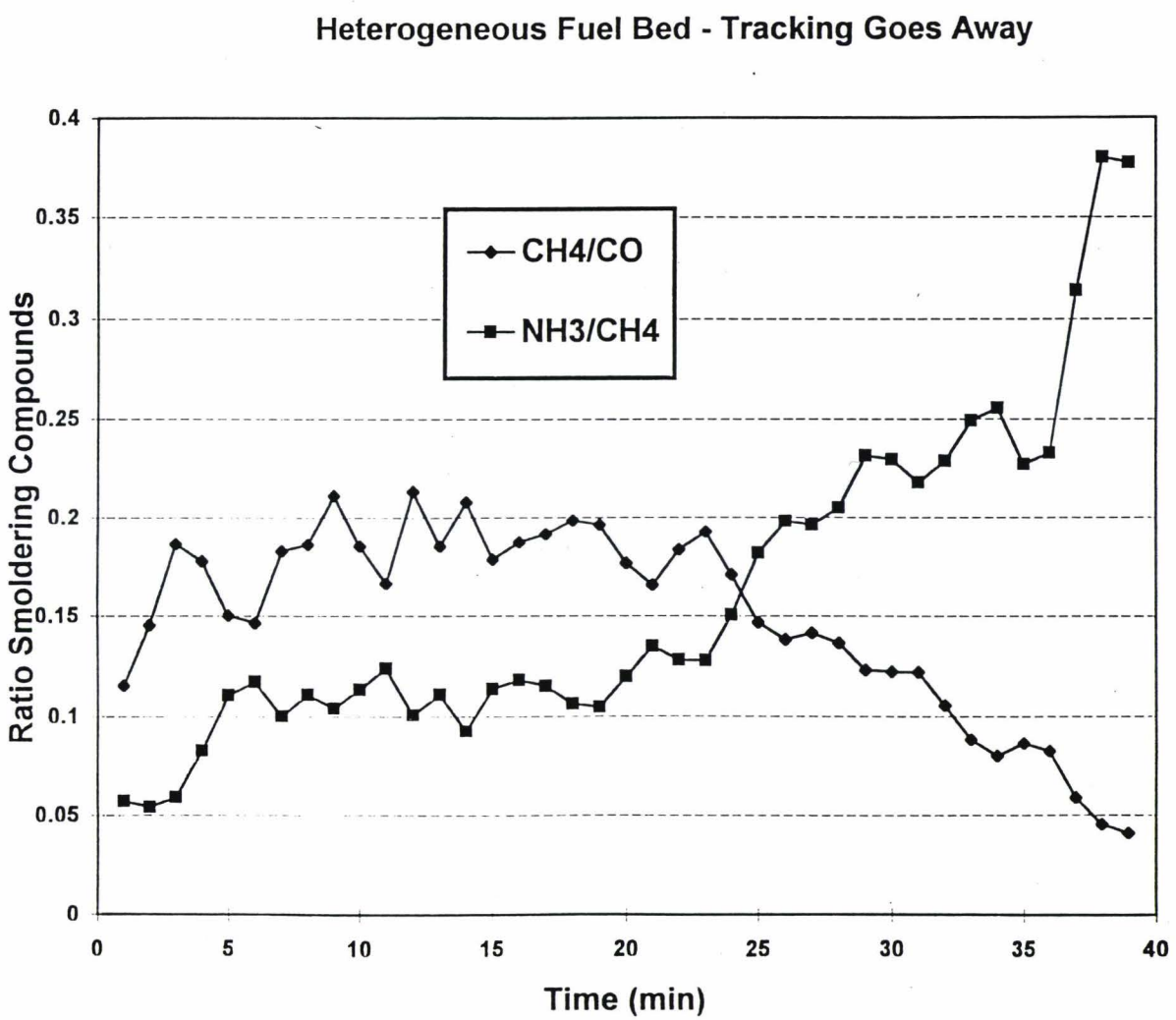

Figure 10. Emissions estimates for oxygenated organic compounds.

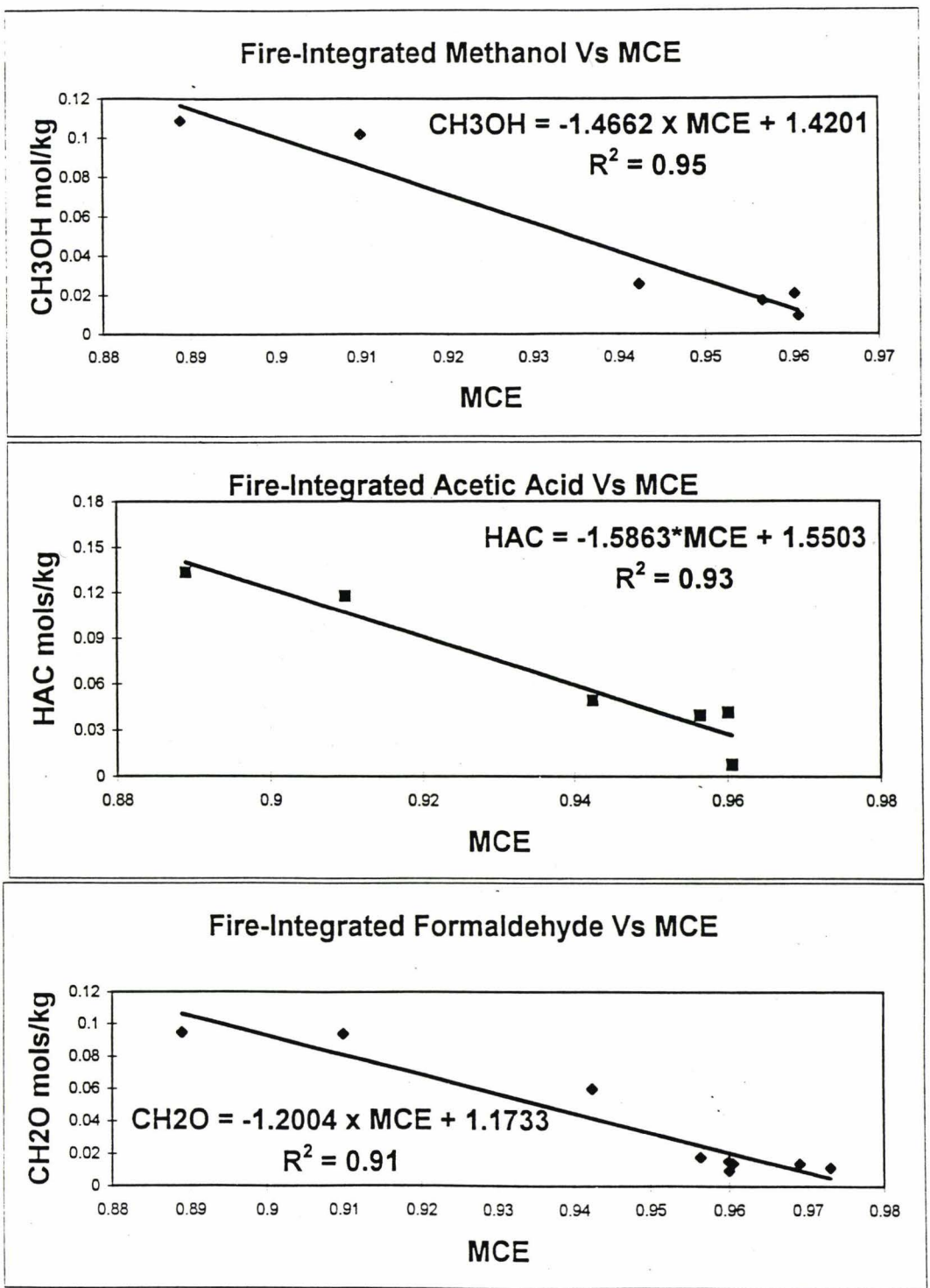

Figure 11. Pathways for secondary acid production in biomass burning plumes.

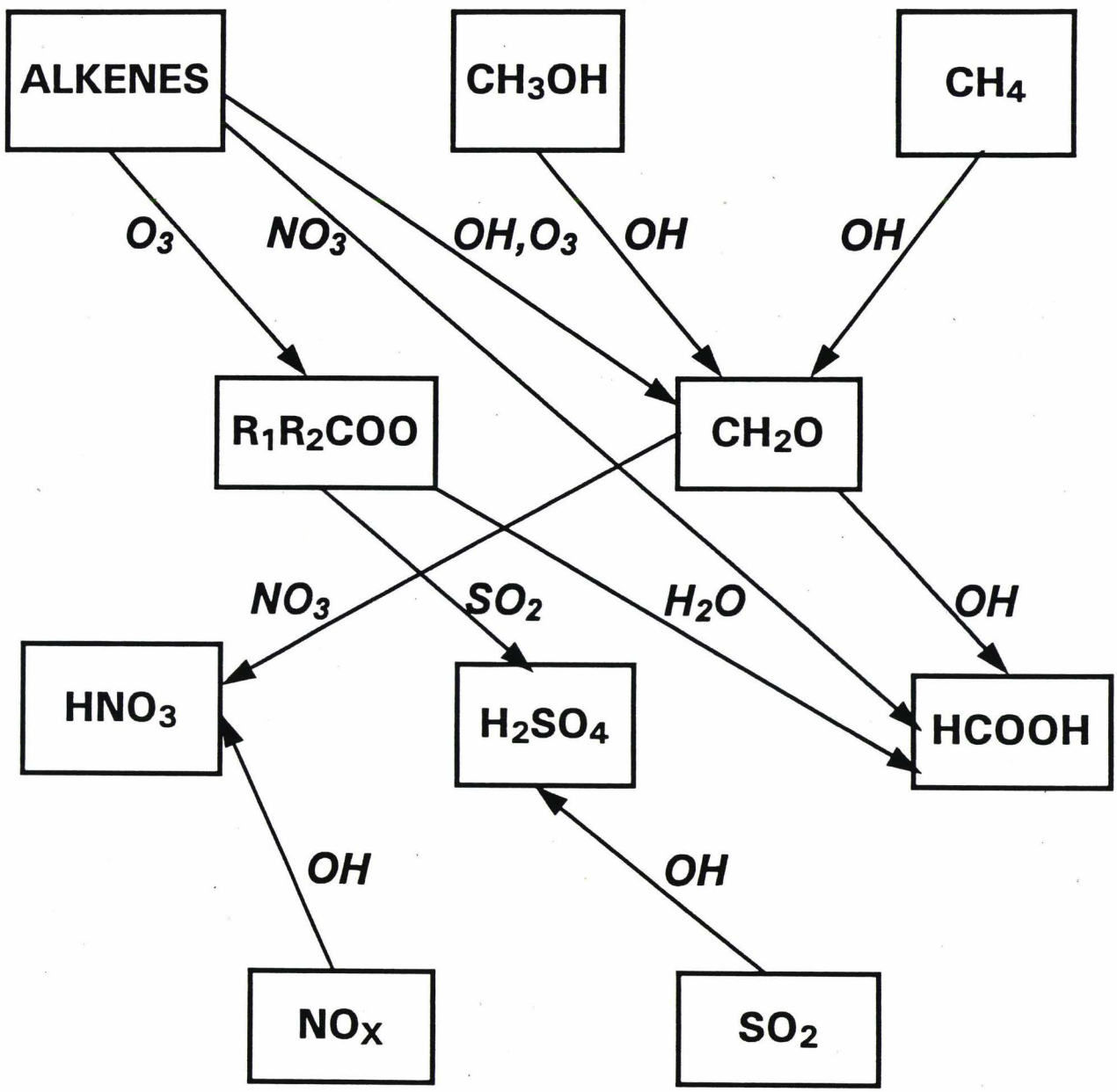

Figure 12. Comparison of NH_3 and HCN emissions for fire #11.

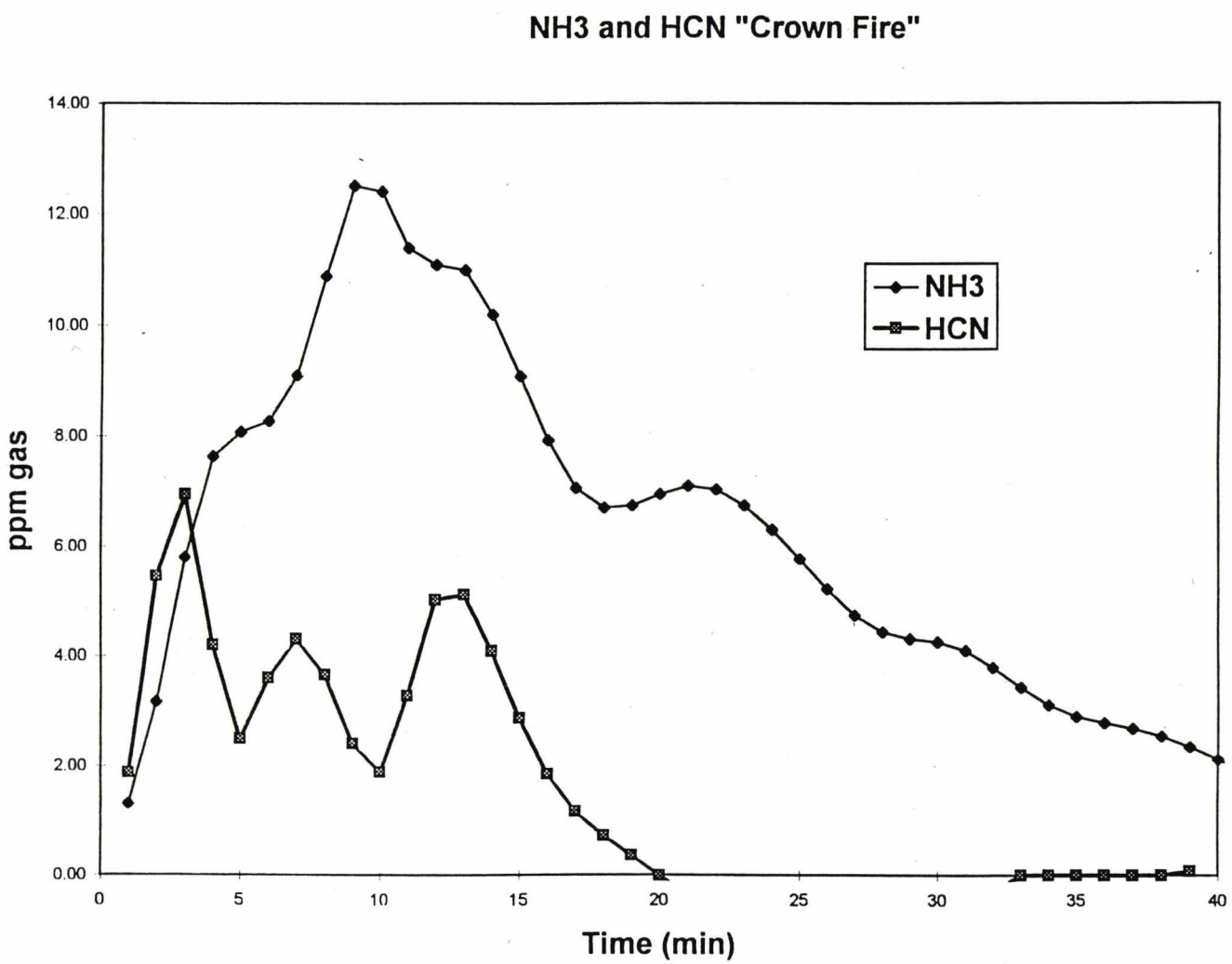

Figure 13. Illustration of the dependence of measured N emissions on fuel type.

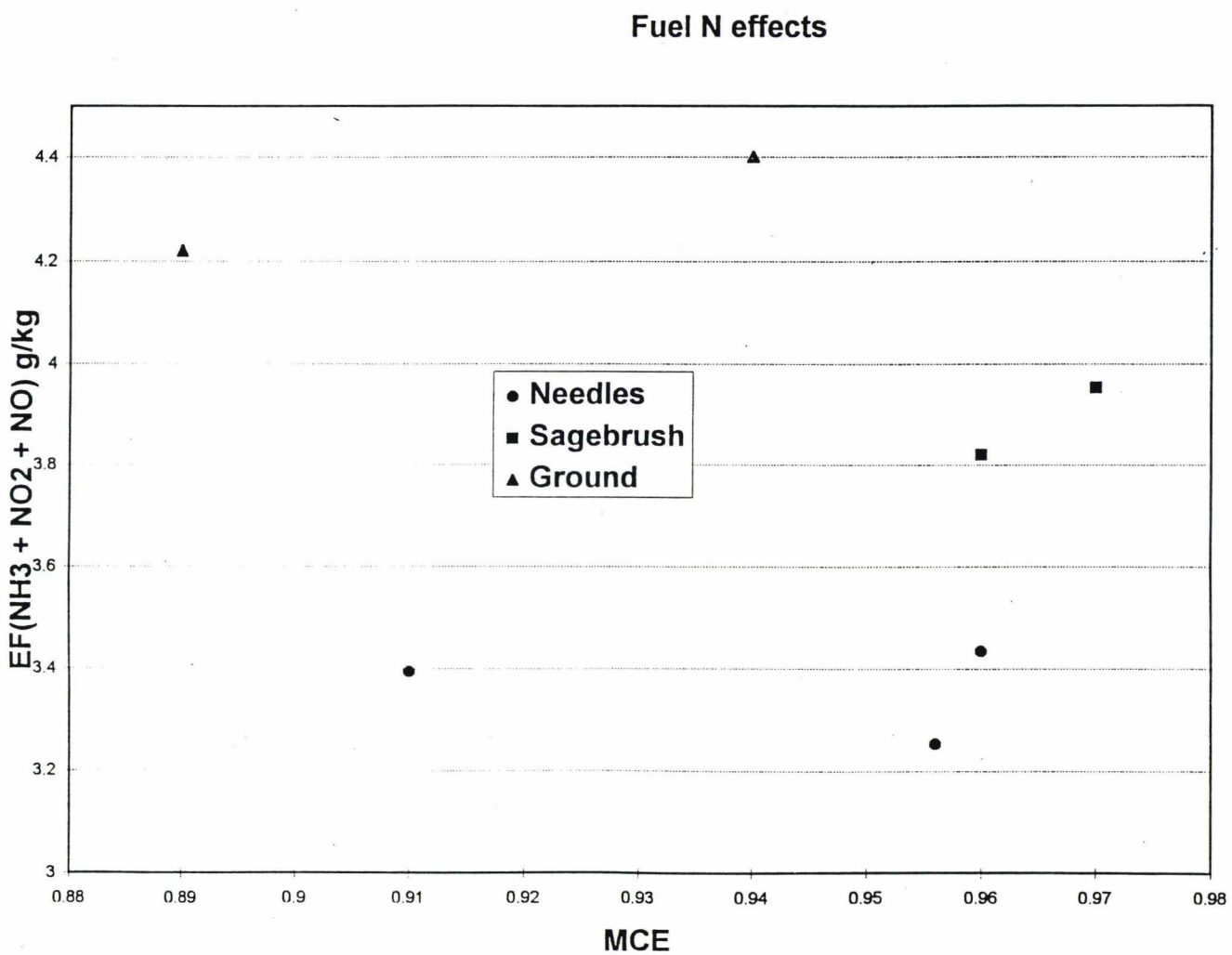

Figure 14. NH_3/NO_x as a function of modified combustion efficiency.

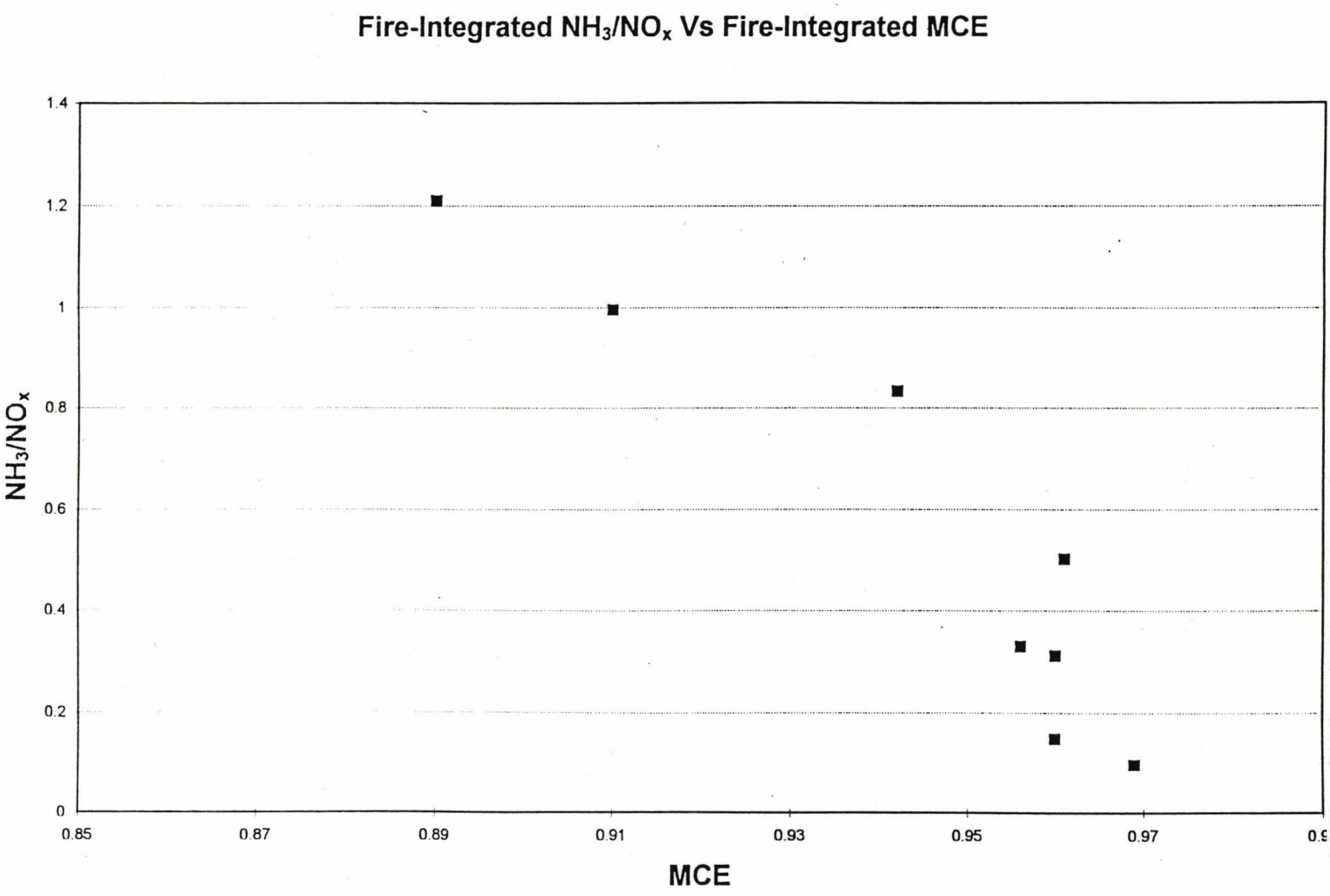

Figure 15. Spectrum in the C-H stretch region presumably due to terpenes.

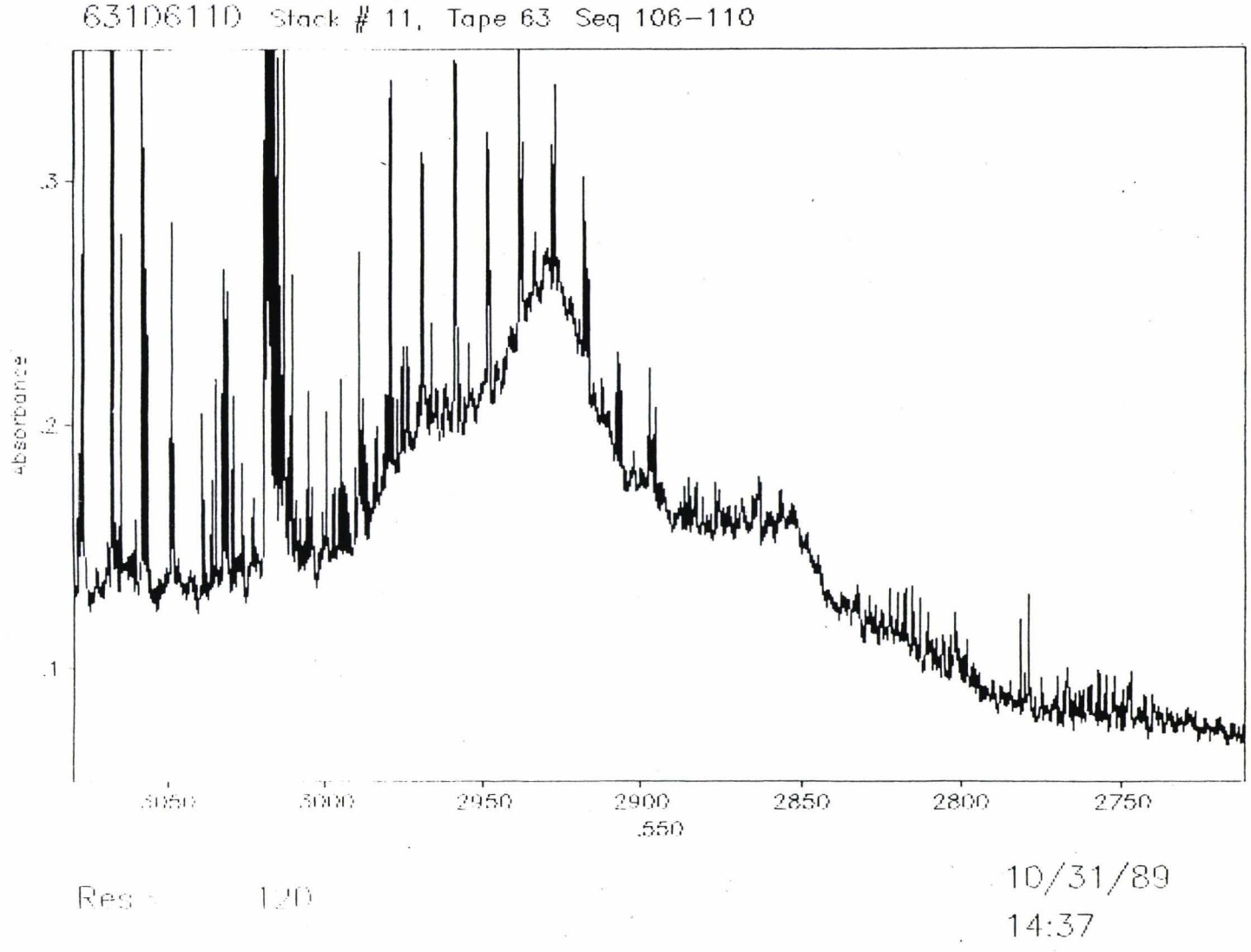

Figure 16. Comparison of lab and field measurements.

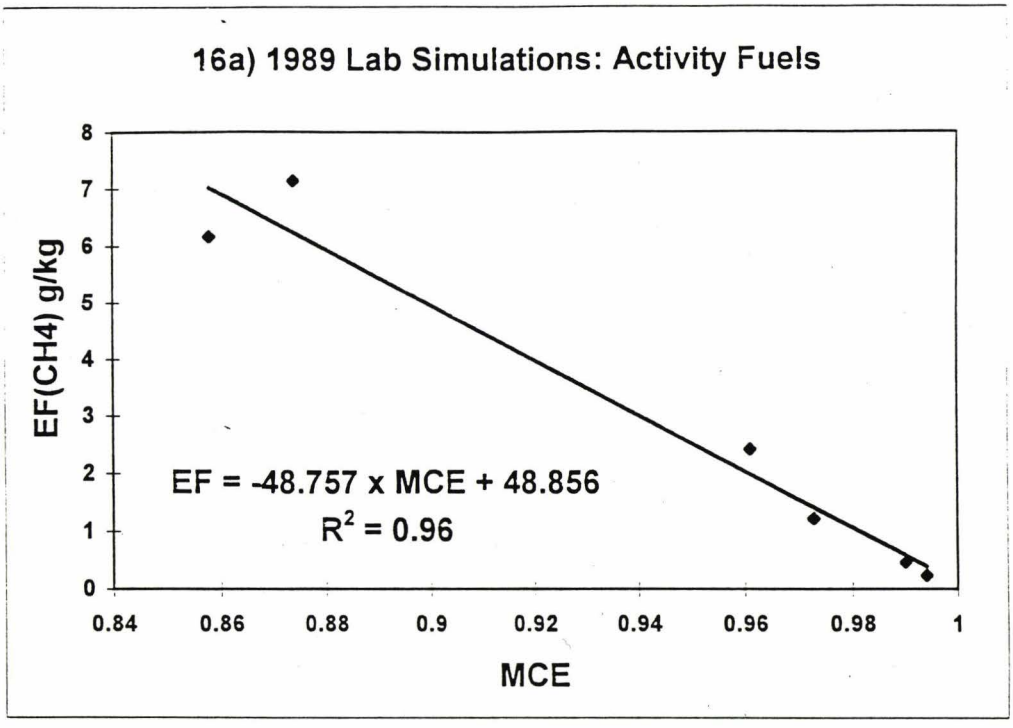

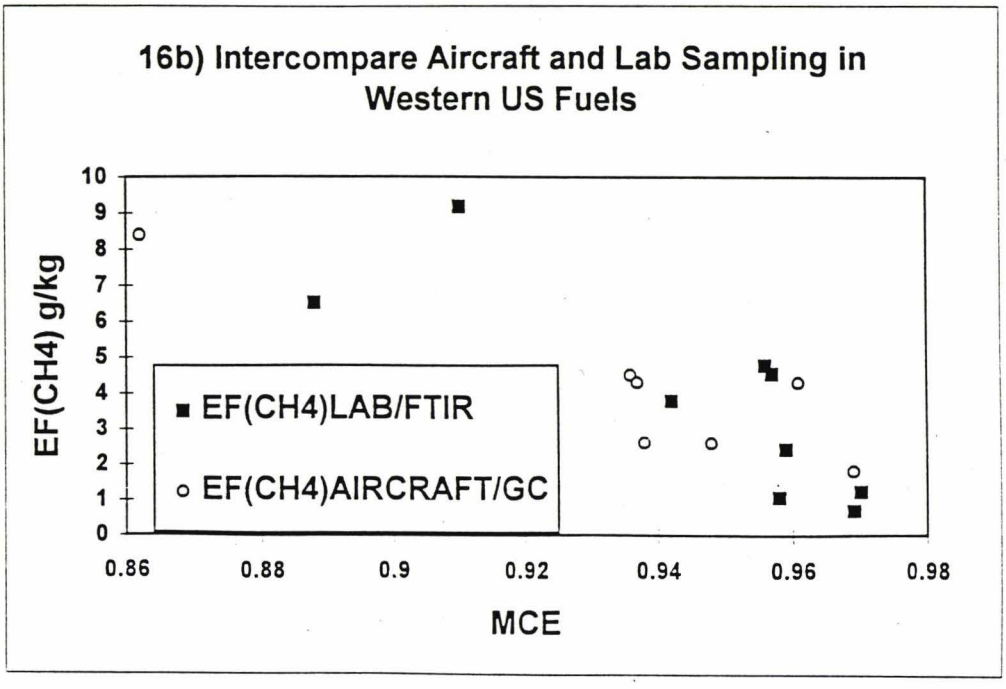

TABLE 1

Fire Type	No.	Fuel Bed Composition	(mass%)	Comments
PINE NEEDLE1	3	Pine Needles	100%	Pinus ponderosa
PINE NEEDLE 2	5	Pine Needles	100%	Pinus ponderosa
SAGEBRUSH 1	8	Sagebrush	100%	Artemisia tridentata
SAGEBRUSH 2	12	Sagebrush	100%	Artemisia tridentata
BROADCAST	6	Duff	44%	
		Pine Needles	14%	Pinus ponderosa
		Twigs	18%	
		Wood	24%	
SLASH	7	Twigs and Needles	10%	Pinus ponderosa
		Small Branches	90%	
GROUND 1	9	Pine Needles	27%	Pinus ponderosa
		Pine Needles and Duff	73%	
GROUND 2	10	Duff	39%	
		Twigs and Needles	35%	Pinus contorta
		Pine Needles	26%	Pinus ponderosa
CROWN	11	Twigs and Needles	26%	Pinus contorta and
		Wood < 30mm	19%	Pseudotsuga menziesii
		Pine Needles	19%	
		Green Needles and Twigs	36%	Pinus ponderosa

TABLE 2

Molecule	Spectral Regions
H_2O	3020.0 - 3007.1
CO_2 and CO	2242.7 - 2210.9
CO_2	737.01 - 727.92
CO_2	2252.8 - 2239.9
CO	2055.8 - 2049.5
^{13}CO	2062.2 - 2061.7
CO	2179.7, 2176.2, 2172.8
CH_4	3020.0 - 3007.1
CH_4	2997.3 - 2976.1
CH_4	1306.7 - 1299.0
NO	1913.4 - 1911.0
NO	1907.1 - 1905.1
NO	1903.8 - 1902.3
NO	1901.1 - 1899.9
NO	1906.9 - 1899.5
NO_2	1599.5 - 1597.7
NH_3	1047.3 - 1045.1
NH_3	968.73 - 961.67
NH_3	933.458 - 926.521
CH_2O	2782.7 - 2777.3

Molecule	Spectral Regions
C_2H_6	2987.0 - 2985.7
C_2H_6	2984.7 - 2982.7
C_2H_2	3271.2 - 3254.7
C_2H_2	743.4 - 728.8
SO_2	1348.5 - 1347.7
HCOOH	1107.4 - 1102.7
HCN	3272.1 - 3270.7
OCS	2071.4 - 2069.9

Molecules Analyzed Manually

Molecule	Frequency
CH_3OH	1033.3
C_2H_4	949.4
CH_3COOH	1176
Volatiles	2930

TABLE 3 (Preliminary, Full Report Version)

Fire # 3
Fuel 15.126 kg Pine Needles

C	H	N	% Fuel Moisture
50.7	6.75	0.31	

Fire Behavior Measurements

	T	F	S
Combustion Efficiency	0.956	0.99	0.835
Combustion Factor		77.7	22.3

Emission Factors (g/kg dry fuel)

PM2.5	total				
CO2	total	1754	HAC	total	2.37
	flaming	1836		flaming	0.244
	smldrng	1467		smldrng	10.23
	%S	22.3		%S	21.3
CO	total	50.79			
	flaming	11.3	NO	total	2.5
	smldrng	183.9		flaming	3.17
	%S	22.9		smldrng	0.252
CH4	total	4.78		%S	23.1
	flaming	0.742	NO2	total	0.253
	smldrng	20.1		flaming	0.525
	%S	20.9		smldrng	-0.633
C2H6	total	1.22		%S	23.4
	flaming	0.175	NH3	total	0.5
	smldrng	5.37		flaming	0.0151
	%S	20.1		smldrng	2.17
C2H4	total	0.712		%S	22.4
	flaming	0.157			
	smldrng	3.03	SO2	total	0.991
	%S	19.3		flaming	1.73
C2H2	total	0.378		smldrng	-0.29
	flaming	0.25		%S	36.5
	smldrng	0.769			
	%S	24.6			
CH2O	total	0.54			
	flaming	0.376	Lobert et al %S		24.2
	smldrng	1.09			
	%S	23			
CH3OH	total	0.539			
	flaming	0.0343			
	smldrng	2.14			
	%S	24			

TABLE 3 (Preliminary, Full Report Version)

Fire # 5
Fuel 15 kg Pine Needles

C	H	N	% Fuel Moisture
50.7	6.75	0.31	

Fire Behavior Measurements

	T	F	S
Combustion Efficiency	0.96	0.99	0.823
Combustion Factor		81.7	18.3

Emission Factors (g/kg dry fuel)

PM2.5	total	30.4			
CO2	total	1773	HAC	total	2.5
	flaming	1838		flaming	0.0841
	smldrng	1480		smldrng	7.45
	%S	18.3		%S	32.8
CO	total	46.89			
	flaming	11.89	NO	total	2.38
	smldrng	201.9		flaming	2.69
	%S	18.4		smldrng	0.293
CH4	total	4.55		%S	12.9
	flaming	0.741	NO2	total	0.567
	smldrng	22.5		flaming	0.614
	%S	17.5		smldrng	0.0397
C2H6	total	1.31		%S	8.1
	flaming	0.221	NH3	total	0.487
	smldrng	6.94		flaming	0.0694
	%S	16.2		smldrng	2.37
C2H4	total	0.743		%S	18.2
	flaming	0.244			
	smldrng	3.18	SO2	total	1.73
	%S	16.9		flaming	2.56
C2H2	total	0.418		smldrng	-0.26
	flaming	0.175		%S	-0.32
	smldrng	1.53			
	%S	17.9			
CH2O	total	0.296			
	flaming	0.147	Lobert et al %S		24.5
	smldrng	1.46			
	%S	11.3			
CH3OH	total	0.656			
	flaming	0.0698			
	smldrng	1.07			
	%S	58.6			

TABLE 3 (Preliminary, Full Report Version)

Fire # 6
Fuel Broadcast

C	H	N	% Fuel Moisture
45			

Fire Behavior Measurements

	T	F	S
Combustion Efficiency	0.961	0.99	0.874
Combustion Factor		74.9	25.1

Emission Factors (g/kg dry fuel)

PM2.5	total	5.93			
CO2	total	1579	HAC	total	0.464
	flaming	1630		flaming	0.0123
	smldrng	1425		smldrng	1.41
	%S	25.3		%S	32.2
CO	total	41.24			
	flaming	11.62	NO	total	1.51
	smldrng	130.6		flaming	1.97
	%S	24.9		smldrng	0.505
CH4	total	2.43		%S	31.3
	flaming	0.464	NO2	total	0.8
	smldrng	7.14		flaming	0.872
	%S	29.5		smldrng	0.087
C2H6	total	0.581		%S	9.1
	flaming	0.168	NH3		0.577
	smldrng	1.84			0.102
	%S	30.1			1.81
C2H4	total	0.621			27.7
	flaming	0.286			
	smldrng	1.37	SO2	total	0.43
	%S	31		flaming	0.439
C2H2	total	0.3		smldrng	0.0608
	flaming	0.229		%S	2.2
	smldrng	0.405			
	%S	40.6			
CH2O	total	0.676			
	flaming	0.431	Lobert et al %S		45.8
	smldrng	0.881			
	%S	54.5			
CH3OH	total	0.299			
	flaming	0.103			
	smldrng	0.969			
	%S	22.7			

TABLE 3 (Preliminary, Full Report Version)

Fire # 7
Fuel Slash

C	H	N	% Fuel Moisture
45			

Fire Behavior Measurements

	T	F	S
Combustion Efficiency	0.973	0.994	0.858
Combustion Factor		84.4	15.6

Emission Factors (g/kg dry fuel)

PM2.5	total	1.48			
CO2	total	1602	HAC	total	d
	flaming	1640		flaming	
	smldrng	1402		smldrng	
	%S	15.6		%S	
CO	total	28.17			
	flaming	6.33	NO	total	0.881
	smldrng	147.3		flaming	1.15
	%S	15.5		smldrng	0.0641
CH4	total	1.23		%S	24.6
	flaming	0.239	NO2	total	0.602
	smldrng	6.16		flaming	0.7
	%S	16.8		smldrng	0.0465
C2H6	total	0.234		%S	15
	flaming	0.026	NH3	total	d
	smldrng	1.51		flaming	
	%S	14		smldrng	
C2H4	total	d		%S	
	flaming				
	smldrng		SO2	total	1.18
	%S			flaming	1.2
C2H2	total	0.223		smldrng	3.18
	flaming	0.176		%S	-1
	smldrng	0.485			
	%S	15.5			
CH2O	total	0.351			
	flaming	0.13	Lobert et al %S		23.6
	smldrng	1.32			
	%S	18.7			
CH3OH	total	d	"d" indicates damage to spectral region		
	flaming				
	smldrng				
	%S				

TABLE 3 (Preliminary, Full Report Version)

Fire # 8
Fuel Sagebrush

C	H	N	% Fuel Moisture
45			

Fire Behavior Measurements

	T	F	S
Combustion Efficiency	0.960	0.978	0.879
Combustion Factor		81.9	18.1

Emission Factors (g/kg dry fuel)

PM2.5	total	2.32			
CO2	total	1581	HAC	total	bld
	flaming	1612		flaming	
	smldrng	1443		smldrng	
	%S	18.1		%S	
CO	total	41.99			
	flaming	23.16	NO	total	2.78
	smldrng	126.7		flaming	2.84
	%S	18.2		smldrng	2.34
CH4	total	1.07		%S	11.4
	flaming	0.742	NO2	total	0.764
	smldrng	2.92		flaming	0.989
	%S	15.1		smldrng	0.0778
C2H6	total	0.141		%S	24.7
	flaming	0.0831	NH3	total	0.276
	smldrng	0.524		flaming	0.124
	%S	13.1		smldrng	0.959
C2H4	total	0.485		%S	18.2
	flaming	0.445			
	smldrng	0.752	SO2	total	1.19
	%S	12.9		flaming	1.67
C2H2	total	0.389		smldrng	-0.42
	flaming	0.433		%S	22.8
	smldrng	0.329			
	%S	42.00			
CH2O	total	0.467			
	flaming	0.440	Lobert et al %S		70
	smldrng	0.743			
	%S	8.9			
CH3OH	total	bld			
	flaming				
	smldrng				
	%S				

TABLE 3 (Preliminary, Full Report Version)

Fire # **9**
Fuel Ground 1

C	H	N	% Fuel Moisture
45			

Fire Behavior Measurements

	T
Combustion Efficiency	0.8888
Combustion Factor	0.3559

Emission Factors (g/kg dry fuel)

CO2	total	1451	HAC	total	8.02
CO	total	115.4			
CH4	total	6.52	NO	total	1.25
C2H6	total	1.98	NO2	total	1.46
C2H4	total	2.08	NH3	total	1.51
C2H2	total	0.899			
CH2O	total	2.84	SO2	total	2.67
CH3OH	total	3.48			

Fire # **10**
Fuel Ground 2

C	H	N	% Fuel Moisture	31
45				

Fire Behavior Measurements

	T
Combustion Efficiency	0.942
Combustion Factor	0.625

Emission Factors (g/kg dry fuel)

CO2	total	1545	HAC	total	2.95
CO	total	60.07			
CH4	total	3.79	NO	total	1.7
C2H6	total	1.08	NO2	total	1.45
C2H4	total	1.16	NH3	total	1.25
C2H2	total	0.556			
CH2O	total	1.8	SO2	total	1.68
CH3OH	total	0.813			

TABLE 3 (Preliminary, Full Report Version)

Fire # **11**
Fuel "Crown"

C 45 H N % Fuel Moisture 61

Fire Behavior Measurements

	T	G
Combustion Efficiency	0.91	0.907
Combustion Factor		

Emission Factors (g/kg dry fuel)

CO2	total	1478	HAC	total	7.07
	green	1471		green	8.55
CO	total	93.1	HCOOH	total	1.12
	green	95.2		green	1.21
CH4	total	9.18	NO	total	1.58
	green	10.4		green	1.57
C2H6	total	2.04	NO2	total	0.674
	green	2.39		green	0.68
C2H4	total	3.24	NH3	total	1.14
	green	3.53		green	1.2
C2H2	total	1.32	SO2	total	1.42
	green	1.24		green	0.896
CH2O	total	2.82	HCN	total	0.392
	green	3.08		green	0.554
CH3OH	total	3.26			
	green	3.92			

TABLE 3 (Preliminary, Full Report Version)

Fire # **12**
Fuel Sagebrush

C	H	N	% Fuel Moisture
45			

Fire Behavior Measurements

	T	F	S
Combustion Efficiency	0.969	0.982	0.862
Combustion Factor		89.1	10.9

Emission Factors (g/kg dry fuel)

CO2	total	1596	HAC	total	bld
	flaming	1618		flaming	
	smldrng	1419		smldrng	
	%S	10.9		%S	
CO	total	32.86			
	flaming	19.37	NO	total	2.95
	smldrng	144.1		flaming	3.17
	%S	10.8		smldrng	1.46
CH4	total	0.702		%S	13
	flaming	0.533	NO2	total	0.811
	smldrng	1.51		flaming	0.921
	%S	17.3		smldrng	0.141
C2H6	total	0.0914		%S	14.1
	flaming	0.0842	NH3	total	0.192
	smldrng	0.191		flaming	0.121
	%S	6.8		smldrng	0.75
C2H4	total	0.306		%S	11.4
	flaming	0.306			
	smldrng	-	SO2	total	1.69
	%S	-		flaming	1.99
C2H2	total	0.33		smldrng	
	flaming	0.31		%S	
	smldrng	0.67			
	%S	5.6			
CH2O	total	0.418			
	flaming	0.491	Lobert et al %S		20
	smldrng	0.139			
	%S	21			
CH3OH	total	bld			
	flaming				
	smldrng				
	%S				

TABLE 4

Fuel		Needles	Needles				Duff	Litter	Duff and Litter	
Method		(GC/MS)	(FTIR)				(GC/MS)		(FTIR)	
Fire		AVG	3		5		AVG	AVG	9	10
Process		T	F	S	F	S	T	T	T	T
MCE		0.76	0.99	0.835	0.99	0.823	0.83	0.77	0.89	0.94
Emission	units									
CH_3CO_2H	g/kg	**7.6**	**0.24**	**10.23**	**0.08**	**7.45**	**0.85**	**2.4**	**8.02**	**2.95**
CH_3OH	g/kg	**4.9**	**0.034**	**2.14**	**0.07**	**1.07**	**0.69**	**2**	**3.48**	**0.81**

TABLE 5

	FIELD DATA		LAB DATA				coniferous
Fuel	sage, grass, and litter		sage only				duff, litter
Fire No.	1	2	8		12		9
Fire Process	T	T	T	S	T	S	T
<u>Trace Gas</u>							
CO	181	141	83	117	90	165	143
CH_4	12.5	12.7	3.2	4.2	2	2.6	14.8
CH_2O	2.4	2.3	0.7	0.8	0.5	bld	3.1
NO	0.8	1.1	2.4	2.2	2.1	1.5	1.4
NO_2	0.4	0.6	0.5	bld	0.5	bld	0.9
NH_3	8.4	8.3	1.3	2	0.9	1.4	3.7

Field fires colder temps higher RH and lower CE

Appendix 3.1

Sources of Uncertainty in Global Emissions Estimates.

An analysis of the uncertainties in source strength estimates should start with a consideration of how these source strengths are often calculated.

(1) Source Strength = (Biomass Exposed to Fire) X (Fraction of Biomass Burned) X (Amount of Emission per unit Amount of Fuel)

In practice there are 5 major types of uncertainties that arise in global source strength estimates and they are briefly summarized: roughly in the order of potential importance.

1) For gases other than CO_2, there can be a very large, real variation in the amount of emitted gas per unit mass of dry fuel. This problem is addressed directly in this work.

2) Other than for large areas of homogeneous Savannah, there is a large uncertainty in the attempt to determine the type of fires that occur. The type of vegetation exposed to fire and the combustion characteristics are often poorly known. Vast areas of Imperata Cylindrica now exist as "fire subclimax" enclaves within areas where tropical forests traditionally flourished. For example, 18 million hectares of *Imperata cylindrical* (blady grass or "alang-alang") are reported to exist in parts of Indonesia where tropical forest was previously established. [*Jacobs*, 1981] If only 30% of this grassland was burned this year, that would account for all 5 million hectares that are estimated to have burned in Indonesia in 1994.) Another example, the last vegetation map for Malaysia was completed in 1958 and since then perhaps one-third of Malaysia's forests have disappeared if the global average of 1% deforestation is assumed. [*Whitmore*, 1985] Without up to date information on the vegetative cover, a fire in these areas might be assigned to tropical forest on the basis of antiquated and low resolution vegetation maps with a resulting significant overestimate of biomass burned. The combustion characteristics of a fire are, in addition, often effected by the fuel moisture which changes seasonally. The possibility of using tracers for different fuel types is briefly discussed in this work. It should be possible to study how fuel moisture effects combustion effectively in the laboratory.

3) On the global scale it is difficult to determine the area burned. The prospects for reducing the uncertainty in the area of biomass burned also depend on properly

quantifying the amount of the various types of fires. Ground-based surveys are time consuming and may be biased to the more accessible areas where more burning may occur. In principle, satellites could provide information without "access bias", but there are problems. Thermal detectors, while excellent for detecting new deforestation frontiers, cannot distinguish between a large cool fire and a small hot fire. They may saturate when a small portion of a pixel is burning. Since most fires are small, using smaller pixel sizes may increase the number of fires that are large enough to saturate a pixel and actually increase the measurement error. There is always a chance that fires will occur when the satellite is out of range. The low resolution used for global coverage (1 km) is insufficient to determine the ecosystem which is actually burning and the high resolution (30 or 70 m) which can provide ecosystem information is not practical for global coverage. Careful high resolution subsampling with Landsat photographs should receive more attention than it has.

4) A single correct "value" for the above ground biomass of tropical ecosystem does not exist, but is often assumed. The mean of the figures for tropical forest in Table I is 364 tonnes/hectare with a standard deviation of 188 tonnes/hectare. The mean reported here is considerably higher than the widely used values of [*Brown and Lugo,* 1984] Their estimates are based on extensive forest volume surveys, but it has been suggested that their values may need to be increased by 65% because they do not consider all the biomass. [*Fearnside*, 1993] It has also been suggested that *all* reported measurements suffer from a bias towards measuring sites with more biomass.

5) The variation in combustion factors, which are also presented in Table I, is considerably smaller; but there is not a lot of data and the effects of reburning, a common practice, are not always included. There are also, evidently, no measured or estimated combustion factors for tropical wildfires. At least two other major uncertainties are associated with combustion factors. It has been argued [*Ewel et al.*, 1981] that the practice of cut, dry and burn is now less common than the situation where a portion of the biomass is harvested for polewood, timbers, primary fuel, or charcoal production before burning of the site. These authors found that this type of harvest accounted for 34% of the biomass on their site. As accessibility is improving in tropical areas this practice will continue to grow. Also, Latin America, where most biomass burning now occurs and where timber production is currently low, is projected to become the world leader in tropical hardwood production in the near future. Another source of uncertainty is the relative contribution of

decomposition of cut slash during the drying period as opposed to consumption during the burn. *Ewel et al.*, [1981] found that during an 11 week drying period all the leaves decomposed. This corresponds to a mass decomposition rate of 9%/week for this "exposed site". [*Uhl and Jordan*, 1984] measured a leaf decomposition rate of 5%/week within intact forest. Information on decompositon before burning is rare, but necessary in order to take full advantage of the data on the varying chemistry and combustion factors of the different plant parts.

Crutzen et al., [1991] estimate the global amount of carbon exposed to fire to be between 2700 and 6800 Tg a-1 or 4750 Tg a-1 +- 43%.

As serious as the problems are in estimating biomass burned, the uncertainty in emission factors is often comparable. For many species other than CO or CO_2, including particulate, the reported emission ratio for a species to CO_2 or CO varies widely from measurement to measurement. These measurements are too extensive to tabulate here, but the variation in published measurements for NH_3 can serve as an example. [*Hegg et al.*, 1988] report values for NH_3/CO_2 as low as 0.14 mmoles/mole, while [*Griffith et al.*, 1991] report a value of 8 mmoles/mole: a factor of 57 difference. In this study we report emission ratios for formic acid as much as 338 times greater than previously reported [*Talbot et al.*, 1988]. Thus emission ratios can evidently vary as much as any term in global source strength estimates. This is primarily due to the large, and often poorly characterized, variety of fuels and combustion characteristics that occurs in fires globally and also the difficulty of making these types of measurements. In summary, it is apparent that reduction of the uncertainty in source strengths *and* the design of effective mitigation strategies both clearly depend on accurate, detailed knowledge of how fuel parameters and combustion characteristics effect emissions.

Table I

Some Above-Ground Biomass Density and Combustion Factor Measurements in Tropical Ecosystems.

Ecosystem Type (age)	Dry Biomass (tons/ha)	Combustion Factor (%)	Reference
Tropical Grassland	7.1	100	Ward et al (1992)
Tropical Dry (fuel load)	10.0	84	Ward et al (1992)
Imperata Grassland	11.5		Soerjani (1970)
Secondary (2)	12.8		Uhl et al (1982)
Secondary (2)	13.0		Ewel (1971)
Secondary (2)	14.2		Snedaker (1970)
Secondary (2)	15.8		Gamble et al (1969)
Secondary (4)	27.1		Snedaker (1970)
Secondary (5)	36.7		Snedaker (1970)
Secondary (4)	38.0		Ewel (1971)
Secondary (6)	42.9		Ewel (1971)
Secondary (6)	44.7		Snedaker (1970)
Secondary (6)	46.1		Nye et al (1960)
Secondary (4)	48.4		Gamble et al (1969)
Secondary*	50.2	80	Ewel (1981)
Secondary (7)	52.7		Williams-Linera (1983)
Secondary (5)	76.7		Bartholemew et al (1953)

Table I (cont.)

Some Above-Ground Biomass Density and Combustion Factor Measurements in Tropical Ecosystems.

Ecosystem Type (age)	Dry Biomass (tons/ha)	Combustion Factor (%)	Reference
Pennisetum Purpureum (grass)	84.0		in Skerman et al (1990)
Secondary (15)	121	42.87	Ward et al (1992)
Open Upland	143		Revilla Cardenas (1987)
Tropical Moist	181		Fearnside (1985)
High Forest (type b)	182		Revilla Cardenas (1982)
High Dense Forest (type b)	183		Revilla Cardenas (1982)
Medium High Forest (type b)	188		Revilla Cardenas (1982)
Dense Riparian	206		Revilla Cardenas (1987)
Dense Upland	219		Revilla Cardenas (1988)
Montane	223		Tanner (1977)
Montane	228		Jordan (1971)
Tropical Moist	233		Greenland and Kowal (1960)
Shallow humus podzol	246		Brunig (1977)
Alluvial	250		Proctor, Anderson (1983)
Oxisol	264		Jordan (1985)
Tropical Moist	264		Nepstad (1989)
Dense Lowland	265	29.25	Fearnside

Table I (cont.)

Some Above-Ground Biomass Density and Combustion Factor Measurements in Tropical Ecosystems.

Ecosystem Type (age)	Dry Biomass (tons/ha)	Combustion Factor (%)	Reference
Amazon Caatinga	268		Herrera (1979)
Tropical Moist (fuel load)	292	52.56	Ward et al (1992)
Montane	310		Edwards (1977)
Tropical Moist	316		Golley et al (1975)
Dense Riparian	320		Revilla Cardenas (1988)
Tropical Moist	326		Golley et al (1975)
Submontane Open	328		Martinelli (1988)
Tropical Moist	335		Sanford
Medium High Forest (type a)	340		Revilla Cardenas (1982)
Peat Forest	350		Brunig (1977)
Open Upland	373		Revilla Cardenas (1986)
Limestone	380		Proctor, Anderson (1983)
Lowland Rain	382		Werner (1982)
Dense Lowland	390		Klinge et al (1973, 75)
Dense Upland	403		Revilla Cardenas (1986)
Tropical Moist	406		Klinge (1976)
Submontane Dense	438		Russell (1983)

Table I (cont.)

Some Above-Ground Biomass Density and Combustion Factor Measurements in Tropical Ecosystems.

Ecosystem Type (age)	Dry Biomass (tons/ha)	Combustion Factor (%)	Reference
Medium humus podzol	452		Brunig (1977)
Heath	470		Proctor, Anderson (1983)
Dipterocarp	475		Kato et al (1978)
Evergreen	513		Lemee undated
High Forest (type a)	607		Revilla Cardenas (1982)
Dipterocarp	650		Proctor, Anderson (1983)
High Dense Forest (type a)	666		Revilla Cardenas (1982)
Mature Dipterocarp	709		Brunig (1977)
Mature Dipterocarp	1160		Brunig (1977)

Note: Shifting cultivators normally burn secondary forest 8 - 15 years of age: the lack of data for this age class is conspicuous. The data for combustion factors is sparse, with none for wild fires. The reported numbers reflect both direct measurements and estimates based on various allometric equations. The total variation includes a contribution from measurement error and from natural variation. Data for grasslands is included for comparison purposes. The study of Ewel et al., [1981] was in an 8 - 9 year old secondary forest with some later interplanting of timber species and some remnants of a 70 year old secondary forest. The combustion factor is determined after 30% of the wood was harvested. The drying period was 11 weeks which is apparently longer than that of other studies.

Selected References For Appendix 1

not including previously cited references.

Brown, S., and A. E. Lugo. 1984. Biomass of tropical forests: a new estimate based on forest volumes. *Science* 223, 1290 - 1293.

Ewel, J., C. Berish, B. Brown, N. Price, and J. Raich. 1981. Slash and burn impacts on a Costa Rican wet forest site. *Ecology* 62, 816 - 829.

Fearnside, P. M. , N. Leal, and F. M. Fernandes. 1993. Rainforest burning and the global carbon budget: biomass, combustion efficiency, and charcoal formation in the Brazilian Amazon. *J. Geophys. Res.* 98, 16733 - 16743.

Hegg et al., 1988 cited in *Griffith et al.*, 1991 part 3.

Jacobs, M. 1981. *The Tropical Rain Forest: A First Encounter*. Berlin: Springer.

Uhl, C. and C. F. Jordan. 1984. Succession and nutrient dynamics following forest cutting and burning in Amazonia. Ecology 65, 1476 - 1490

Whitmore, T. C. 1985. *Tropical rain forests of the Far East: Second Edition*. Oxford: Clarendon.

Appendix 3.2

Forest Management Implications.

Phosphorus Loss from Tropical Soils.

Phosphorus is most often the limiting nutrient in the tropics. [*Jordan*, 1985]. Fire is important in redistributing large quantities of phosphorus both through volatilization and wind removal of P-containing ash. [*Raison et al.*, 1984] determined that up to 60% of the total fuel phosphorus was lost from Australian sites during burning with as much as 50% of this loss being due to volatilization during hot fires and the rest due to convective transport from the site in the fine gray/white ash which contained P levels 50 times greater than the fuel. These authors note the great significance of this loss as natural rates of phosphorus replacement are very low as phosphorus is very insoluble. In tropical ecosystems a high percentage of the available P is stored in leaves with a P:N ratio of about 0.05. Higher temperatures are required to volatilize inorganic P (~ 774 oK) than N (300 oK). However, P bound in organic compounds is expected to volatilize at lower temperatures. Furthermore, the temperature of volitalization for inorganic K is the same as that of P and the biomass burning haze layer over the Amazon was measured to have almost 14 times the level of K present in the free troposphere [*Andrea et al.*, 1988]. These authors give a global source strength for K from biomass burning as 2.4 Tg yr-1. This may be also take as a rough estimate of the P source strength although this number may have more agricultural than atmospheric significance). To our knowledge there have not yet been any actual measurements of gas phase P compounds in biomass burning plumes. If gas phase P flaming compounds peaked near 5% of the peak NO levels that would imply about 1.5 ppm as an upper limit for a single compound. PH_3 is the only P compound on HITRAN and several spectra at high temperature were searched for this compound at 991.88 cm-1. A small feature corresponding to about 1.5 ppm was seen in one spectra, but the identification of this compound, which is not oxidized, is far from conclusive. Our new system should have lower detection limits and we are assembling a library of spectra for phosphorus compounds. We plan to search for volatilized P in tropical fuels.

Biomass burning actually causes a short-lived increase in P available to crop plants. This is because the ash raises the pH and frees P that has been immobilized in the clay. The immobilized P normally represents a large fraction of the total ecosystem P, but to burn

frequently to try to maintain high levels of available P degrades soil N and C levels.) In a related note, FTIR has been identified as a method of choice to analyze soil for phosphorus compounds. Future field work with our instrument may be able to develop knowledge about the effects of fire on these compounds. This may be valuable in determining the optimum return cycle for fire for sustained productivity in various important tropical ecosystems.

Fire-fighter Exposure to Toxic Compounds in Smoke.

Our plot of formaldehyde vs. MCE, shows a negative linear correlation and thus is a useful step towards a source strength estimate. (See preceding paper draft.) If we crudely assume that formaldehyde is a smoldering stage compound, then our measured ratio of formaldehyde to CO can be combined with the CO exposure levels measured for fire-fighters in the Pacific Northwest by Reinhardt et al. The results indicate that these personnel, and probably the inhabitants of the rural tropics, are frequently exposed to levels above the 8 hour average dose recommended by OSHA and that in fact formaldehyde exposure is more serious than CO exposure especially when carcinogenicity is taken into account. This can be demonstrated informally in several ways. The maximum observed CO concentration of 587 ppm is a little over one-third of the level "immediately dangerous to life or health" (IDLH) of 1500 ppm. Formaldehyde peaked at 25 ppm or more than 80% of its IDLH. The recommended limit for an 8 hour day, known as the time weighted average (TWA), for CO and formaldehyde are 35 and 0.016 ppm respectively. The quantity TWA(CO)/TWA(HCHO) * ER(HCHO/CO) = 94. This indicates that the toxicity of HCHO in smoke may be about 100 times more serious than CO, before even considering the carcinogenic effects of HCHO.

An important observation, first made in this work, is that HCHO is in fact not a smoldering compound: i.e. it is not emitted in a constant ratio to CO (see Figure P3A3.2.1 below). The implication of this is that the worst case exposure scenario may be significantly higher than previously reported by Reinhardt et al.

Figure P3A3.2.1. Formaldehyde to CO ratio.

This figure illustrates that the ratio of HCHO/CO is not constant during a fire. Our worst case exposure scenario corresponds to highest observed value as indicated. The horizontal lines are the worst case exposure scenario and average exposure scenario of Reinhardt et al..

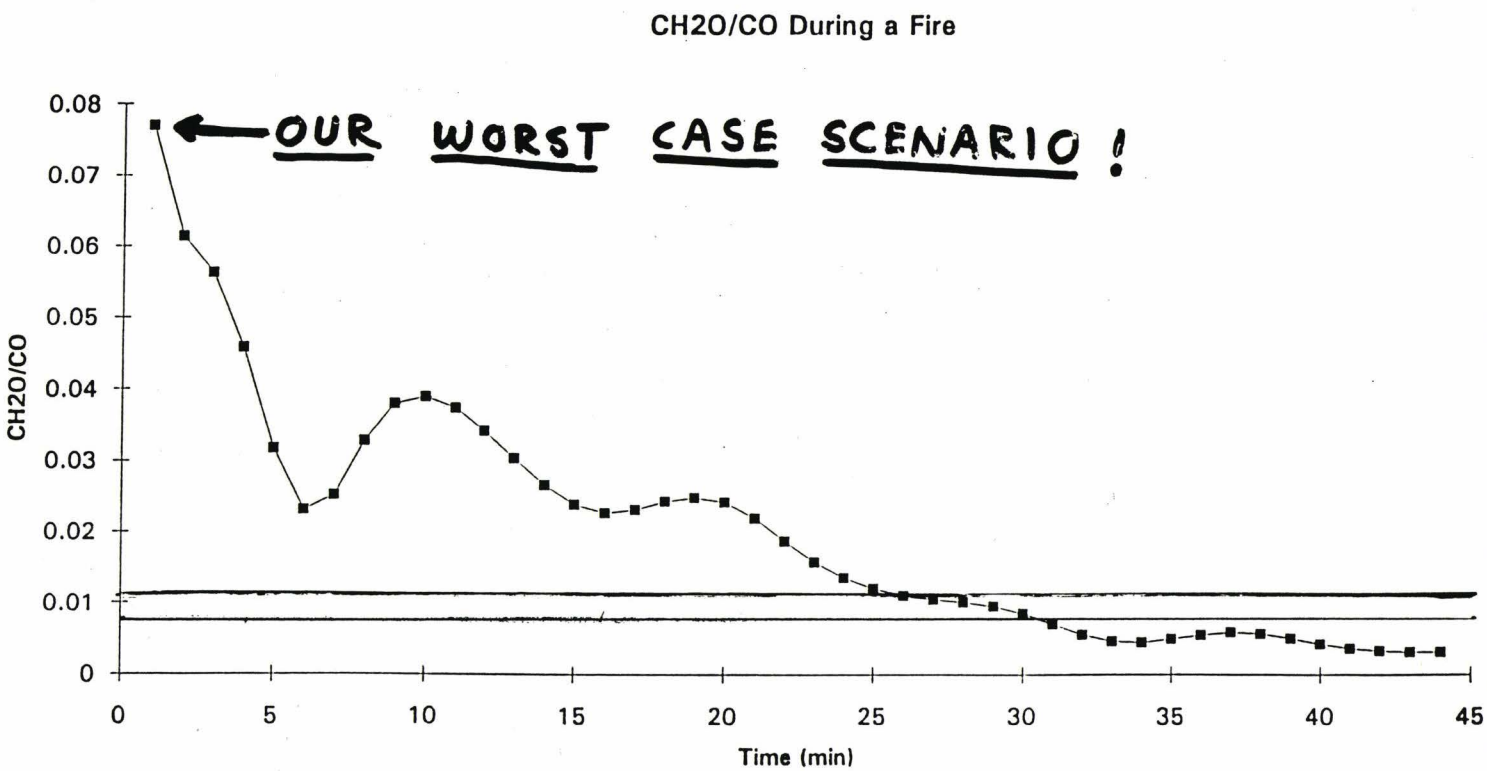

Management implications for local impacts.

The emissions of air toxics appear to be worse from live vegetation and this makes a contribution to the analysis of the trade-offs involved in the impacts of frequent low intensity burns in fire adapted ecosystems as opposed to less frequent stand replacement fires. By supressing the natural role of fires in areas with seasonal climates, greater fuel loading and fire danger results with the probable, eventual result being more biomass burned and under conditions where the emissions are more deleterious. The effects of unnatural stand-replacement fires are likely to be more serious on soils as well.

In ecosystems where fire is naturally infrequent we can also add to an evaluation of the true costs. The negative effects of fires may include degradation of soil organic matter; increased erosion and damage to public water supplies; reduction of precipitation, and photosynthetic radiation , and thus crop yields; species extinction, loss of timber, and finally serious air pollution as this work helps to quantify. Since management of evergreen forests for timber production usually leads to increased flammability of the forest these factors should be included in the true cost of logging tropical evergreen forests as well as the replacement cost and "scarcity" value of the timber and the loss of an enormous variety of "minor forest products" whose net present value may exceed that of the timber. [*Panayotou*, 1992]

Implications from the global perspective.

Tropical countries face a management dilemma with respect to biomass burning. Shifting cultivation has long been known to be the most labor and fuel efficient form of sustainable tropical agriculture under conditions of low population density. [*Steinhart and Steinhart* 1971, *Seavoy* 1976]. Logging provides a crucial source of revenue for strapped governments, but selective logging, liberation thinning, and nearly all other tropical silviculture techniques greatly increase the flammability of the forest. The transition from forest to ranching, tree plantations, some agroforestry systems, or continuous cultivation increases flammability and may have questionable sustainability. The rapid increase and coexistence of these various land conversion practices has created a literally explosive situation. These countries are in dire need of realistic solutions that will enable them to feed their population, produce revenues and exports, and maintain the environmental

services of their forested lands. The design of these solutions will draw on knowledge of how biomass burning effects local ecosystems and *quantifying the negative global impacts.*

This data makes a contribution to evaluating the environmental services of forests on a global scale. Panayotou has argued that a high value can be assigned to tropical forests based on their carbon storage (the contain about two-thirds as much C as the atmosphere) and the fact that reduction of carbon emissions in developed countries costs $28/ton. Many of the emissions quantified in this work may have negative values to society because of their role, not only as greenhouse gases, but also as air toxics, precursors to tropospheric ozone or acid rain, and other aspects of atmospheric chemistry. Thus this work may further a more detailed calculation of the total value of the environmental services of forests on a global scale. Ultimately this value may be a source of revenue for developing countries and rural area of developed countries to promote better forest management practices.

Another aspect of forest valuation is touched on here. The emissions from wildfires are explicitly addressed in this work for the first time. The emissions from "crown" fires in the boreal forest attain a significant vertical velocity in regions where the tropopause is low. Using an average needle density for western US coniferous forests of ~1 ton/hectare we can make a preliminary simple estimation of the emissions from a western crown fires.

Tropical forests often have about twice the leaf : wood ratio of temperate forests with leaf densities of 2.8 - 13.4 t ha-1 being reported. During droughts in the tropics wildfires may be a significant component of total biomass burning. The largest wildfire in recorded history occurred during the 1982-3 ENSO-induced drought in Kalimantan, The prevailing winds would presumably have directed these emissions toward the intertropical convergence zone and possibly into the stratosphere. From Southeast Asia to the western US, an abnormally large pulse of biomass burning emissions would then be expected due to droughts associated with ENSO events that cause an increase in wildfires every 3 - 4 years. These anomalous pulses may be especially large for compounds which are associated with burning green vegetation.

Smoke effects on plant growth.

In interpreting the significance of biomass burning data it is worth noting several facts about the potential effects of smoke on plant growth.

1) Many of the substances in smoke can cause severe reduction in plant growth at very low concentrations. Examples include SO_2, NO_2, and C_2H_4.

2) Reduction of photosynthetically active radiation (PAR) by the particles in smoke is a concern for developing countries food supply. (New Straits Times)

3) Preliminary work indicates that increased CO_2 causes changes in photosynthate allocation in plants which favors the production of more stemwood with relatively less production of fine fuels or food.

Some Future Research Needs.

The most important areas of future study are outlined and the use of the FTIR technique will play a major role in some of these projects.

1) More work needs to be done, with larger sample sizes (> 1 hectare), on biomass density by ecosystem and by stand age as this will effect the calculation of carbon storage, carbon loss, and carbon re-placement after the fire. The methods used should be completely described to facilitate intercomparison.

2) Better high resolution satellite estimates are needed of the area of biomass burned and in which ecosystems.

3) It may be possible to develop tracers for the biomass burning in various ecosystems as an independent method to check on what ecosystems are burning especially for aircraft based studies. It is known, for instance, that vinyl phenol is always emitted by burning grasses, but not by burning wood as its origin is from a type of lignin found only in grasses. It may be possible to find compounds unique to certain fuels which are stable or have known decomposition rates. This would enable a simple emission ratio measurement to be used in estimating source strengths of various fuels. This would be important in sorting out the contribution from repeated burning of degraded ecosystems as opposed to destruction of new primary forest.

4) More complete field studies are needed; especially in Southeast Asia which features some unique ecosystems and transport.

5) Better and more complete laboratory-FTIR measurement of emission factors should be carried out; especially for tropical fuels in a complete matrix, isolated one at a time. Some current fuel priorities are:

i) Burning of *Imperata* type grasses accounts for a large fraction of the global fire.

ii) Fuels from heath forests (known as *kerangas* in Southeast Asia or *caatinga* in the Rio Negro region) and their related everwet formation the peat swamp forest. These forests represent tropical ecosystems where potential fuel accumulates due to the presence of phenolic compounds in the litter which retards decomposition (and lends a brown color to river waters). These forests are then especially flammable during droughts. Furthermore the fuel chemistry of these forests, which are also quite extensive, is of considerable interest. Organic soils have been reported to contain up to 3.5% nitrogen and one expects very high levels of ammonia from fires smoldering in these ecosystems. Peat also contains about 50% lignin ($C_{10}H_{11}O_2$) which is known to contribute heavily to charcoal formation, may be a precursor for methanol and formaldehyde production, and contains 74% C by mass. Furthermore these are coastal ecosystems and thus likely to contain high levels of Cl and Br in the fuels and resulting emissions. Fires in these ecosystems can smolder for extremely long times and produce almost total consumption of biomass including the trees which tend to topple over and be added to the fuel. Supression of these fires has been noted to be especially difficult.

iii) Agricultural waste from tropical crops such as rice straw.

iv) Charcoal production kilns as fuel accounts for the bulk of harvested biomass and the fastest growing use of biomass.

v) Fuels representative of tropical secondary forests which are characterized by fast growing species with wood of low specific gravity such as *Cecropia* in the Amazon or *Macaranga* in Southeast Asia. Dead fuels also deserve more attention in this context. Secondary forests often have a high percentage of their total biomass as residual dead fuels from the former primary forest. For example, some

measurements of this in tropical forests of various ages include: 7.3% primary, 24% 8 - 9 years, and 31% 5 years. Dead wood is high in lignin with Evans et al reporting up to 65% and Rothermel reporting up to 77%.

Selected References For Appendix 3.2

Jordan, C. F. 1985. *Nutrient Cycling in Tropical Forest Ecosystems: Principles and Their Application in Management and Conservation*. Chichester: Wiley.

Panayotou, T. and P. S. Ashton. 1992. *Not By Timber Alone: Economics and Ecology For Sustaining Tropical Forests*. Washington D. C.: Island Press.

Steinhart, J. S. and C. E. Steinhart. 1971. Energy use in the US Food System. *Science* 184, 307.

Raison, R. J., P. K. Khanna, and P. V. Woods. 1985. Mechanisms of element transfer to the atmosphere during vegetation fires. *Can. J. For. Res.* 15, 132 - 140.

Appendix 3.3

Miscellaneous Experimental Notes.

H_2O

H_2O is the dominant species measured in smoke from biomass fires because it has the highest background levels, it is made in the combustion reaction, and natural fuels have bound or excess water adsorbed on and in them which is gassified and desorbed during fires. Perhaps surprisingly, the measurement of water concentrations is not at all straightforward. Strong water peaks in greatly separated parts of the spectra can lead to concentration predictions, at peak values, with an absolute variation as high as 1% compared to total levels of less than 4%. This is because the total water levels peak at the same time as temperatures. A typical smoke spectrum at peak water levels actually contains the sum of contributions from .7% water at room temperature absorbing over a 3 meter path and about 2.3% water at 400 oK also absorbing over a 3 meter path. Fortunately, we were able to identify a region of the water spectrum that is fairly temperature independent.

CH_3OH

This is the first measurement of methanol from large scale open fires. An earlier study of laboratory "smolder" fires (CE 75 - 80%) reported that the emissions of methanol and methane were very nearly equal. (McKenzie et al) An earlier study of the pyrolysis of biomass by TG-FTIR found that methanol was one of 5 gases that accounted for 60% of the mass loss in the fuel. (DeGroot et al 1988) (These authors estimate that 40% of the pyrolysis products condensed before entering the measurement area which makes quantitative intercomparison of their results difficult.) However, they estimate that about 4 g of methanol was produced for every kilogram of wood consumed which is not inconsistent with our values of. 0.8 to 3.5 in our quite different fires. (DeGroot et al do not report methane as a product.) As expected, in contrast to the studies of DeGroot et al and McKenzie et al, we find that the methanol emissions are about 20 % of the methane The MS study of pyrolysis of coal by Chu et al reported the production of methanol as did the study of Evans et al of the pyrolysis of lignin and the study of Hileman et al of the pyrolysis of Douglas Fir. In light of the findings in the five above mentioned studies we conclude that it is likely that the methanol produced in our fires is due to pyrolysis. This conclusion is also supported indirectly by the following argument. DeGroot et al

presented evidence that much of the methanol they detected had its origin in the pyrolysis of the lignin portion of the biomass fuel. No features due to methanol were seen in our smoke spectra from burning sagebrush which contains about half the lignin as do the other fuels we burned. Temporally the methanol behavior is complex, as might be expected for a pyrolysis compound. In fires 5 and 6 which have well-separated combustion processes the methanol peaks with the smoldering compounds. However after the peak its production drops off faster than the other smoldering compounds. In fires 9 - 11, which were essentially all smoldering, the methanol production ceases well before the other smoldering compounds. In these smolder fires the methanol release correlates quite well with the release of the fuel moisture. (See Figure X.) . While, the temporal behavior of the methanol emissions cannot be explained by a simple assumption that it is a smoldering compound this can be a useful assumption for the purposes of source strength estimates. The methanol emission factors are always higher for smoldering and the plot of the methanol emission factors Vs CE is reasonably linear given the number of points.

The GC-MS study of McKenzie et al reported concentrations of about 40 compounds including methanol, acetic acid and formic acid. Our study which measures the latter three as well as "non-condensable" gases under realistic conditions serves to link the work of McKenzie et al to realistic fires. However we do not detect some of their major emissions such as acetol.

HCHO

Formaldehyde emissions are important in odd Hydrogen atmospheric chemistry as it is a source of HO_2 and also HCOOH. The temporal behavior of the formaldehyde emissions is complex. On three fires that had very high S/N for formaldehyde the flaming and smoldering combustion peaks were clearly well separated temporally. In two of these fires, the fuel was sagebrush, and the HCHO peaked even before CO_2. In the third fire, the broadcast simulation, the HCHO peak was midway between the CO_2 and CO peaks.

The study of the pyrolysis of lignin at constant temperatures between 800 and 900 °C by Evans et al reports the formation of formaldehyde in an "early wave". Burton studied the pyrolysis of carbohydrates found in Tobacco in helium and air as a function of temperature from 200 - 900 °C. Burton detected peaks for HCHO formation from various biomass components at temperatures between 225 °C and 400 °C in air. Hileman et al studied pyrolysis of Douglas fir in inert and oxidative atmospheres between 340 and 550

°C. They found that for fresh samples, subjected to constant temperatures in an inert atmosphere, that formaldehyde production peaked at 550 °C. However for samples exposed to sequentially increasing temperature formaldehyde production was not observed above 400 °C. Douglas Fir samples sequentially heated in an oxidative atmosphere showed no formaldehyde production above 400 °C. Finally DeGroot et al observed no formaldehyde in the pyrolysis of cottonwood at 250 °C. From these observations we can tentatively conclude that formaldehyde is produced by the pyrolysis of specific components of biomass wood both at low and high temperatures. Finally, it is possible that one or both of these production mechanisms produced the formaldehyde observed in our fires.

HCOOH

Formic acid is a ubiquitous component of the atmosphere whose sources are not fully understood. *Goldman et al.*, report 0.5 ppb formic acid in the upper troposphere. *Talbot et al.*, report that formic acid levels in the lower troposphere over Virginia were ~ 1.9 ppb in the summer and 0.7 ppb in the winter (with the simultaneously measured amounts of acetic acid being 1.3 and 0.7 ppb respectively. *Andrea et al.*, found that formate was more common than acetate in both the free troposphere over the dry season Amazon and in the boundary layer haze due to biomass burning. They attributed the presence of these compounds to the photochemical oxidation of formaldehyde and acetaldehyde. *Talbot et al.*, found that 98 % of organic acids were partitioned into the gas phase and conclude that gas phase concentrations of formic and acetic acid are around 2 ppb in boundary layer air during the dry season in the Amazon. In remote areas organic acids are the chief acidic constituent of rainwater [*Keene et al.*, 1983: *Keene and Galloway*, 1984]. *Talbot et al.*, assessed some sources of these carboxylic acids. They found a formic acid/acetic acid ratio from motor vehicles of 0.51 ± 0.05 and this ratio from flaming combustion of biomass was 0.098 ± 0.010. *Talbot et al.*, report an emission ratio of formic acid to CO_2 of 6.9 E-6 ± 4.2E-6. *McKenzie et al.*, found a ratio of formic/acetic acids of 0.22 from the smoldering combustion of biomass. *DeGroot et al.*, measured formic acid and acetic acid from the pyrolysis of cottonwood in an *inert* atmosphere by FTIR. They report a formic/ acetic ratio of 0.30 with production of 8.75g formic acid per kg of fuel. We find an emission ratio of acetic to formic acid of at least four. In the atmosphere and in aged plumes formic acid is more common than acetic acid and this is probably due to oxidation of pyrolysis compounds and alkenes.

C_2H_2

The atmospheric and combustion chemistry of C_2H_2 is poorly understood. Previous studies (Griffith, Bonsang, Lobert) have found that the emission of this compounds correlates with CO_2. Our results indicate that C_2H_2 is a pyrolysis compound. Our C_2H_2 measurements are likely to be quite accurate as they are made with fair precision and high time resolution in two widely separated spectral regions. If we compute our C_2H_2/CO_2 levels they are about 50% higher than reported by Lobert et al. Olbu et al report a C_2H_2/CH_4 level of 0.073 (r2 = 0.93) for African savannah fires. Our average value for this ratio is about 0.12. This difference is quite possibly due to the difference in fuels.

C_2H_6

Ethane is representative of the higher alkanes which drop off in concentration rapidly along the homologous series. Our ethane/ methane plot is very linear with an average ratio of 0.16 more than double that reported by Lobert et al. (See Figure 12) It was thought that this difference is related to the different fuels in the studies rather than some instrumental artifact as FTIR has been used in the past to confirm GC measurements of C_2H_6. (Hanst 1994) However, extensive intercomparison of the IFSL data from similar fuels shows that the FTIR approach consistently gives about twice the ethane/methane ratio measured by the IFSL technique in similar fuels. The reason for this is still not known.

C_2H_4

C_2H_4 is measured in a clean area of the spectrum and is a strong absorber of IR radiation. Previous studies agree that it is the most abundant non-methane hydrocarbon. With the possible exception of terpenes our average data for all fires agrees with that conclusion. In fire # 11 the ethene peak is 37 ppm using the cross-section of Hanst et al. This compares with peak values for ethane and ethyne of 13 and 16 ppm respectively. (Peak values are of interest as they tend to reflect high signal to noise measurements which should be weighted heavily) Consideration of all the C_2 compounds shows that at least 80% of them have at least one pi bond. This may be useful in determining the origin of these compounds. Our value for C_2H_4/CH_4 emission ratio is about .29, again, about twice the value reported by Lobert et al. In general, we find, using forest fuels, that we measure higher ratios of C_2 hydrocarbons to CH_4 than other workers have obtained.

Implications of the lack of features due to some compounds.

The spectroscopy literature literally contains hundreds of references to retrievals for certain compounds at certain wavelengths. A thorough search was made for numerous compounds with negative results in most cases. A complete list of undetected compounds may not be that useful, but some important ones should be mentioned.

Griffith et al mentioned a lack of features attributable to N_2O in their smoke spectra. In this work as well we see no evidence of N_2O which in this case places an upper limit on its ratio to CO_2 of 6.7e-5 .

Methyl Chloride emissions from biomass burning are of some concern. The published emission ratios of Lobert et al for CH_3Cl to CO and CH_4 imply that our "richest" smoldering spectrum (587 ppm CO, 120 ppm CH_4) would have 1 - 2 ppm of CH_3Cl. If so this molecule would be detectable in our spectra by isolated peaks near 2966 cm-1. We did not see CH_3Cl in this area. However, we are in the process of continuing these types of measurements with a system with a longer pathlength by a factor of 12. This should be sufficient for good measurements of CH_3Cl at its peak values and an important way to cross check the emission ratios for this compound.

Field-sampling methodology of other workers summarized.

A great deal of useful information about biomass fires has been learned through canister sampling based measurement programs where only CO_2 and CO are measured in real time, but there are certain limitations. Most previous work of this type has been based on an approximate temporal division of the fire into flaming and smoldering "phases". An attempt is made to acquire a canister sample during each phase. The sum of the CO and CO_2 is approximately the total carbon emission in real time, and this fact, combined with knowledge of the carbon mass percentage of the fuel, and the vertical velocity, allows an estimate of the fuel consumed in each "phase". To arrive at the total fire emissions of a compound one then sums "phase" emissions from the appropriate canister weighted by the fuel consumption of the "phases". This approach, while ingenious, does have some problems. Grass fires have a very short "smoldering phase" and, in general, it may be difficult to program sample collection ahead of time to coincide with the actual "phase occurrence". If a canister collection is not spread over the whole "phase" then the sample is only representative if "tracking" is occurring.

Mass Balance.

As discussed above, the production of "combustion water" (CW) during complete combustion can be assumed to be determined by the chemical formula of the fuel. Complete combustion of a fuel with the formula $C_lH_mO_n$ would create CW/CO_2 in a ratio (mH/2)/lC. (Thus for complete combustion of $C_6H_9O_4$ one expects the combustion to produce 3 moles of water for every four moles of CO_2. Fuels enriched in carbon, such as charcoal (70 - 80% C), emit a much lower ratio of CW/CO_2.) In practice the gassification of excess fuel moisture can be followed in real time using equation (2)

(2) fuel moisture evolved = (total water) - (background water + combustion water)

This equation is very accurate for complete combustion and we observed that in all our fires featuring flaming combustion the fuel moisture was completely driven off early in the fires when the combustion efficiency was greater than 97%. As discussed above, we can also check this measurement in principle by summing all the evolved fuel moisture and calculating the original % mass H_2O of the fuel which is easily measured by subsampling before the fire. Unfortunately, in these experiments the fuel moisture was not measured before the fire, an oversight easily corrected in future experiments. However, the calculated fuel moistures fall in the middle of the expected range based on other measurements. The measurement of fuel moisture is important for two chief reasons.

1) Only by knowing the temporal profile of the evolution of the fuel moisture can the mass data be made meaningful. The corrected mass data is an important check on the accuracy of the flow. For the last four fires the flow was actually calculated from the change in mass as a malfunction arose with the flow meter.

2) We found, with the exception of one fire, that the distilling fuel moisture tracks the production of CO_2 very closely early in the fire and a simple calculation based on the measured heats of combustion of biomass fuels shows that gassification and desorption of the fuel moisture consumes a remarkably consistent 10% of the energy released by the fire during this time. In fire number 11 the fuel bed contained green needles and the energy consumption by fuel moisture was about 20%. These observations shed light on the energy transfer aspects of fires propagating in natural fuels.

Byram gives a "time-honored" approximate formula for biomass as $C_6H_9O_4$ based on the average of many mass percentage analysis. This formula implies a mass percentage of 49.7 for C, 6 for H, and 44.3 for O. This formula also implies a combustion water CW/CO_2 ratio of 0.75: assuming complete combustion. This is important in correcting the mass record for fuel moisture. (See the section on water for more details on the fuel moisture calculation.) The great majority of C:H:N analyses carried out at the IFSL have C mass percentages very close to 50% and this is also the finding in at least one other study (Fearnside). Our mass percentage for pine needles was measured as 50.7 and this value was used for fires 3 and 5 for which the fuel was 100% pine needles. The C:H:N analysis was not performed specifically for the fuels in our other lab fires. However, the C:H:N analysis was carried out for the fuels burned in the companion fires in the field which were nominally similar. The average of these measurements was originally thought to be 45% C, which is also a figure widely used in global estimates. For our data reduction purposes, the mass percent C may not be constant during a single fire. We know that pyrolysis preferentially removes the "hydrate" part of the fuel. This probably contributes to the formation of charcoal which is about 75%C. In one field measurement, only 2 - 3 % of the fuel was converted to charcoal, but this is a significant fraction of the remaining fuel near the end of the fire. Another noticeable effect near the end of the fire may be build-up of ash and possibly even chemiabsorption of O_2. If all the fuel moisture is not driven off during flaming combustion then the CW/CO_2 ratio is unknown. During flaming combustion there may be some error in the mass record due to buoyancy effects.

In this work we assumed a constant mass percent C during a single fire. Variation of only the coefficient for carbon in Byram's formula generates formulas for fuel which have different mass percentages of C and different implied CW/CO_2 ratios under conditions of complete combustion. We modeled our mass loss record with the following combinations for %C and CW/CO_2: 43, 1.25; 45,0.9; 47, 0.83; and 49.7, 0.75; all derived from the stoichemetric assumptions given above. As expected, we find that with each of these combinations, the fuel moisture evolution peaks and ends at the same moment, but that the total moles of fuel moisture evolved varies by +- 12%. Because we did not measure the fuel moisture before these fires it is not possible to check our calculation in this way. (The fractional error in the fuel moistures reported here is probably less than .2.) In all the fires the fuel moisture evolution was complete near the beginning of the fire and in the fires which featured flaming combustion; the fuel moisture was evolved under conditions of MCE greater than 97%. We compared the evolved moles of C as calculated from the

concentration and flow data with the evolved moles of C as calculated from the "fuel-moisture corrected" mass loss record. We find that calculations based on the mass record, assuming the above stoichemetrically derived conditions, yield from 8 - 12 % more C than the flow based data. We were able to correct this as described earlier by assuming an error in the flow meter calibration.

Wood is about 50% cellulose which has the chemical formula $C_6H_{10}O_5$. The cellulose formula implies a mass percent C of 44.44 and a CW/CO_2 ratio of 0.833. Using these assumptions significantly improves the agreement between our mass and flow records with the total based on mass being only 3.6% higher than the total based on flow. However, we obtain the best agreement between the mass and flow records if we simply assume the fuel is 45% C and adopt a CW/CO_2 ratio of 0.75. In this case the totals are within one-half of a percent of each other. (See Figure 9) The theoretical explanation for this agreement is not clear. There may be experimental error or errors in the assumptions about the fuel stoichiometry. The greatest discrepancy between the records occurs after the flow, CO_2, and H_2O have already peaked indicating that experimental error in these quantities is not the dominant contribution to the observed small discrepancies. Further progress in understanding this will come with planned, detailed experiments. Future experiments will include fuel moisture and fuel chemistry analyses as well as weighing residual ash, charcoal, and chemiadsorbed O2 in the charcoal as necessary. The quantities derived in this work for fires 6 - 12 are based on the assumptions then that the mass % C is 45 (except for fires 3 and 5) and that the CW/CO_2 ratio is 0.75. These assumptions are also used to back-calculate the flow for fires 9 - 12 for which the flow meter malfunctioned.

NO_X Partitioning.

We plotted the NO_2 emission factors vs the NO emission factors and found that the various fuel types seem to occupy distinct regions in "NO - NO_2 space". Although this has limited atmospheric significance, more work could be done to see if this is a generally useful relationship.

Fuel H balance.

The fuel moisture was only estimated, but our estimate led to the conclusion that the combustion water and other hydrogen containing compounds accounted for about 92% of the fuel H with the bulk of the unseen H probably emitted as H_2.

Percentage of heat released absorbed in convection column.

Calorimeter measurements make it possible to calculate heat release from the CO_2 data. From the temperature and flow data for fire 8 we calculated that roughly 50% of the heat released is absorbed by the convection column above the fire. This puts an upper limit on the horizontal radiative transfer of the fire near 50% and indicates another class of potentially useful future measurements.

Effects of Volatile Constituents.

The volatile components in biomass, commonly referred to as "extractives", have relatively high vapor pressure, flammability, and heats of combustion and thus allow sustained combustion of live fuels at higher fuel moistures than dead fuels will burn. The general effect of fuel moisture will be to reduce the heat value of the fuel and the temperature wihin the flame structure resulting in a greater proportion of incompletely oxidized products. Fuel moisture is also one of the factors that can limit O2 available for combustion (Byram). Our highest intensity fires were with the freshly cut sagebrush fuels which are high in moisture content, but also high in extractive content. Green needles are also high in extractives, but this fire did not burn with as high intensity possibly due to even higher fuel moisture or a less optimized fuel geometry.

Preliminary assessment of effects of green fuels.

Little laboratory work has been done on emissions characteristics of "green" vegetation. The "fireplace study" of Talbot et al monitored CO_2, CO, formic acid, and acetic acid and concluded that there was no difference in emissions due to the "green" or dry state of the vegetation. Laboratory work on open burning of agricultural wastes shows differences between dry and high moisture content fuel, but this was ascribed only to the increased importance of smoldering of the fuel with higher moisture contents. In contrast we find that there may be *chemical and physical* reasons for the difference in emissions between green and brown needles. Some of these differences are doubtless due to the fact that green needles burned at lower combustion efficiency than the brown needles. We can

factor out the effect of combustion differences to some extent in the following way. The emission factors for fire 11 were computed only for the time that green needles were burning and these can be compared to the emission factors for smoldering combustion of dry needles in fire five. The ratio for green needles/dry needles for methane, ammonia acetylene, formaldehyde, methanol, and acetic acid 0.468, .515, 0.821, 2.14, 3.73, and 7.5. In general for smoldering combustion of the two fuels the hydrocarbons and ammonia (smoldering compounds) decrease in relative importance while formaldehyde, acetic acid, and methanol (pyrolysis compounds) increase in importance.

We may predict differences in emissions from a consideration of the chemical changes during the process of "curing" vegetation. In live foliage nutrients, sugars, and extractives are maintained at high levels and the foliage is protected from leaching by a waxy coating. Some of these compounds are drawn back into the plant just before abscission. After abscission, as vegetation dries the waxy coating quickly degrades and any rainfall event will act to leach out soluble constituents such as sugars. Volatile compounds (extractives) continue to be emitted from curing foliage for many weeks. In alignment with our formaldehyde results, Burton found that sugars in tobacco leaves subjected to pyrolysis are excellent precursors for formaldehyde.

More work is in progress to determine the size of the pulse of "biogenic" emissions that may occur during fires of compounds normally associated with intact forests. The terpenes have been identified as a potential precursor for particulate from biomass fires. We found that our average PM2.5 concentration was proportional to the mass percent of pine needles in the fuel bed, but this was only measured for three fires. The relative importance of changes in combustion chemistry and changes in fuel chemistry as vegetation drys bears further work.

The observation that there are differences in the emissions may have considerable significance in that they point to potential large differences between "cut/dry/burn" fires and wildfires.

PART 4. CHARACTERISTICS OF THE NEW SYSTEM

S/N improvements incorporated into the new system

Faster scan speed allowing more signal averaging.

In the system used in the experiment described in part 3 it was only possible to acquire 5 scans in one minute. With the new system, it should be possible to coadd about 300 scans in 30 seconds resulting in a factor of 7.7 more S/N from this change alone: and with twice the time resolution.

Longer path length.

The new system will have a 50 meter path length rather than the 3 meter path used previously. The result should be a factor of 17 improvement in S/N.

Optical Configuration.

Placing the "sample" after the interferometer should result in 10 to 100 times better S/N.

Combined effect of improvements.

The theoretical increase in S/N should be from 1300 to 13000 before considering the decrease in resolution which should only effect compounds with sharp lines such as CO and not compounds such as formic acid. For compounds with sharp lines the increase in S/N is theoretically about 300 to 3000 which should be possible at twice the time resolution used previously. As the current S/N is adequate for our research goals we may be able to target new questions.

Experimental Improvements

1) Auxiliary measurements of fuel chemistry and moisture are crucial with ash and char weights and analysis being useful.

2) Particulate characterization with nephelometer and filter samples.

3) There is a desperate need for some long-term field studies which include detailed characterization of the site before and after the fire, as well as detailed emissions characterization.

Implementation schedule for new system

A summary discussion follows of the most important remaining events anticipated in implementing the use of the new system. It is divided into three sections.

1) The contract for building the system has been awarded to Infrared Analysis Inc. We anticipate that during the summer of 1995 we will have an opportunity to review and approve a final design. At that point, in preparation for fall delivery of the system, we will concentrate on preparing the combustion lab for installation. This would involve enlarging the window in the stack if necessary and providing a secure base for supporting the system within the stack. This is also the time to install the necessary utilities such as power, computer hookups, and the N_2 purge lines for the windows. Assuming delivery, inspection, and installation proceed without problems, the next major event would be "test fire 1." During test fire 1 we would ensure that that the optical alignment of the system is maintained when exposed to temperature changes, that the purge lines are adequately clearing the mirrors, that our CO_2 is in reasonable agreement with the NDIR instruments, and that the system S/N and resolution are acceptable. At this point, we would anticipate rectifying any problems that are design related and covered under our warranty. We would also determine the best way to carry out the flow and temperature measurements in the stack.

2) A second, extensive, treatment of the data from test fire 1 would be made to develop a full set of analysis "library files". At this point we would address any problems relating to non-linearity (due to underresolved lines) and interference. A rigorous assessment of the measurement capabilities will be made which will assist in the development of a detailed study plan that specifies the fuels burned, emissions monitored, and the necessary auxiliary measurements. Decisions will also be made on the optimum fuel loading and laboratory pressure etc...

3) To facilitate the implementation of the study plan it will be necessary to develop the data acquisition system. A program will be written in the vendor provided language which will accomplish the following tasks:

i) Initiate scans and control the signal averaging in proper temporal relation to the other simultaneous measurements.

ii) Accept information, such as temperature and flow, as necessary from the simultaneously acquired data.

iii) Store the raw spectra and call and apply the required routines for wavelength correction and spectral analysis and then display the concentrations and fluxes on the screen as well as storing them in a file.

With this program in place, it will be possible to carry out the study at an accelerated pace and with information from each fire available to guide the remaining part of the study.

Figure 4.1. Simulation of data from new system

Simulation of 1989 apparatus: 7 ppm NO_2 at .12 cm-1 res. and 3 m path.

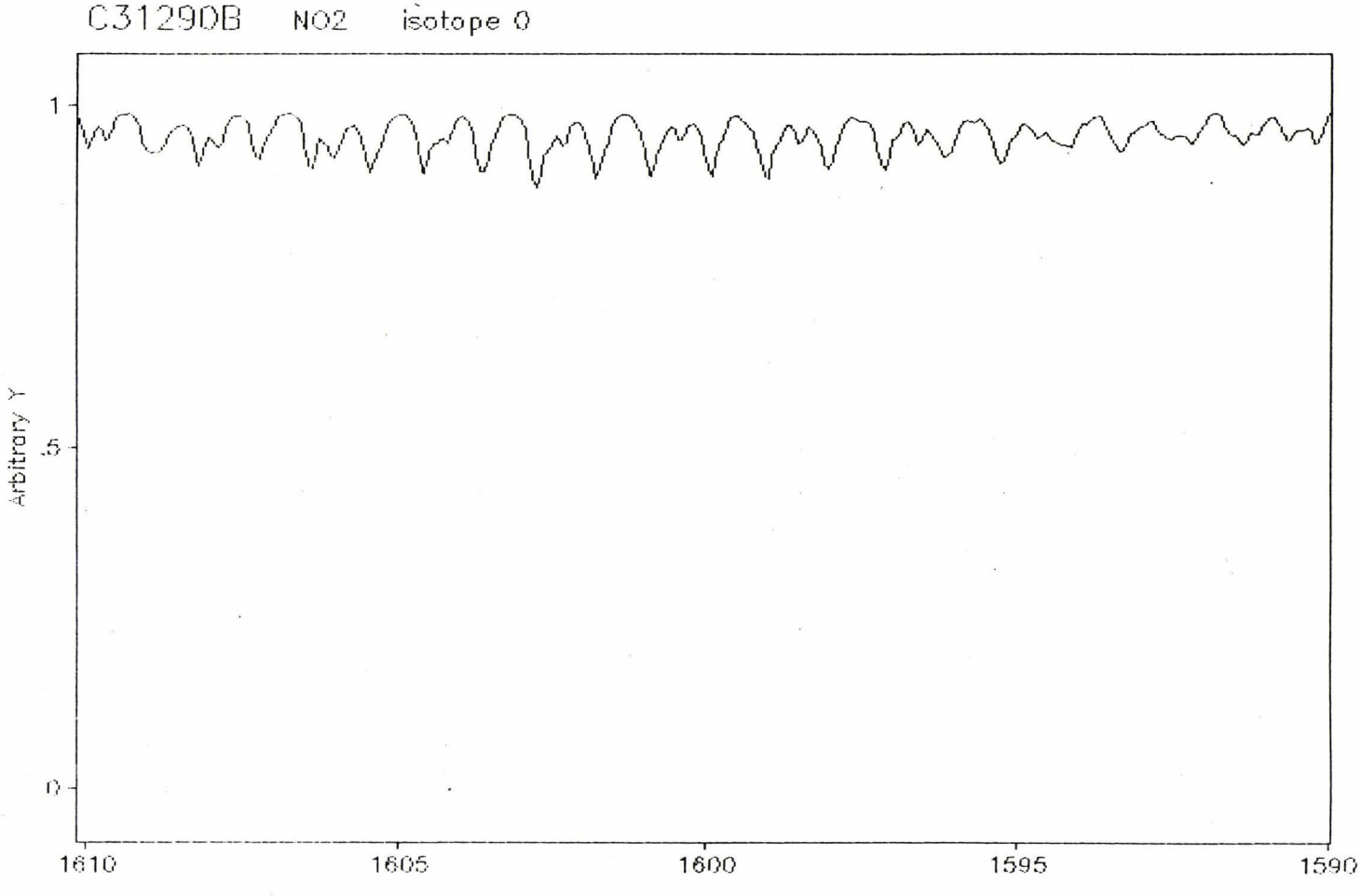

Coadded 2% H_2O and 7 ppm NO_2 at .12 cm-1 res. and 3 m path.

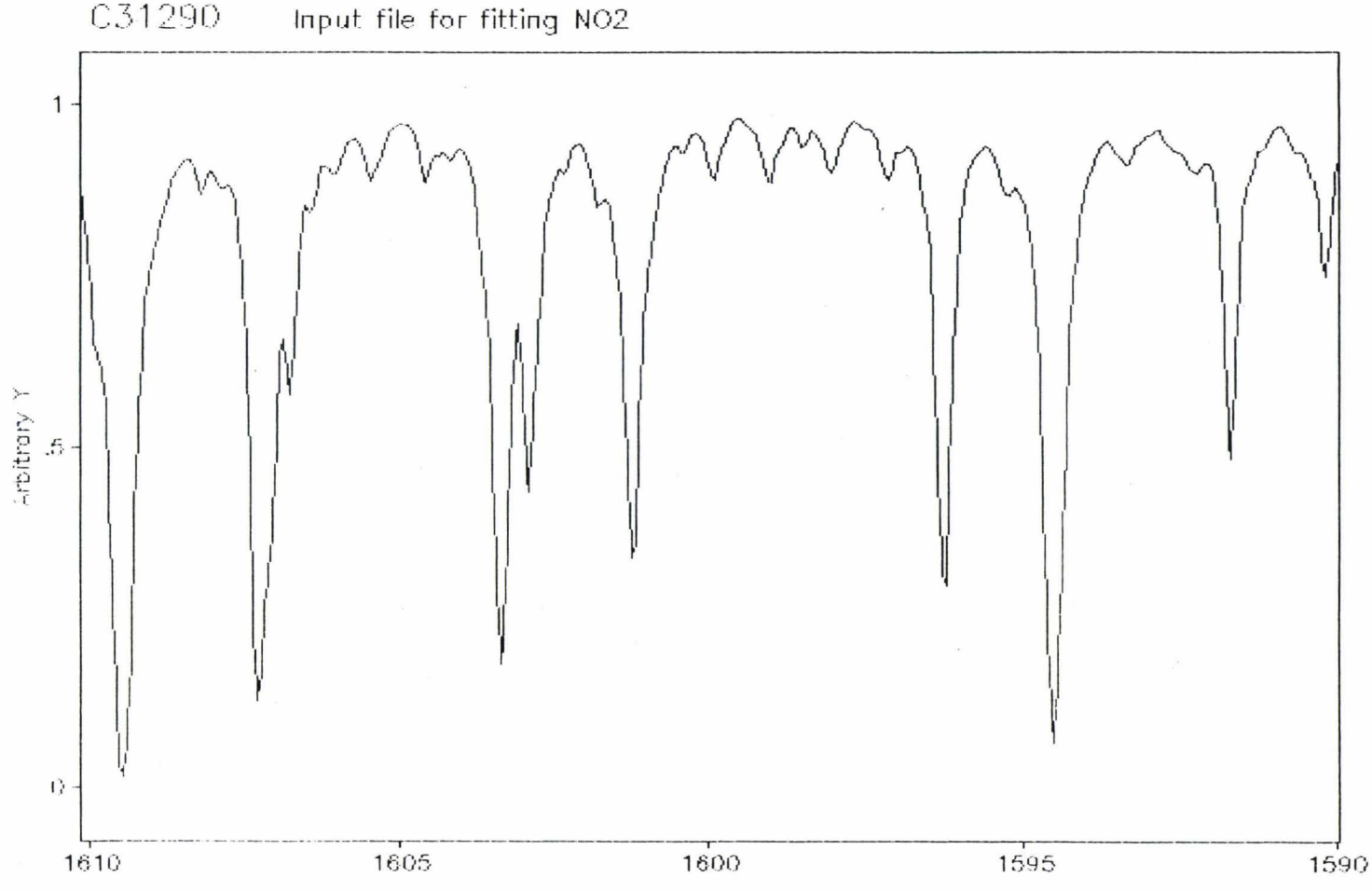

Offset spectra of 2% H_2O and 7 ppm NO_2 at .5 cm-1 res. and 50 m path.

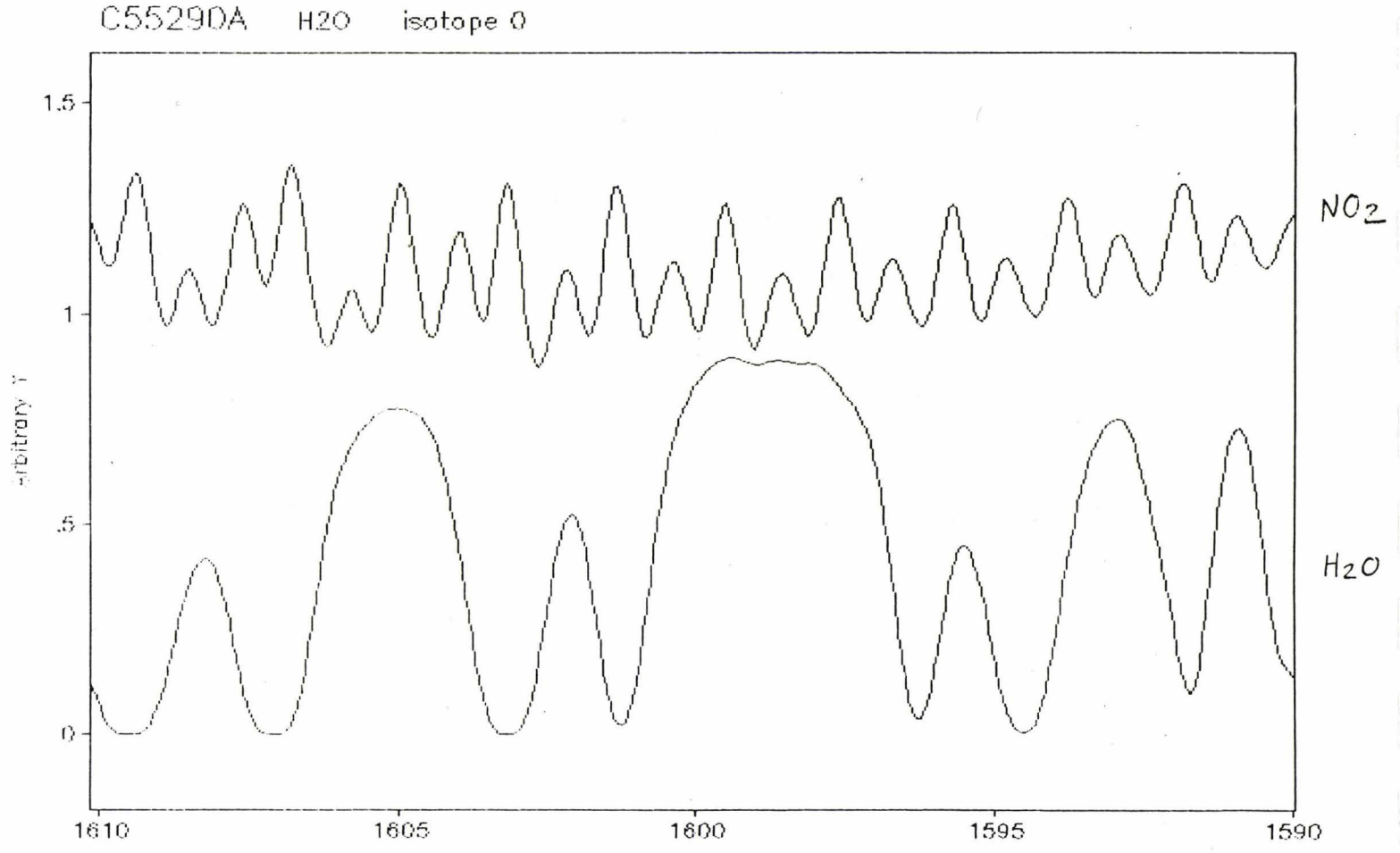

Coadded 2% H_2O and 7 ppm NO_2 at .5 cm-1 res. and 50 m path.

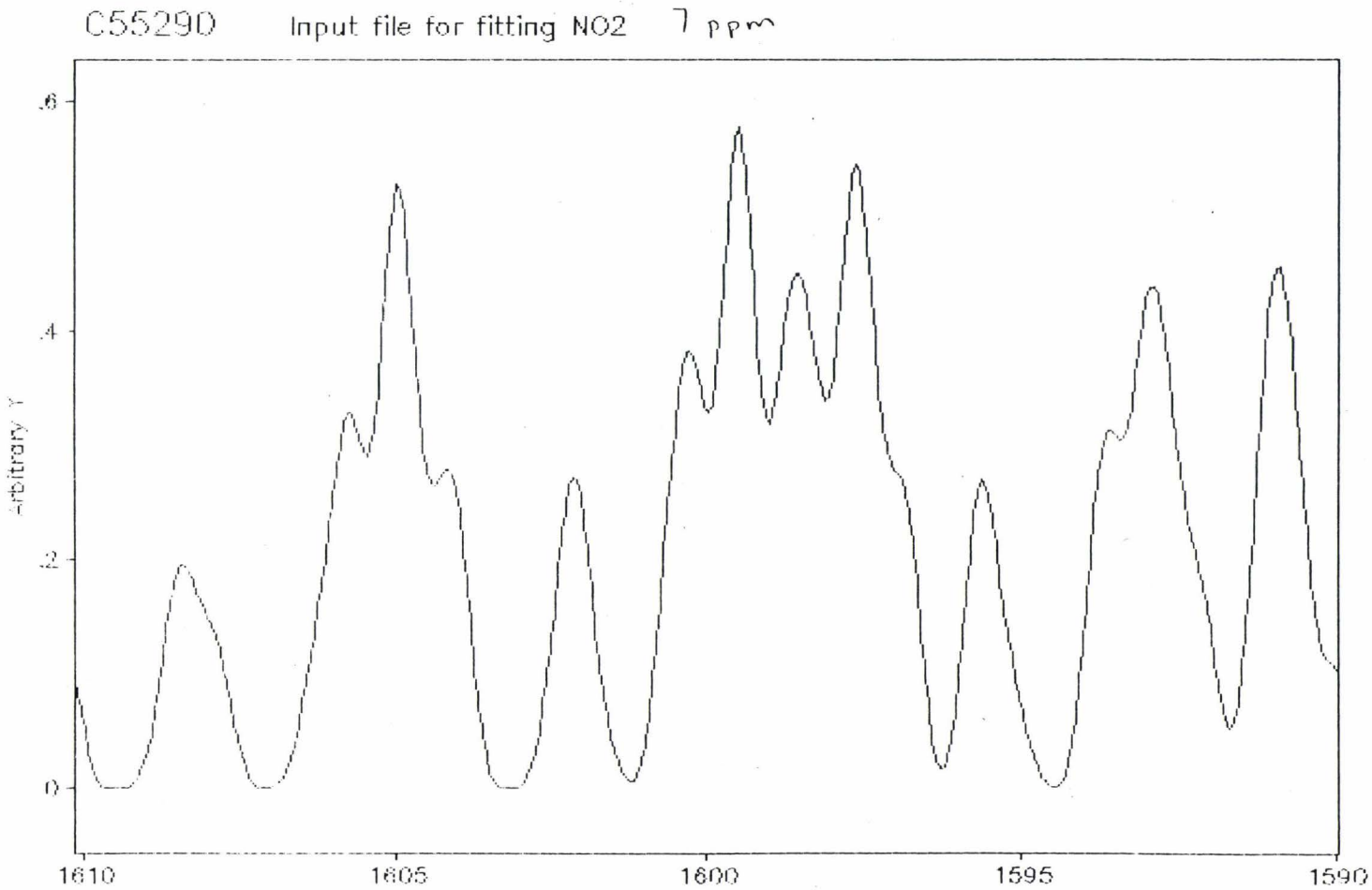

Coadded spectrum at high res. and coadded spectrum at low res. plotted together.

"Old and new system compared in same smoke."

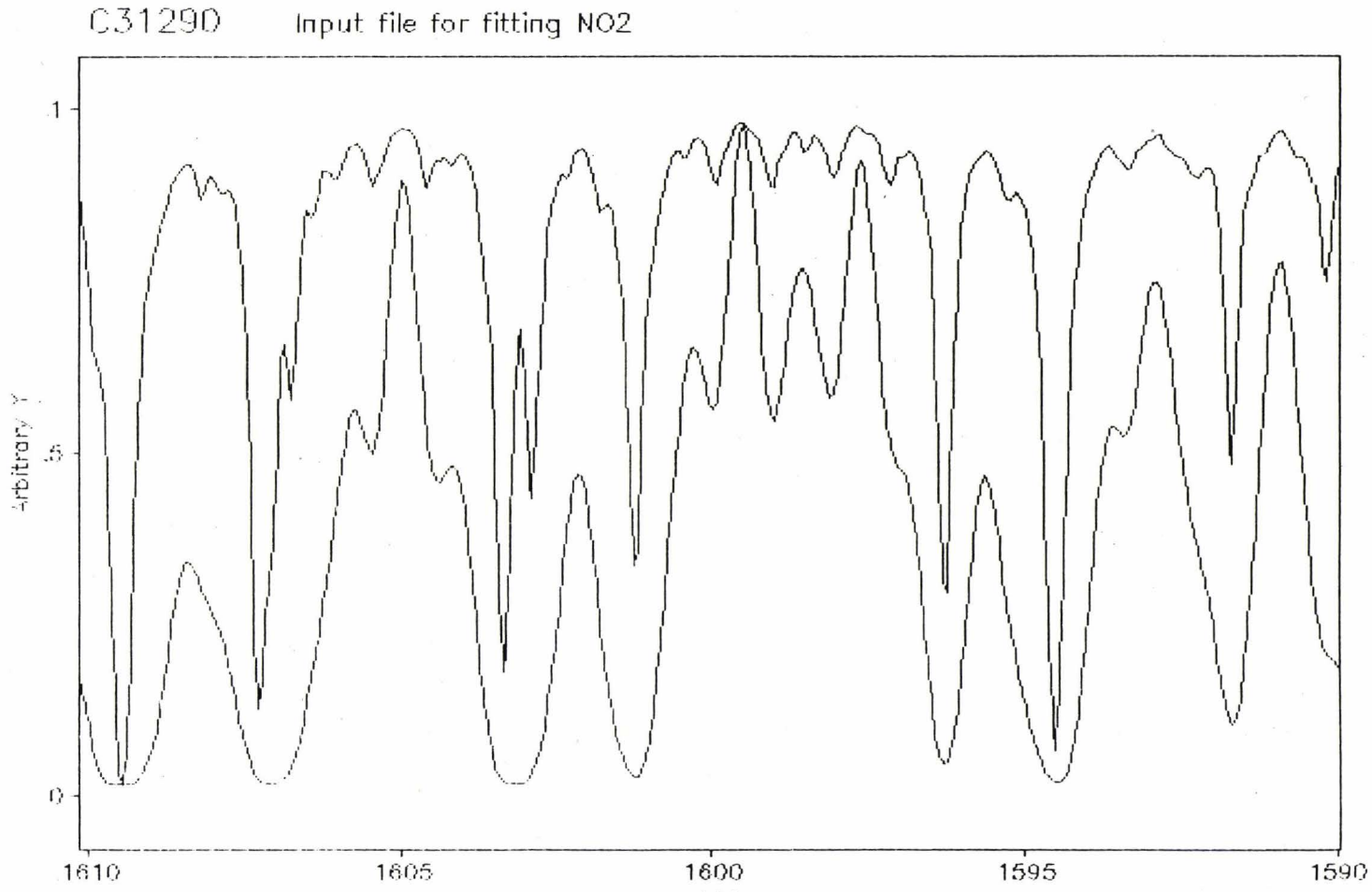

"Worse conditions - new system."

Offset spectra of 3% H_2O and 2 ppm NO_2 at .5 cm-1 res. and 50 m path.

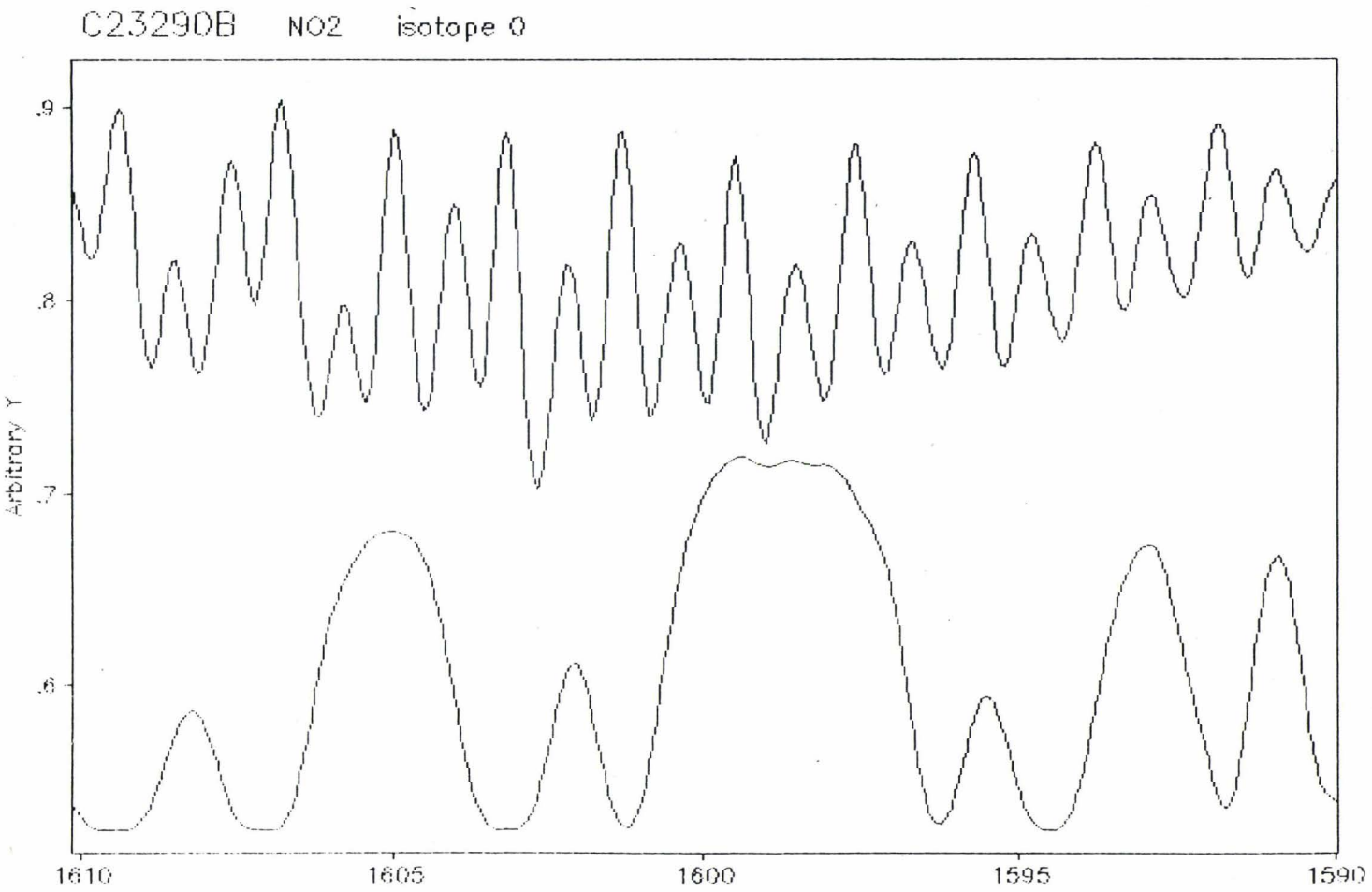

Coadded spectra of 3% H_2O and 2 ppm NO_2 at .5 cm-1 res. and 50 m path.

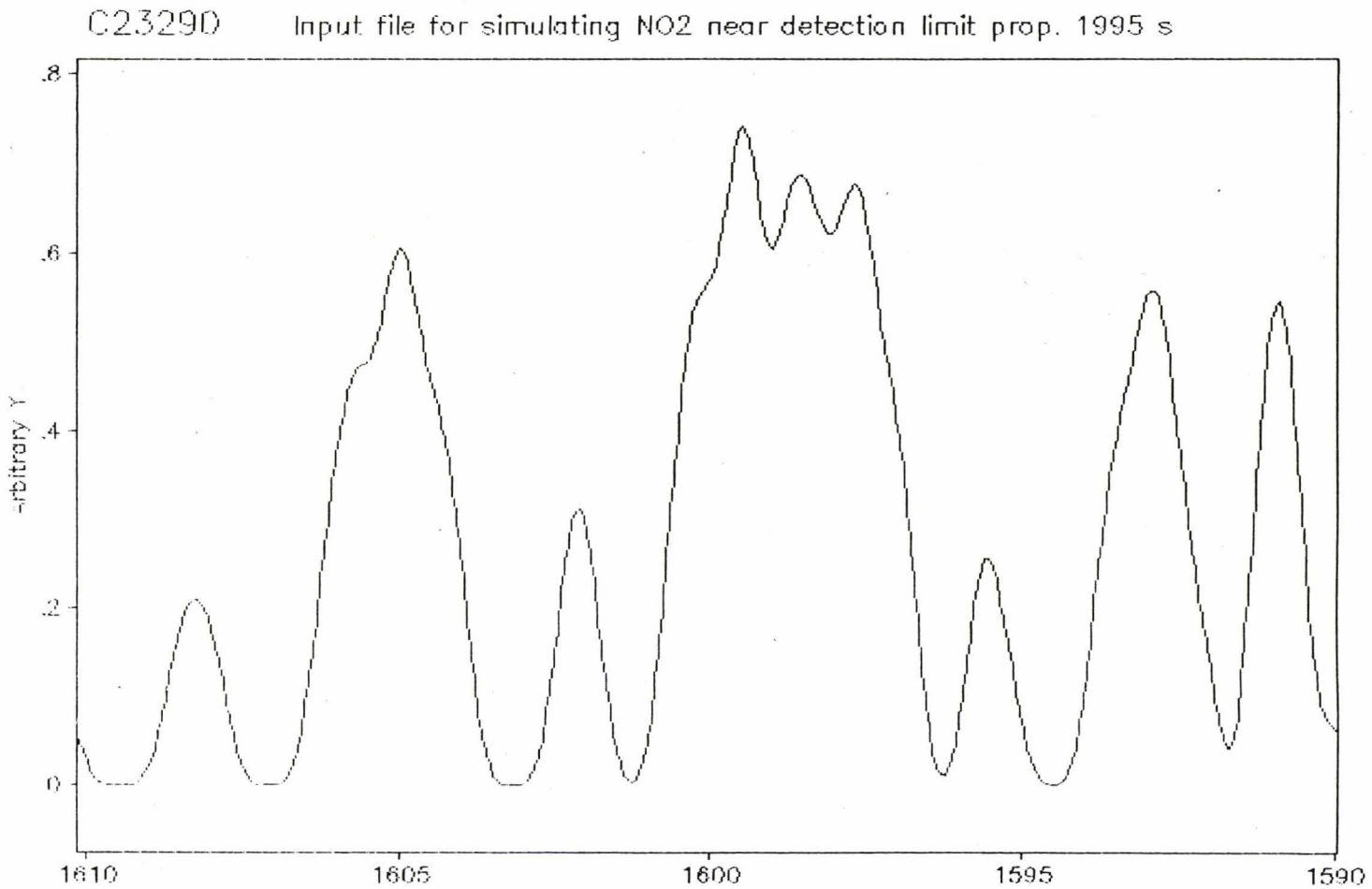

Co-*plotted* spectra of 3% H_2O and 2 ppm NO_2 at .5 cm-1 res. and 50 m path.

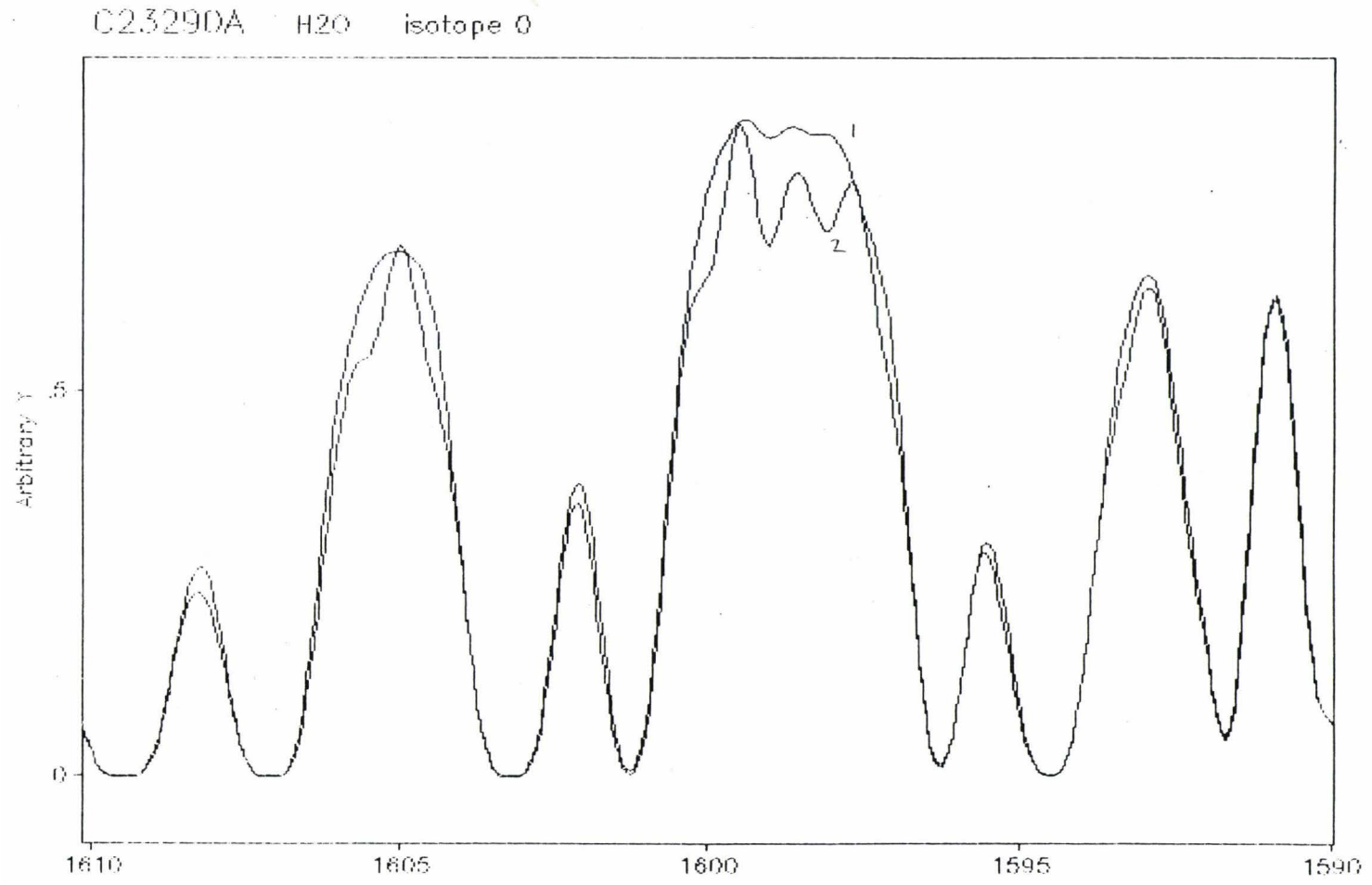

PART 5. CO2, CO AND HYDROCARBONS EMITTED FROM SAVANNA FIRES IN AFRICA DURING 1992 AND 1993

Emissions of CO_2, CO and Hydrocarbons from Fires in Diverse African Savanna Ecosystems

Wei Min Hao[a], Department of Chemistry, University of Montana, Missoula, Montana

Darold E. Ward, Gerald Olbu and Stephen P. Baker, Intermountain Research Station, Forest Service, U.S. Department of Agriculture, Missoula, Montana

Abstract

Emissions of CO_2, CO, and hydrocarbons from thirteen savanna fires (2-6 hectares) were investigated in Zambia and South Africa in August and September, 1992. The experiments were conducted at two moist woodland savanna sites, a moist grassland savanna site, and a semi-arid woodland savanna site in Zambia, and nine semi-arid woodland savanna sites in South Africa. The hydrocarbons measured were CH_4, C_2-C_6 alkanes, alkenes and alkynes, and aromatic compounds. There is no apparent difference in combustion efficiency for these ecosystems. The linear relationship between the emission factor of CH_4 and the combustion efficiency is similar regardless of the phase of combustion (flaming or smoldering), the climatic zone, the herbaceous species, or the amount of aboveground biomass. Concentrations of emitted nonmethane hydrocarbons are linearly correlated with those of CH_4. The emission ratio of a trace gas to CH_4 is constant for either phase of combustion in these ecosystems. Biomass burning in African savannas is a significant source of CO, ethyne, propene, and benzene in the atmosphere. The amount of CO, ethene, ethane, ethyne, propene, propane, and benzene emitted per year from these fires is about 20%-95% of the amount released from global industrial activities.

a. Currently at Intermountain Research Station, USDA Forest Service, Missoula, Montana

Submitted to Journal of Geophysical Research, July 21, 1994; Revised on May 21, 1995

1. INTRODUCTION

Africa is the largest continent in the tropics. About 20% of Africa is humid savannas and about 15% is arid savannas. African savannas account for about two-thirds of the tropical savannas [*Hao et al.*, 1990]. Savannas are often burned during the dry season for the purpose of agriculture and animal grazing. The frequency of burning varies considerably in Africa. More than half of the area is burned every year in the humid Guinea zone, but less than 15% of the area is burned in the arid Sahel zone [*Menaut et al.*, 1991]. The amount of aboveground savanna grass also differs, with high amounts of biomass in the humid region and low amounts of biomass in the dry region [*Bille*, 1977; *Menaut et al.*, 1991]. Land-use practices in Africa are changing rapidly because of high population growth during the last decade. The annual deforestation rate has increased about 12% from 1980 to 1990 [*Food and Agriculture Organization (FAO)*, 1993; *Hao et al.*, 1994] and the fallow cycle of shifting cultivation has shortened from 10 years to 5 years.

It is known that significant amounts of trace gases and aerosol particles are emitted from biomass burning [*Crutzen and Andreae*, 1990]. These trace gases and particulate matter are important in regional air pollution, in the chemistry of the troposphere and stratosphere, and in climate change. Considerable research has been done to investigate the emissions of CO_2, CO, and hydrocarbons from African savanna fires [*Delmas*, 1982; *Greenberg et al.*, 1985; *Bonsang et al.*, 1991; *Delmas et al.*, 1991]. However, there has been no systematic study to compare quantitatively the release of these gases from fires in different savanna ecosystems, nor has there

been any effort made to examine the interrelationship among emitted trace gases. The emission factor of CH_4 is, in fact, strongly correlated with combustion efficiency (CE) [*Hao and Ward*, 1993]. For lower combustion efficiencies, the emissions of CH_4 are higher. Combustion efficiency is the molar ratio of emitted CO_2 to the sum of CO and CO_2 above ambient levels. The definition of combustion efficiency is somewhat different from that used by *Ward et al.* [1992], which was defined as the percentage of fuel carbon emitted as CO_2. An emission factor of CH_4 is defined as grams of CH_4 produced per kilogram of dry fuel burned.

In this paper, we present the results of field measurements from fires in diverse African savanna ecosystems in August and September, 1992. There were four sites in Zambia: two in moist woodland savannas, one in moist grassland savannas, and one in semi-arid savannas. In contrast, the nine sites in South Africa were all in semi-arid savannas near Kruger National Park. The work in South Africa is part of the SAFARI-92 program. The impact of savanna fires in Africa on the chemistry of the atmosphere will be discussed.

2. EXPERIMENT

2.1. Field Sites

The meteorological conditions, the characteristics of soil and biomass, and the fire behavior at the thirteen sites studied in Zambia and South Africa have been described in detail by *Shea et al.* [this issue]. The type of savannas in each country, the number of sites, location,

elevation, annual precipitation, minimum and maximum temperatures, and the amount of aboveground biomass in each savanna ecosystem are summarized in Table 1. The total aboveground biomass includes grass, litter, and wood debris. The dominant herbaceous species are *Hyparrhenia spp.*, *Themeda triandra*, and *Diheteropogon amplectans* in moist grassland and woodland savannas near Kasanka National Park in Zambia. *Hyparrhenia spp.*, *Shizachyrium jeffreysii, and Brachiaria serrata* are the major grasses in semi-arid woodland savannas near Choma, Southern Province, Zambia. The amount of aboveground biomass in moist woodland savannas is substantially greater than that in moist grassland savannas, because of the large quantity of litter and wood debris in woodland savannas. The amount of biomass in semi-arid woodland savannas is only 12% less than that in moist woodland savannas. The dominant species of semi-arid woodland savanna grasses at Kruger National Park in South Africa are *Hyperthelia dissoluta, Diheteropogon amplectans, Heteropogon contortus, Setaria flabellata, and Elionurus muticus*. The average amount of aboveground biomass is about 4 tons ha^{-1} in areas which are burned every other year. The amount of biomass is greater as the length of time between successive fires becomes longer. The aboveground biomass is about 5.5 tons ha^{-1} in areas which are not burned for 4 years, or about 7.1 tons ha^{-1} for 28 years [*Shea et al.*, this issue].

2.2. *Sampling Methods*

The Fire Atmosphere Sampling System (FASS) [*Ward et al.*, 1992] was used for collecting canister samples. The FASS was enclosed in an aluminum box and buried below

ground to minimize the effects from high heat intensity. The operation of the sampling system was controlled by a software program of the main FASS system. Ambient air or smoke was drawn from the top of a 5-10 m tower through a ¼" teflon line by a modified KNF pump with a flow rate of 1.8 L min^{-1}. It passed through two Nupro stainless steel filters before entering the pump. The sample air then was directed through a manifold which had 4 solenoid valves (Angar Scientific), one attached to each canister. The sample was pumped into an 850 ml electro-polished stainless steel canister over the duration of the phase of combustion. Pressure in each canister was monitored as it was filled to 28 psia by a Kavlico pressure sensor. Excess sample was exhausted from a Nupro pressure relief valve to outside the box. The flow rate of the sample to fill the canister was regulated by a Tylan FC-280SA mass flow controller and was dependent on the length of time for each phase of the fire. The sampling time was 6 minutes during the flaming phase and 15 minutes during the smoldering phase for savanna fires. A canister of background air was collected prior to the fire. It is useful to differentiate between the "flaming" and "smoldering" samples. The flaming samples were predominantly from flaming combustion, even though the samples contained some emissions from smoldering combustion. The CO_2 concentrations of flaming samples were generally above 1,600 ppm. Likewise, the "smoldering" samples were predominantly from smoldering combustion and the CO_2 concentrations were less than 900 ppm. Power for all components was supplied by a 12 volt rechargeable battery. Overall, 36 canister samples were collected from 4 fires in Zambia and 81 canister samples from 9 fires in South Africa.

2.3. Analytical Methods

Canister samples were analyzed at the Intermountain Fire Sciences Laboratory within two months after being collected. Concentrations of identified compounds in the canisters did not show apparent change during storage for three months, except 1,3-butadiene. Fresh smoke samples of similar concentrations were collected from laboratory experiments for testing storage. Concentrations of 1,3-butadiene in the canisters have been found to decrease about 75% within two months.

Two Hewlett Packard (HP) 5890 Series II gas chromatographs (GC) were used for analyzing CO_2, CO, CH_4, C_2-C_6 aliphatic compounds, and aromatic compounds. Samples for CO_2 and CO analysis were injected through a 1 ml sample loop. They were separated using a packed Carbosphere column (1/8" O.D. x 6' long) with helium as carrier gas at a flow rate of 20 ml min^{-1}. The oven temperature was held at 30°C for 6 minutes and then was increased to 90°C at a rate of 10°C min^{-1}. Separated CO and CO_2 were reduced to CH_4 by a methanizer heated at 375° C before reaching to the flame ionization detector (FID). The detection limit was 1 ppm for CO_2, and 0.2 ppm for CO. The accuracy of duplicate analysis was $\pm$ 2%.

Methane, and C_2-C_3 alkanes, alkenes and alkynes were separated using a HP-1 precolumn (0.53 mm I.D. x 4 m long) and a J&W Scientific GS-Q megabore column (0.53 mm I.D. x 30 m long) with a 0.25 ml sample loop. Helium was used as carrier gas with a flow rate of 4 ml min^{-1} and as makeup gas with a flow rate of 26 ml min^{-1}. The temperature program of the oven

was the same as the one used for CO_2 and CO analysis. The primary standard gases of 9534 ppm CO_2, 477 ppm CO, and 9.65 ppm CH_4 were obtained from National Institute of Standards and Technology (NIST) and the secondary standard gases of 3.0 ppm CH_4 and 2.0 ppm C_3H_8 were from Norco (Boise, Idaho). The accuracy of duplicate analysis was $\pm$ 2% for CH_4, $\pm$5% for C_2 compounds, and $\pm$10% for C_3 compounds. The detection limit was 10 ppb for these compounds.

A cryogenic system was used to pre-concentrate the sample for analysis of hydrocarbons having carbon numbers greater than C_3. The cryogenic system included a 1/16" O.D. stainless steel trap, a Tylan FC-280S mass flow controller, and a Valco 6-port valve in a heated enclosure. The trap was submerged in liquid nitrogen in a dewer to concentrate 100 ml sample at -196°C. After pre-concentration, the sample was desorbed from the cold trap by a beaker of boiling water. The sample entered the GC and was focused at the head of the column at a temperature of -50°C. A DB-1 capillary column (0.25mm I.D. x 30 m long) from J&W Scientific was used for separating the compounds. The flow rate of N_2 carrier gas was 0.7 ml min^{-1} or 11.5 cm sec^{-1} linear flow. The oven temperature was kept at -50°C for 14 minutes initially, then was increased at a rate of 5°C min^{-1} for 16 minutes until reaching 30°C, which was held for 10 minutes. The temperature then was increased at a rate of 3°C min^{-1} for 50 minutes to 180°C, and held at 180°C for 30 minutes. Forty six compounds were identified by comparing their retention times with known compounds and confirmed by gas chromatography/mass spectrometry. About 26 compounds had concentrations consistently above the detection limit (1 ppb). A standard gas of 2 ppm propane and the response factor of different compounds to

the FID were used to calculate the concentrations of the gases. The peaks of the chromatograms were integrated by the HP Chemstation software.

3. RESULTS

3.1. Emission Factor of CH_4 vs. Combustion Efficiency

Concentrations of emitted gases presented here were from integrated canister samples collected either during the flaming phase or the smoldering phase. Combustion efficiency was calculated by the concentrations of CO_2 and CO above ambient levels. The emission factor of CH_4 was derived from the concentrations of CO_2, CO, CH_4, and other hydrocarbons, and the carbon content of biomass [*Ward et al.*, 1992]. Figure 1 summarizes the results from flaming and smoldering phases of fires in Zambia and South Africa. Most of the data from smoldering combustion at Kruger National Park were not included in Fig. 2, since it was mostly caused by cow and/or elephant dung rather than grass.

The emission factor of CH_4 is strongly and linearly correlated with the combustion efficiency. The emission factor of CH_4 is high for a fire of low combustion efficiency. There is no significant difference in the linear relationship between the emission factor of CH_4 and the combustion efficiency for flaming combustion and smoldering combustion. Nor is there any clear distinction in the linear correlation among moist and semi-arid grassland and woodland savannas, which have a wide range of herbaceous species and different amounts of aboveground

biomass in Zambia and South Africa.

3.2. Nonmethane Hydrocarbons vs. CH_4

Concentrations of emitted C_2-C_6 aliphatic compounds and aromatic compounds above ambient levels from flaming and smoldering phases of fires at selected sites in Zambia and South Africa were plotted against concentrations of CH_4 in Figs. 2-6. The slopes of the plots, or the emission ratios of the trace gases to CH_4, and correlation coefficients (r^2) are shown in Table 2. Concentrations of most of these compounds are linearly correlated with that of CH_4, with most of the correlation coefficients greater than 0.8. The weak correlation between 1,3-butadiene and CH_4 was due to instability of the compound in the canister. The emission ratio of 1,3-butadiene to CH_4 shown in Table 2 is the lower limit, because a significant amount of the compound may have decomposed during storage.

There are more unsaturated compounds produced than saturated compounds for the same carbon number. The most concentrated gas is ethene of the C_2 compounds, propene of the C_3 compounds, and *i*-butene and 1-butene of the C_4 compounds. The highest emission of aromatic compounds is benzene, followed by toluene, and *m*- and *p*-xylene. Concentrations of benzene are higher than those of C_4, C_5, and C_6 aliphatic compounds.

4. DISCUSSION

4.1. Combustion Efficiency and CO

The average combustion efficiency of savanna fires in Africa was 0.93 ± 0.02 (n=13), or the emission ratio of CO to CO_2 was 7.1%, which was calculated by weighting the combustion efficiency of the flaming and smoldering phase by the proportion of biomass burned in each phase [*Ward et al.*, this issue]. This value is consistent with that for savanna fires in Brazil (CE = 0.94) [*Ward et al.*, 1992]. It suggests that the degree of oxidation is very similar in combustion of African and South American savanna grass during the dry season. Our average combustion efficiency for savanna fires is very close to the combustion efficiency for flaming fires or mixed fires of chaparral in California [*Cofer et al.*, 1990]. It is difficult to compare directly the average combustion efficiency for savanna fires derived from our field measurements with some of the emission ratios of CO to CO_2 published previously. The arithmetic mean of combustion efficiency was reported to be 0.90 for savanna fires in Ivory Coast [*Bonsang et al.*, 1991] and in Brazil [*Greenberg et al.*, 1984]. However, the phase of combustion was not distinguished among the samples collected. Our average combustion efficiency is similar to the values of $[CO_2]/([CO]+[CO_2])$ in haze layers caused by biomass fires over the Amazon Basin, although the sources of plumes were not identified [*Andreae et al.*, 1988]. The average combustion efficiency may vary considerably during the burning season. Combustion efficiency may be low during the early dry season because of the relatively high moisture content in the biomass. The value may increase, or combustion may be more efficient, as biomass becomes drier toward the end of the burning season.

There is very limited information available about the area burned, the amount of aboveground biomass, and the frequency of burning in various regions of African savannas [*Hao et al.*, 1990; *Menaut et al.*, 1991; *Hao and Liu*, 1994]. We estimate the amount of biomass burned in African savannas on the basis of the savanna area on the vegetation map [*FAO*, unpublished data], the percentage of area burned per year [*Menaut et al.*, 1991], the aboveground biomass density as a function of rainfall in different savanna ecosystems [*Menaut et al.*, 1991], and the proportion of aboveground savanna grass burned [*Menaut et al.*, 1991; *Hao and Liu*, 1994; *Shea et al.*, this issue]. Approximately 2.0 x 10^9 tons of biomass was burned in Africa in 1990 [*Hao*, unpublished data]. For an average combustion efficiency of 0.93 and the corresponding emission factor of CO to be 72.6 g kg^{-1}, approximately 145 Tg (1 Tg = 10^{12} g) of CO were emitted from savanna fires in Africa, which was about 30% of the release from industrial sources globally [*WMO*, 1995].

4.2. CH_4

Our results clearly demonstrate that there is no apparent difference in the linear relationship between the emission factor of CH_4 and the combustion efficiency for flaming and smoldering combustion, or for various amounts of aboveground biomass in different savanna ecosystems. It is consistent with the results of *Hao and Ward* [1993], which were derived from laboratory fires of savanna grass, hay, straw, and pine needles [*Lobert et al.*, 1991], and from fires in African savannas [*Bonsang et al.*, 1991], Brazilian cerrado [*Greenberg et al.*, 1984; *Ward et al.*, 1992], and chaparral and wetlands [*Cofer et al.*, 1990]. The slope of the linear

relationship (-36.5 ± 3.2 g kg^{-1}) is very close to that of our previous work (-34.9 ± 3.3 g kg^{-1}) [*Hao and Ward*, 1993]. It indicates that the combustion chemistry of CH_4 production is the same for all grasslike materials. For the same combustion efficiency, the same amount of CH_4 is produced for various types of savanna fires.

For a combustion efficiency of 0.93, the corresponding emission factor of CH_4 is 2.1 g kg^{-1}. We estimate that about 4.2 Tg of CH_4 is released per year from burning savanna grass in Africa (Table 2). This source contributes less than 1% of the atmospheric CH_4.

4.3. Nonmethane Hydrocarbons

There are strong correlations between most of the nonmethane hydrocarbons and CH_4 (Figs. 2-6). There is no difference in the linear relationship for flaming and smoldering combustion, for various types of savanna grass, or for different amounts of aboveground biomass. It indicates that the mechanisms for producing these gases during combustion processes are the same regardless of the type of grass and the amount of aboveground biomass.

Assuming an average combustion efficiency of 0.93 [*Ward et al.*, this issue] and the average emission factor of CH_4 to be 2.1 g kg^{-1}, emission factors of nonmethane hydrocarbons for savanna fires can be calculated on the basis of their emission ratios to CH_4. Emission factors of these compounds are summarized in Table 2. The amount of these gases emitted per year from fires in African savannas is compared with the amount released from industrial activities

and from all the sources (Table 2). It is difficult to estimate the amount of nonmethane hydrocarbons emitted from global biomass burning, since the emission ratios of these compounds to CH_4 are quite different between forest fires and savanna fires [*Hao*, unpublished data]. Although there are large uncertainties in quantifying the source strengths, it clearly shows that biomass burning in African savannas is an important source of atmospheric ethyne, propene, and benzene. The amount of ethene, ethane, ethyne, propene, propane, and benzene produced from African savanna fires is about 78, 45, 36, 95, 22, and 43%, respectively, of that emitted from industrial activities.

There have been a few measurements of latitudinal distribution of nonmethane hydrocarbons from the northern hemisphere to the southern hemisphere on board ships or aircraft. Significantly high concentrations of nonmethane hydrocarbons from 20°N to 20°S over the Atlantic Ocean were observed in the lower troposphere during the STRATOZ III Experiment in June, 1984 [*Rudolph*, 1988] and during cruises in March and April, 1987 [*Rudolph and Johnen*, 1990] and in September and October, 1988 [*Koppmann et al.*, 1992]. The results indicate the pronounced influence of biomass burning in Africa and Latin America on the chemical composition of the air mass over the Atlantic Ocean. Most of the latitudinal measurements across the Pacific Ocean were performed in February and March [*Donahue and Prinn*, 1993] or in November and December [*Singh and Salas*, 1982; *Singh et al.*, 1988], when little biomass burning occurred in Asia and Latin America [*Hao and Liu*, 1994]. Thus, these studies did not indicate any apparent latitudinal gradients of nonmethane hydrocarbons between 5°N and 40°S over the Pacific Ocean.

5. CONCLUSIONS

Emissions of CO_2, CO, and hydrocarbons from savanna fires were determined in moist and semi-arid grassland and woodland savannas in Zambia and South Africa. The results clearly indicate that the combustion efficiency is the same even though the type of herbaceous species and the amount of aboveground biomass are different in these ecosystems. The linear relationship between the emission factor of CH_4 and the combustion efficiency is similar for flaming and smoldering combustion at all the sites. Concentrations of most of the nonmethane hydrocarbons emitted are linearly correlated with that of CH_4. The ratio of emitted trace gas to CH_4 remains constant regardless of the phase of combustion, the climatic zone, the geographic location, the savanna grass species, or the amount of aboveground biomass. The amount of carbon monoxide, ethene, ethane, ethyne, propene, propane, and benzene emitted from African savanna fires is comparable to that released due to global industrial activities.

REFERENCES

Andreae, M.O. et al., Biomass-burning emissions and associated haze layers over Amazonia, *J. Geophys. Res., 93*, 1509-1527, 1988.

Bille, J.C., Etude de la production primaire nette d'un ecosystème sahélien, *Trav. Docum. ORSTOM, 65*, 1-82, 1977.

Bonsang, B., G. Lambert, and C.C. Boissard, Light hydrocarbons emissions from African savanna burnings, in *Global Biomass Burning: Atmospheric, Climatic, and Biospheric Implications*, edited by J.S. Levine, pp. 155-161, MIT Press, Cambridge, Mass., 1991.

Cofer III, W.R., J.S. Levine, E.L. Winstead, P.J. LeBel, A.M. Koller, Jr., and C.R. Hinkle, Trace gas emissions from burning Florida wetlands, *J. Geophys. Res., 95*, 1865-1870, 1990.

Crutzen, P.J., and M.O. Andreae, Biomass burning in the tropics: Impact on atmospheric chemistry and biogeochemical cycles, *Science, 250*, 1669-1678, 1990.

Delams, R., On the emission of carbon, nitrogen and sulfur in the atmosphere during bushfires in intertropical savanna zones, *Geophys. Res. Lett., 9*, 761-764, 1982.

Delmas, R.A., A. Marenco, J.P. Tathy, B. Cros, and J.G.R. Baudet, Sources and sinks of methane in the African savanna. CH_4 emissions from biomass burning, *J. Geophys. Res., 96*, 7287-7299, 1991.

Donahue, N.M., R.G. Prinn, In situ nonmethane hydrocarbon measurements on SAGA-3, *J. Geophys. Res., 98*, 16915-16932, 1993.

Ehhalt, D.H., J. Rudolph, and U. Schmidt, On the importance of light hydrocarbons in multiphase atmospheric systems, in *Chemistry of Multiphase Atmospheric Systems, NATO ASI Ser. G6*, edited by W. Jaeschke, 321-350, 1986.

Food and Agriculture Organization (FAO), Forest resources assessment 1990: Tropical countries, *FAO Forestry Paper 112*, Food and Agriculture Organization of the United Nations, Rome, 1993.

Greenberg, J.P., P.R. Zimmerman, and R.B. Chatfield, Hydrocarbons and carbon monoxide in African savanna air, *Geophys. Res. Lett., 12*, 113-116, 1985.

Greenberg, J.P., P.R. Zimmerman, L. Heidt, and W. Pollock, Hydrocarbon and carbon monoxide emissions from biomass burning in Brazil, *J. Geophys. Res., 89*, 1350-1354, 1984.

Hao, W. M., M.-H. Liu, and P.J. Crutzen, Estimates of annual and regional releases of CO_2 and other trace gases to the atmosphere from fires in the tropics, based on the FAO statistics for the period 1975-1980, in *Fire in the Tropical Biota (Ecological Studies 84)*, edited by J.G. Goldammer, 440-462, Springer-Verlag, Berlin, 1990.

Hao, W.M., and D.E. Ward, Methane production from global biomass burning, *J. Geophys. Res.,98*, 20657-20661, 1993.

Hao, W.M., and M.-H. Liu, Spatial distribution of tropical biomass burning in 1980 with 5° x 5° resolution, *Global Biogeochem. Cycles, 8*, 495-503, 1994.

Hao, W.M., M.-H. Liu, and D.E. Ward, Impact of deforestation on biomass burning in the tropics, in *Proceedings of Global Climate Change: Science, Policy, and Mitigation Strategies*, edited by C.V. Mathai and G. Stensland, Air and Waste Management Association, 273-278, 1994.

Koppmann, R., R. Bauer, F.J. Johnen, C. Plass-Dülmer,and J. Rudolph, The distribution of light nonmethane hydrocarbons over the mid-Atlantic: Results of the Polarstern cruise ANT VII/1, *J. Atmos. Chem., 15*, 215-234, 1992.

Lobert, J. M., D.H. Scharffe, W.M. Hao, T.A. Kuhlbusch, R. Seuwen, P. Warneck, and P.J. Crutzen, Experimental evaluation of biomass burning emissions: Nitrogen and carbon containing compounds, in *Global Biomass Burning: Atmospheric, Climatic, and Biospheric Implications,* edited by J.S. Levine, 289-304, MIT Press, Cambridge, Mass., 1991.

Menaut, J.-C., L. Abbadie, F. Lavenu, P. Loudjani, and A. Podaire, Biomass burning in west African savannas, in *Global Biomass Burning: Atmospheric, Climatic, and Biospheric Implications,* edited by J.S. Levine, 133-142, MIT Press, Cambridge, Mass., 1991.

Rudolph, J., Two-dimensional distribution of light hydrocarbons: Results from the STRATOZ III Experiment, *J. Geophys. Res., 93,* 8367-8377, 1988.

Rudolph, J., and F. J. Johnen, Measurements od light atmospheric hydrocarbons over the Atlantic in regions of low biological activity, *J. Geophys. Res., 95,* 20583-20591, 1990.

Shea, R.W., B.W. Shea, J.B. Kauffman, D.E. Ward, C.I. Haskins, and M.C. Skoles, Fuel biomass and combustion factors associated with fires in savanna ecosystems of South Africa and Zambia, *J. Geophys. Res.*, this issue.

Singh, H.B., and L.J. Salas, Measurement of selected light hydrocarbons over the Pacific Ocean: Latitudinal and seasonal variations, *Geophys. Res. Lett., 9,* 842-845, 1982.

Singh, H.B., W. Viezee, and L.J. Salas, Measurements of selected C_2-C_5 hydrocarbons in the troposphere: Latitudinal, vertical, and temporal variations, *J. Geophys. Res., 93,* 15861 -15878, 1988.

Singh, H.B., and P.B. Zimmerman, Atmospheric distribution and sources of nonmethane hydrocarbons, in *Gaseous Pollutants: Characterization and Cycling*, Edited by J.O. Nriagu, 177-235, Wiley & Sons, New York, 1992.

Ward, D.E., R.A. Susott, J.B. Kauffman, R.E. Babbitt, D.L. Cummings, B. Dias, B.N. Holben, Y.J. Kaufman, R.A. Rasmussen, and A.W. Setzer, Smoke and fire characteristics for cerrado and deforestation burns in Brazil: BASE-B experiment, *J. Geophys. Res., 97,* 14601-14619, 1992.

Ward, D.E., W.M. Hao, R.A. Susott, R.A. Babbitt, R.W. Shea, J.B. Kauffman, and C.O. Justice, Effect of fuel composition on combustion efficiency and emission factors for African savanna ecosystems, *J. Geophys. Res.*, this issue.

World Meteorological Organization (WMO), Scientific Assessment of Ozone Depletion: 1994, *WMO Global Ozone Res. and Monit. Project, Rep. 37*, WMO, Geneva, 1995.

Table 1. Description of Field Sites

Country	Zambia			South Africa
Type of Savannas	moist grassland	moist woodland	semi-arid woodland	semi-arid woodland
No. of Sites	1	2	1	9
Location	Kasanka National Park (12°35'S, 30°21'E)	Kasanka National Park (12°35'S, 30°21'E)	Choma, South Province (16°50'S, 26°59'E)	Kruger National Park (31°14'E, 25°15'S)
Elevation	~900 m	~900 m	~400 m	~600 m
Annual Precipitation	~738 mm in 1989 ~1170 mm in 1991	~738 mm in 1989 ~1170 mm in 1991	~800 mm	600-1000 mm
Annual Temperature (mini., maxi.)	15°C, 30°C	15°C, 30°C	12°C, 30°C	15°C, 27°C
Aboveground Biomass (tons ha^{-1})	3.1	5.8	5.1	2.2 - 7.1

Table 2. CO and Hydrocarbon Emissions from African Savanna Fires

Compound	Emission Ratio to CH_4 (10^{-3})	Correlation Coefficient with CH_4[a] (r^2)	Emission Factor (g kg^{-1})	Emission from African Savanna Fires (10^{12}g yr^{-1})	Industrial Sources[b] (10^{12}g yr^{-1})	Total Source Strengths[c] (10^{12}g yr^{-1})
CO	19490	0.97	72.6	145	500[d]	2450[d]
Methane	1000	1	2.13	4.26	26	590[b]
Ethene	230	0.96	0.86	1.72	2.2	20-45
Ethane	74	0.96	0.30	0.59	1.3	10-15
Ethyne	73	0.93	0.25	0.51	1.4	3-6
Propene	68	0.98	0.38	0.76	0.8	7-12
Propane	19	0.96	0.11	0.22	1.0	15-20
i- & 1-Butene	17	0.96	0.13	0.26		
1,3-Butadiene	6.2	0.55	0.05	0.09		
trans-2-Butene	3.4	0.83	0.03	0.05		
cis-2-Butene	2.1	0.93	0.02	0.03		
n-Butane	3.4	0.86	0.03	0.05	2.4	1-2
i-Butane	1.1	0.87	0.01	0.02		1-2
1-Pentene	2.6	0.88	0.02	0.05		
n-Pentane	3.3	0.94	0.03	0.06	1.4	1-2
2-Methylbutane	0.9	0.90	0.01	0.02		2-3
Cyclopentene	2.3	0.42	0.02	0.04		
1-Hexene	3.5	0.91	0.04	0.08		
n-Hexane	0.9	0.68	0.01	0.02		
Benzene	20.6	0.85	0.21	0.43	1.0	4-5
Toluene	10.2	0.97	0.13	0.25	3.5	4-5
m- & *p*-Xylene	2.7	0.72	0.04	0.08	2.5[e]	2-3

[a]Derived from slopes of Figs. 2-6.
[b]Derived from *Ehhalt et al.* [1986].
[c]*Singh and Zimmerman* [1992].
[d]*WMO* [1995].
[e]Including o-xylene.

Figure Legends

Fig. 1. Relationship between emission factor of CH_4 and combustion efficiency.

Fig. 2. Relationship between emitted C_2 compounds and CH_4.

Fig. 3. Relationship between emitted C_3 compounds and CH_4.

Fig. 4. Relationship between emitted C_4 compounds and CH_4.

Fig. 5. Relationship between emitted C_5 and C_6 compounds and CH_4.

Fig. 6. Relationship between emitted aromatic compounds and CH_4.

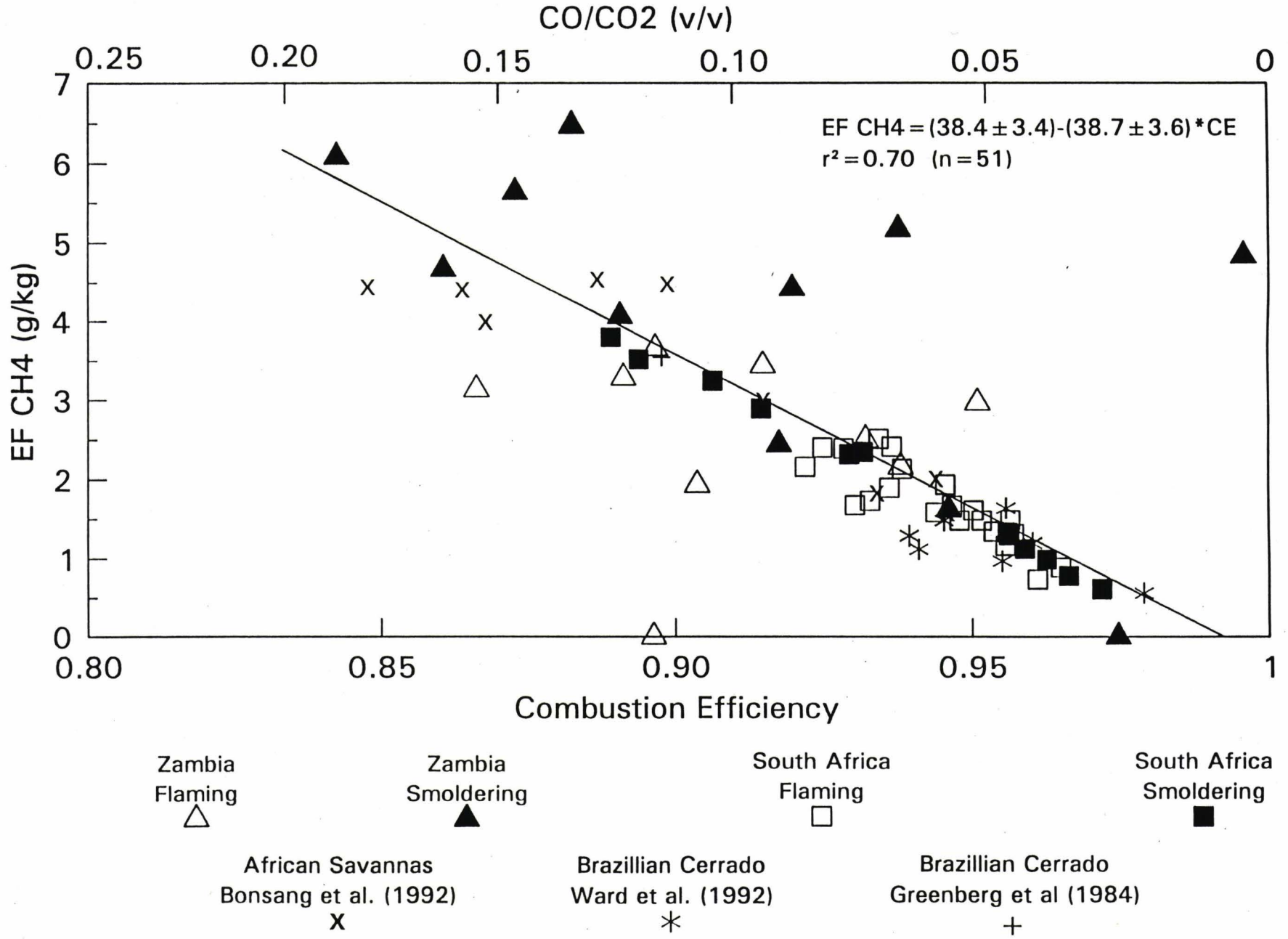
CO/CO2 (v/v)
0.25
0.20
0.15
0.10
0.05
0
EF CH4 = (38.4 ± 3.4)-(38.7 ± 3.6)*CE
r² = 0.70 (n = 51)
EF CH4 (g/kg)
0
1
2
3
4
5
6
7
0.80
0.85
0.90
0.95
1
Combustion Efficiency
Zambia Flaming
Zambia Smoldering
South Africa Flaming
South Africa Smoldering
African Savannas
Bonsang et al. (1992)
Brazillian Cerrado
Ward et al. (1992)
Brazillian Cerrado
Greenberg et al (1984)

Fig. 1

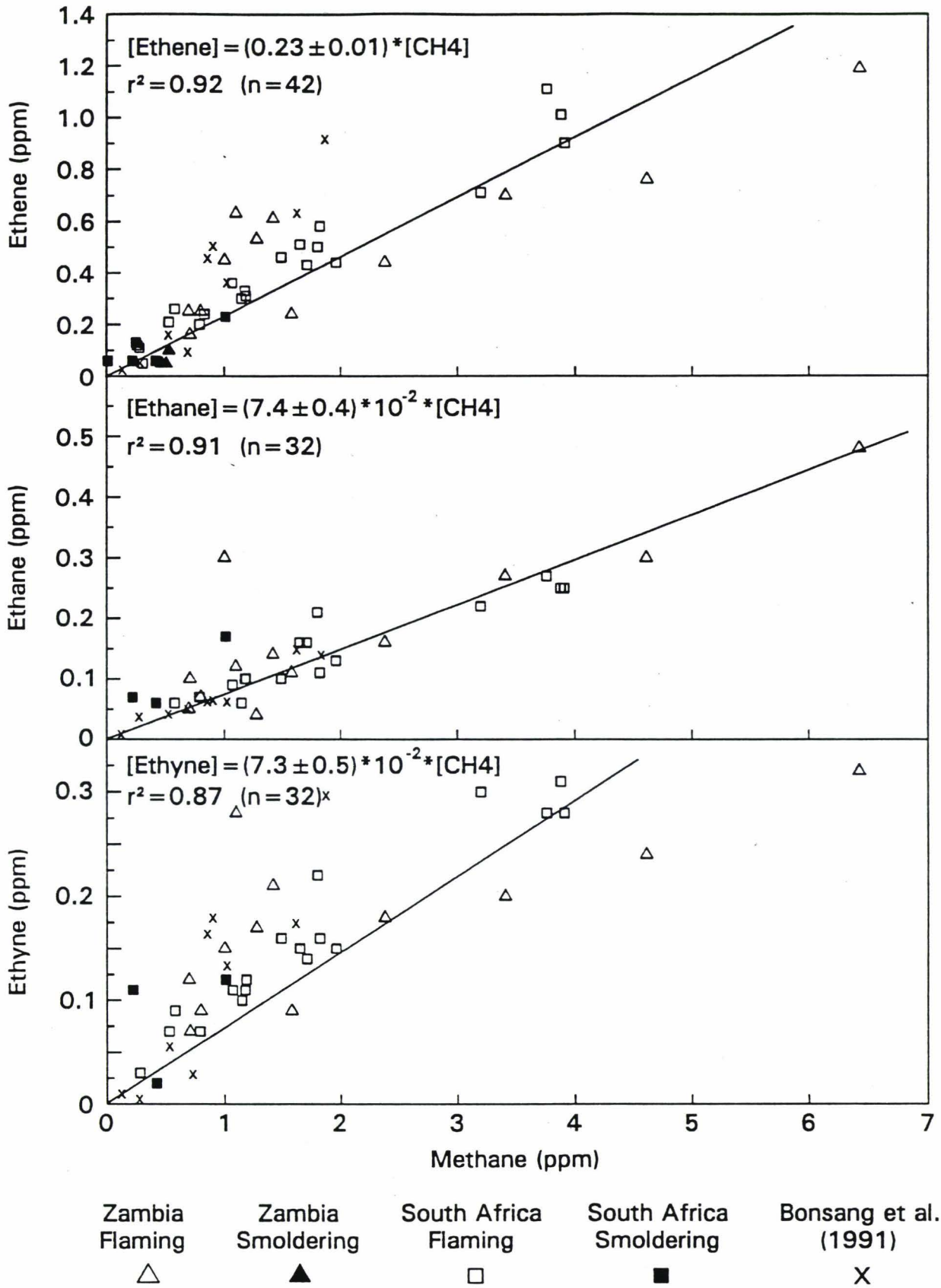
[Ethene] = (0.23 ± 0.01) * [CH4]
r² = 0.92 (n = 42)
Ethene (ppm)
[Ethane] = (7.4 ± 0.4) * 10⁻² * [CH4]
r² = 0.91 (n = 32)
Ethane (ppm)
[Ethyne] = (7.3 ± 0.5) * 10⁻² * [CH4]
r² = 0.87 (n = 32)
Ethyne (ppm)
Methane (ppm)
Zambia Flaming
Zambia Smoldering
South Africa Flaming
South Africa Smoldering
Bonsang et al. (1991)

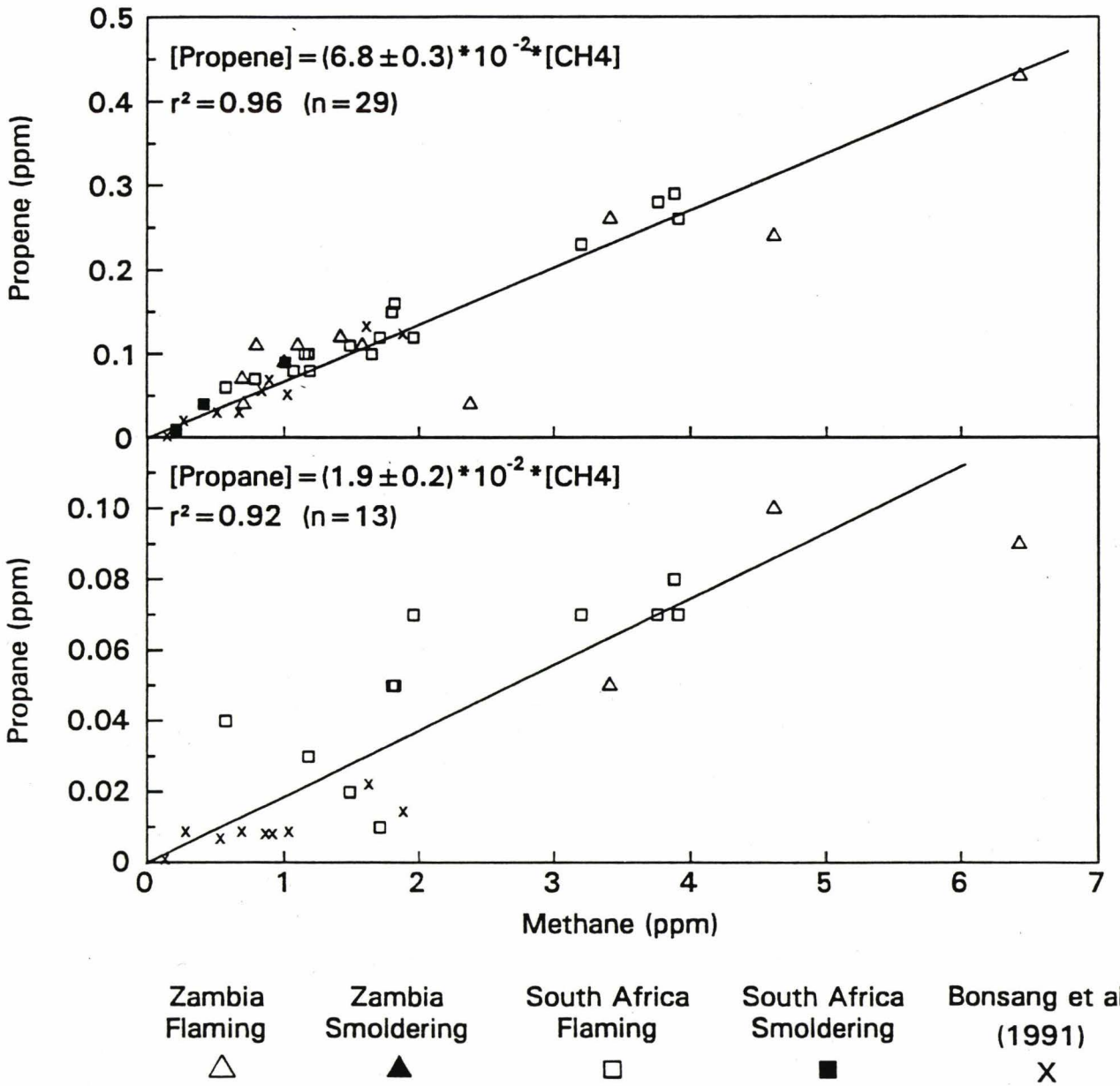
[Propene] = (6.8 ± 0.3) * 10 -2 * [CH4]
r² = 0.96 (n = 29)
Propene (ppm)
0.5
0.4
0.3
0.2
0.1
0
[Propane] = (1.9 ± 0.2) * 10 -2 * [CH4]
r² = 0.92 (n = 13)
Propane (ppm)
0.10
0.08
0.06
0.04
0.02
0
0
1
2
3
4
5
6
7
Methane (ppm)
Zambia Flaming
Zambia Smoldering
South Africa Flaming
South Africa Smoldering
Bonsang et al. (1991)

Fig. 4

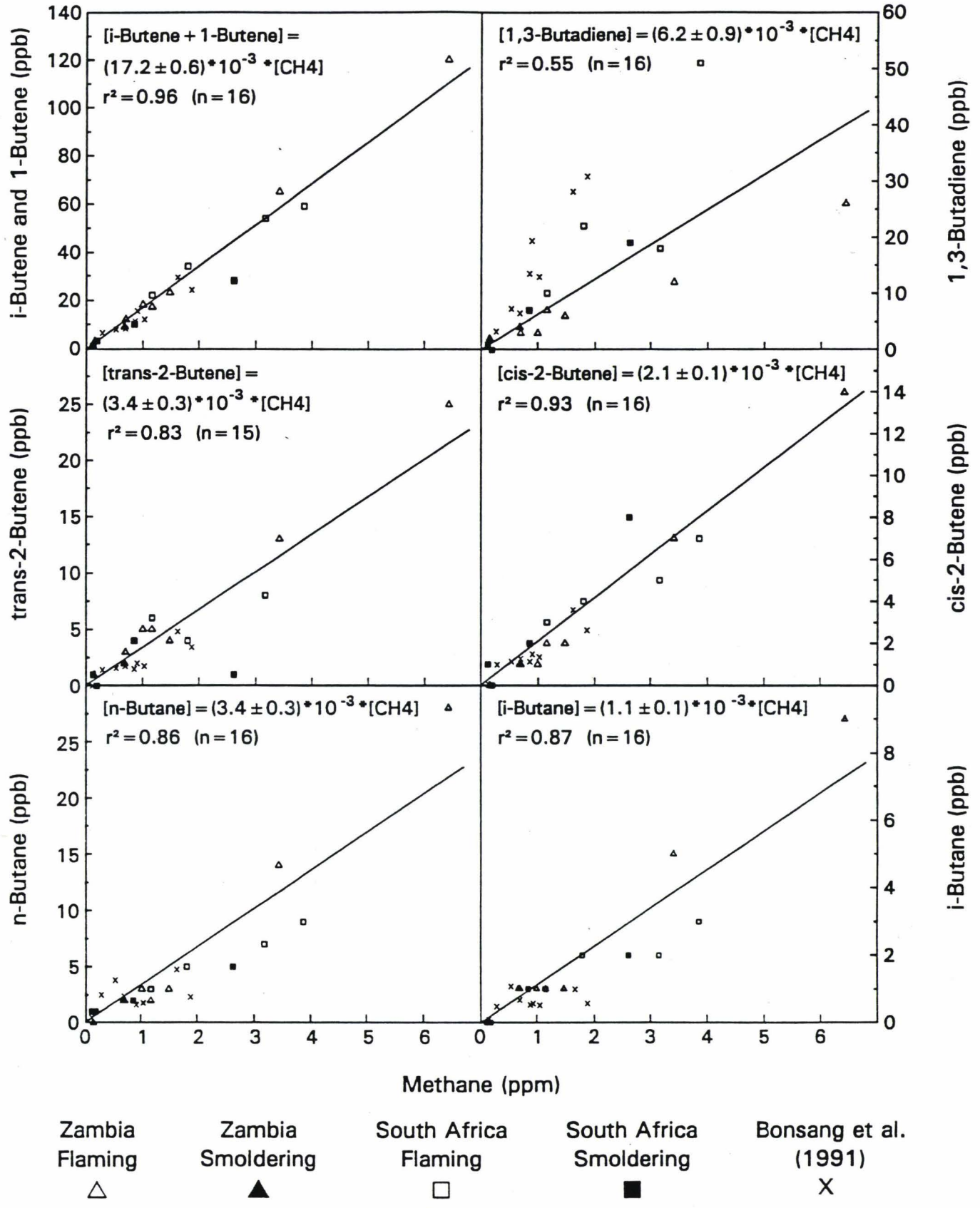
[i-Butene + 1-Butene] =
(17.2 ± 0.6)*10^-3 *[CH4]
r² = 0.96 (n = 16)
i-Butene and 1-Butene (ppb)
[1,3-Butadiene] = (6.2 ± 0.9)*10^-3 *[CH4]
r² = 0.55 (n = 16)
1,3-Butadiene (ppb)
[trans-2-Butene] =
(3.4 ± 0.3)*10^-3 *[CH4]
r² = 0.83 (n = 15)
trans-2-Butene (ppb)
[cis-2-Butene] = (2.1 ± 0.1)*10^-3 *[CH4]
r² = 0.93 (n = 16)
cis-2-Butene (ppb)
[n-Butane] = (3.4 ± 0.3)*10^-3 *[CH4]
r² = 0.86 (n = 16)
n-Butane (ppb)
[i-Butane] = (1.1 ± 0.1)*10^-3 *[CH4]
r² = 0.87 (n = 16)
i-Butane (ppb)
Methane (ppm)
Zambia Flaming
Zambia Smoldering
South Africa Flaming
South Africa Smoldering
Bonsang et al. (1991)

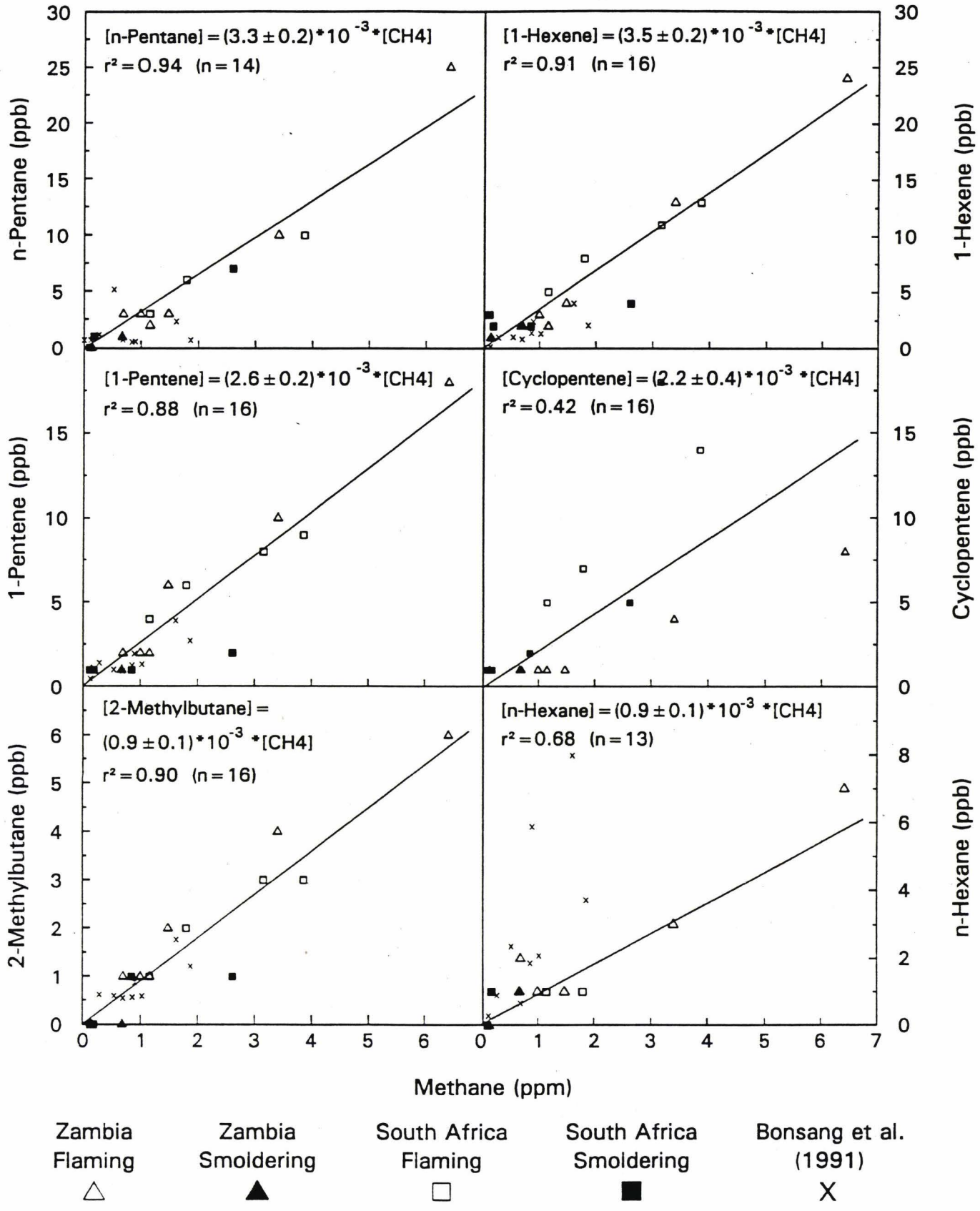
[n-Pentane] = (3.3 ± 0.2)*10 -3 *[CH4]
r² = 0.94 (n = 14)
[1-Hexene] = (3.5 ± 0.2)*10 -3 *[CH4]
r² = 0.91 (n = 16)
[1-Pentene] = (2.6 ± 0.2)*10 -3 *[CH4]
r² = 0.88 (n = 16)
[Cyclopentene] = (2.2 ± 0.4)*10-3 *[CH4]
r² = 0.42 (n = 16)
[2-Methylbutane] =
(0.9 ± 0.1)*10-3 *[CH4]
r² = 0.90 (n = 16)
[n-Hexane] = (0.9 ± 0.1)*10-3 *[CH4]
r² = 0.68 (n = 13)
n-Pentane (ppb)
1-Hexene (ppb)
1-Pentene (ppb)
Cyclopentene (ppb)
2-Methylbutane (ppb)
n-Hexane (ppb)
Methane (ppm)
Zambia Flaming
Zambia Smoldering
South Africa Flaming
South Africa Smoldering
Bonsang et al. (1991)

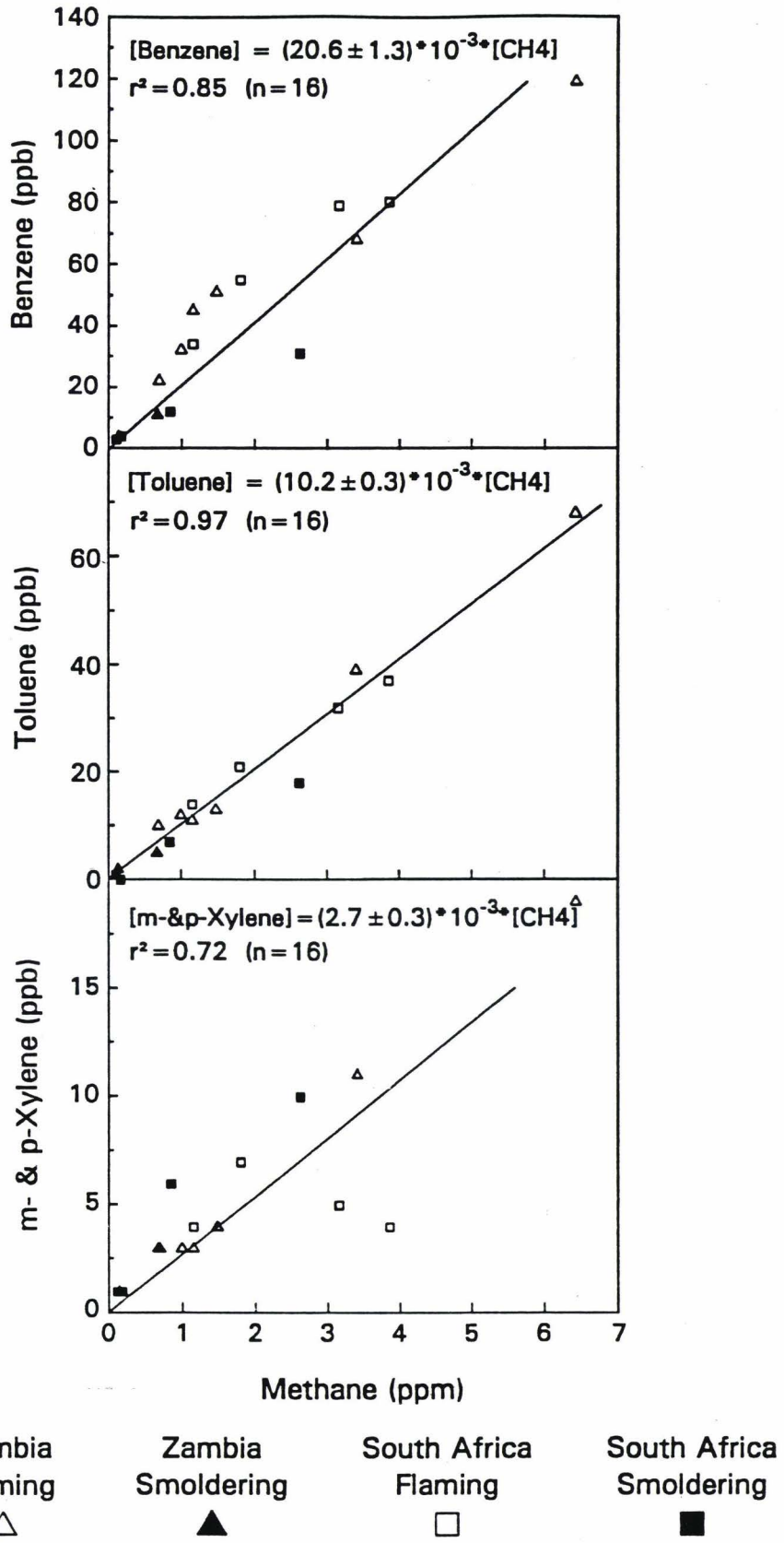
[Benzene] = (20.6 ± 1.3)*10-3*[CH4]
r² = 0.85 (n = 16)
Benzene (ppb)
[Toluene] = (10.2 ± 0.3)*10-3*[CH4]
r² = 0.97 (n = 16)
Toluene (ppb)
[m-&p-Xylene] = (2.7 ± 0.3)*10-3*[CH4]
r² = 0.72 (n = 16)
m- & p-Xylene (ppb)
Methane (ppm)
Zambia Flaming
Zambia Smoldering
South Africa Flaming
South Africa Smoldering

Preliminary Results of CO_2, CO, CH_4 and Nonmethane Hydrocarbons Emitted from Biomass Burning in Africa, 1993

Wei Min Hao

Shafizadeh Center for Wood and Carbohydrate Chemistry

University of Montana

Missoula, Montana

Africa 1993 Fires

C2H6 vs. CH4

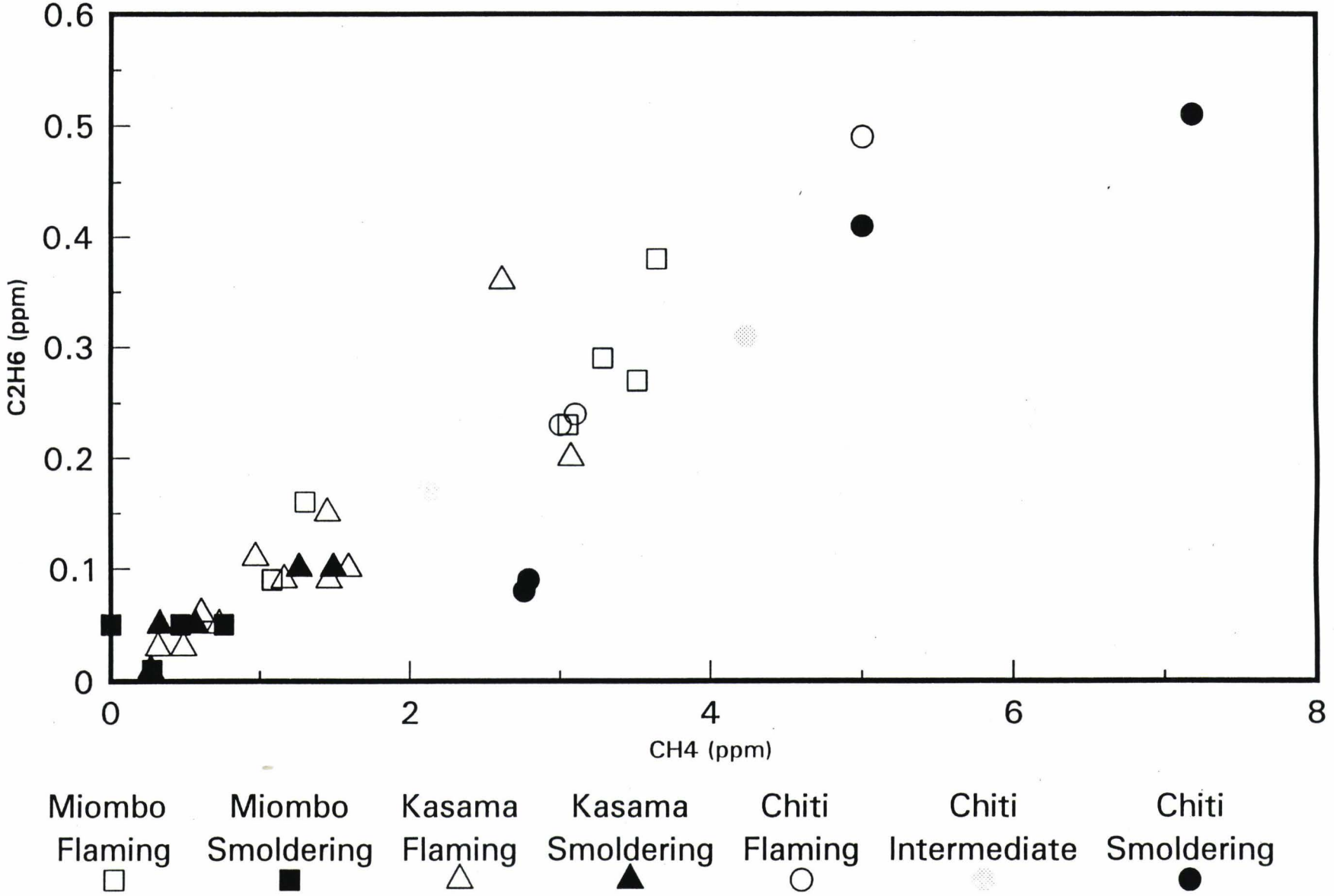

Africa 1993 Fires

C2H4 vs. CH4

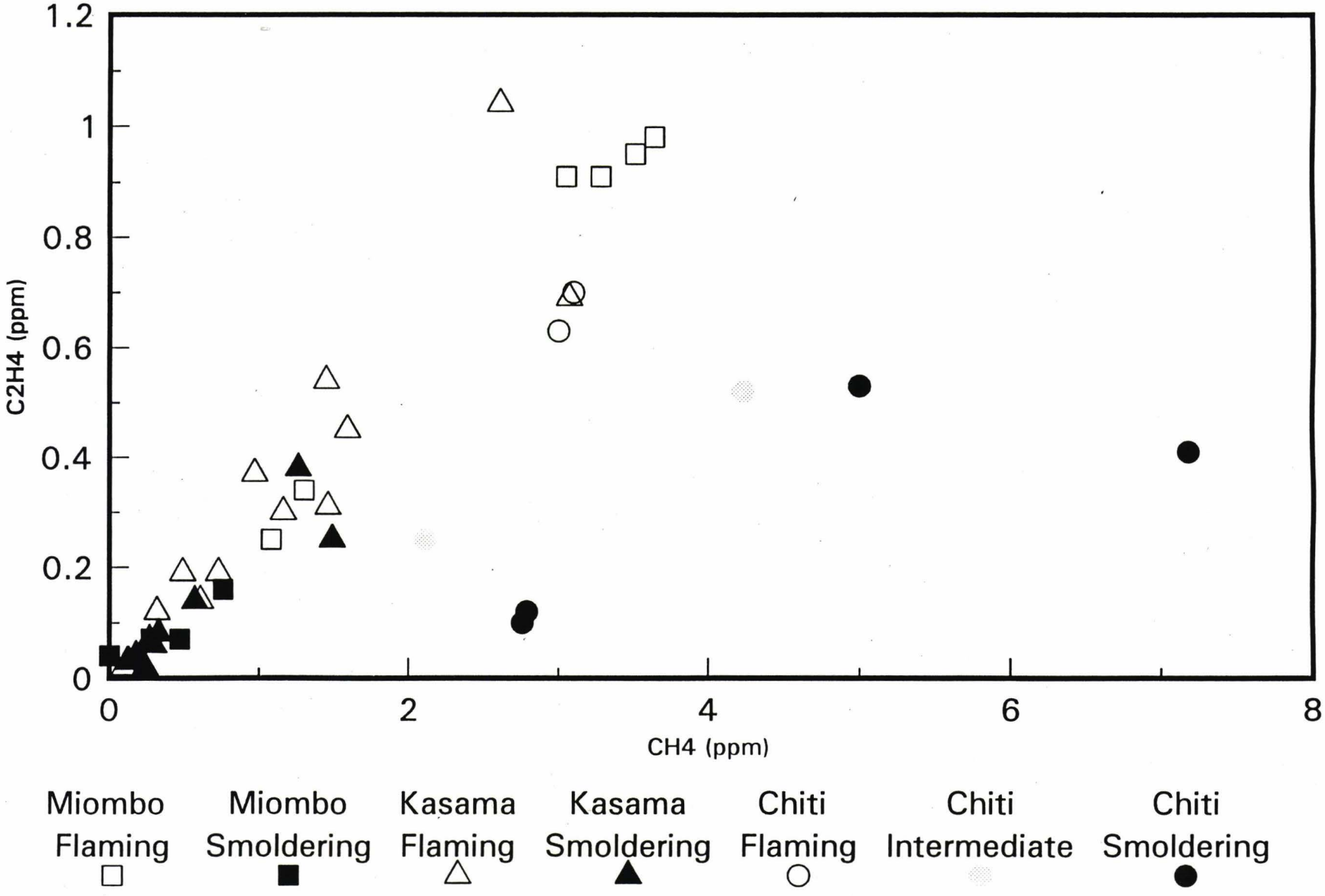

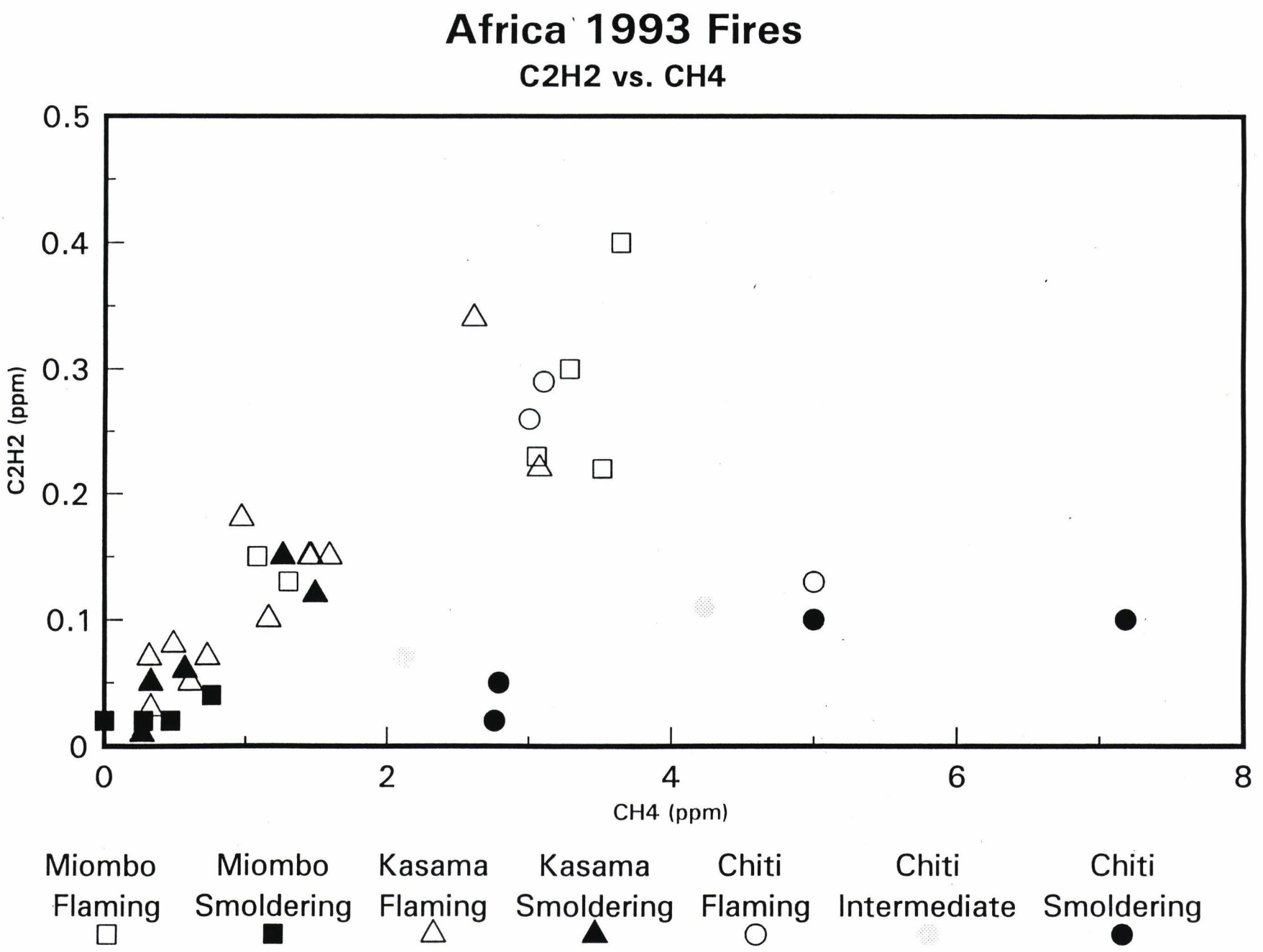
Africa 1993 Fires
C2H2 vs. CH4
0.5
0.4
0.3
0.2
0.1
0
C2H2 (ppm)
0
2
4
6
8
CH4 (ppm)
Miombo Flaming
Miombo Smoldering
Kasama Flaming
Kasama Smoldering
Chiti Flaming
Chiti Intermediate
Chiti Smoldering

Africa 1993 Fires

C3H8 vs. CH4

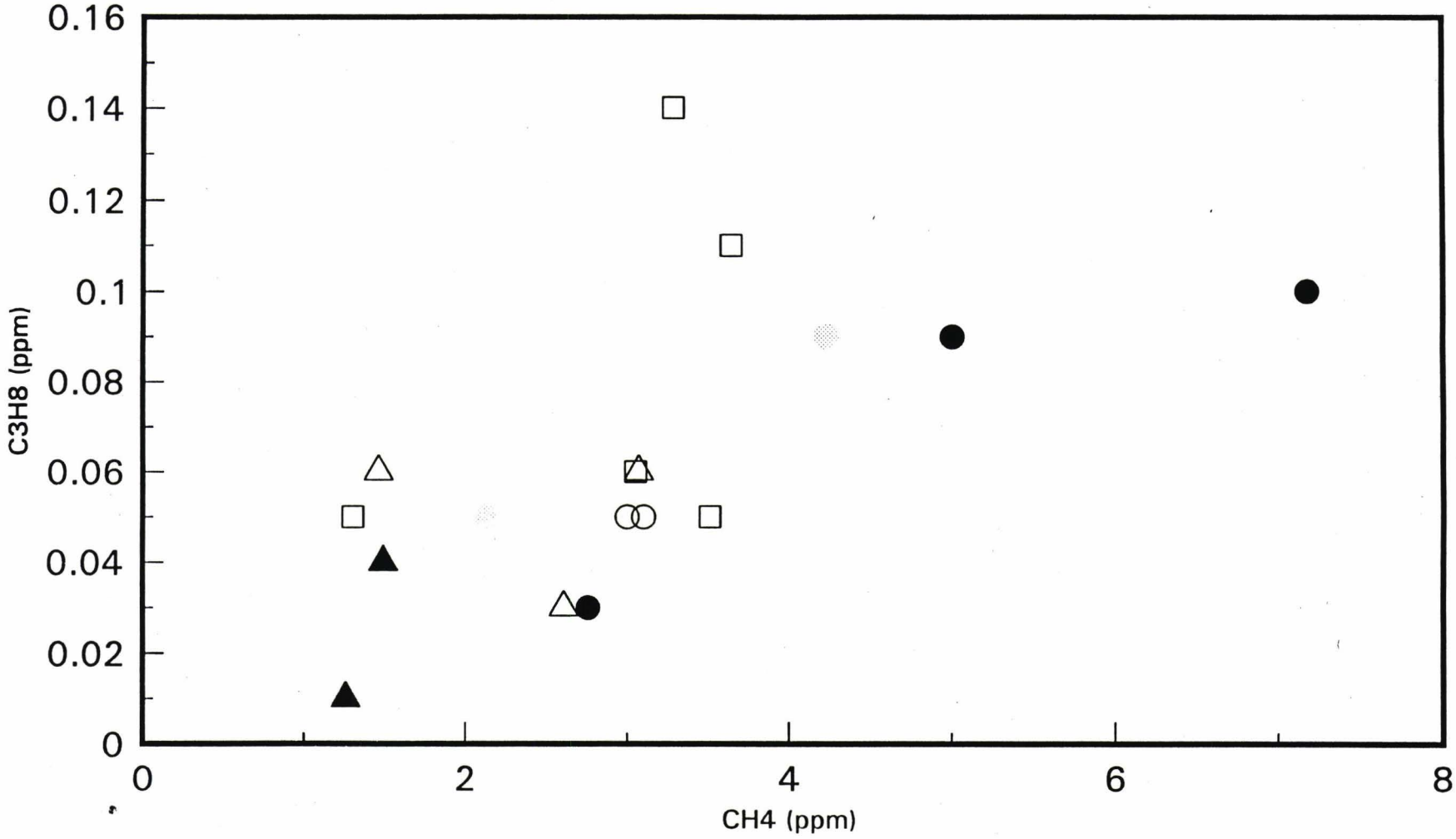

Africa 1993 Fires

C3H6 vs. CH4

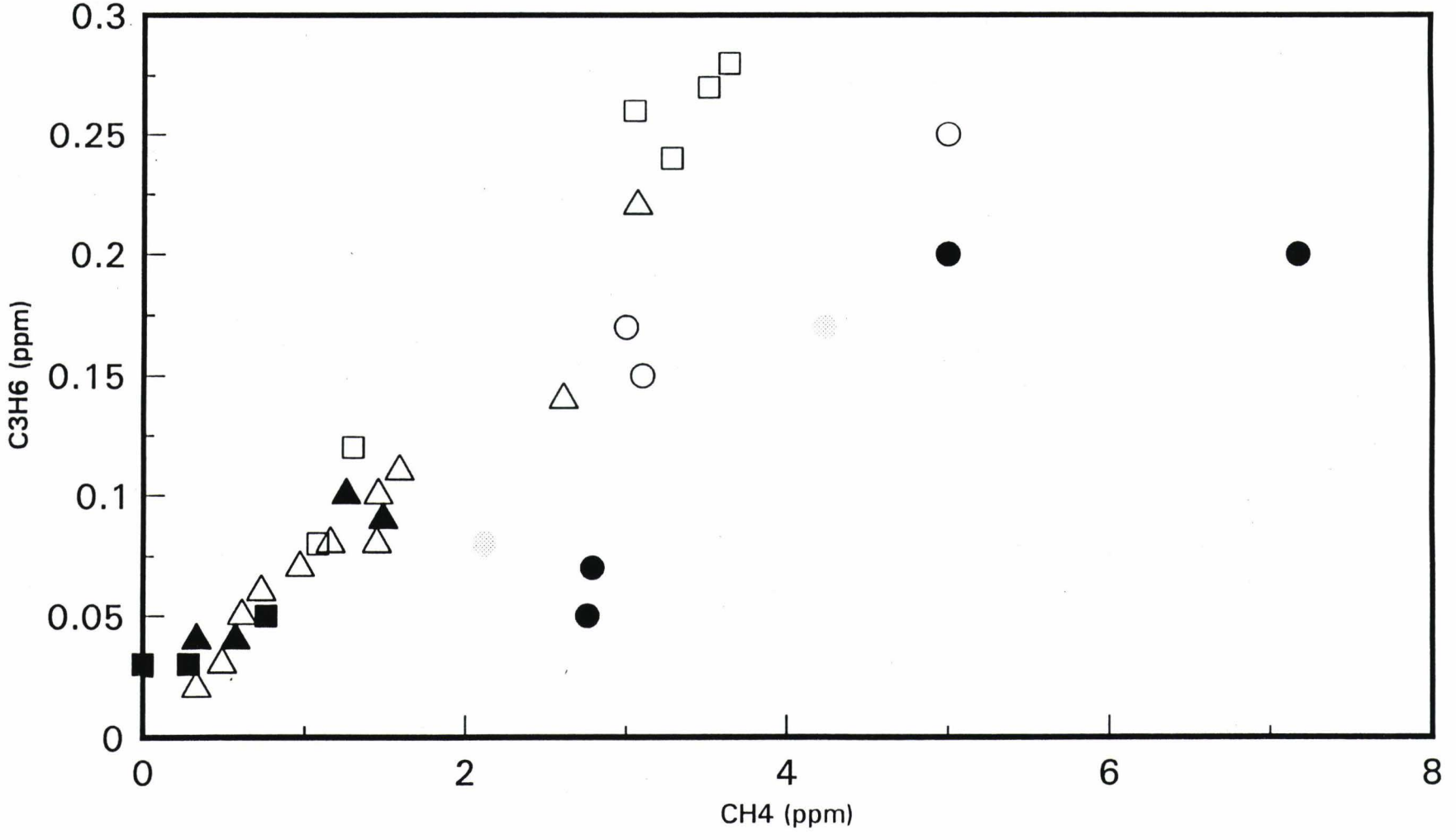

Africa 1993 Miombo + Zambia Fires Combined

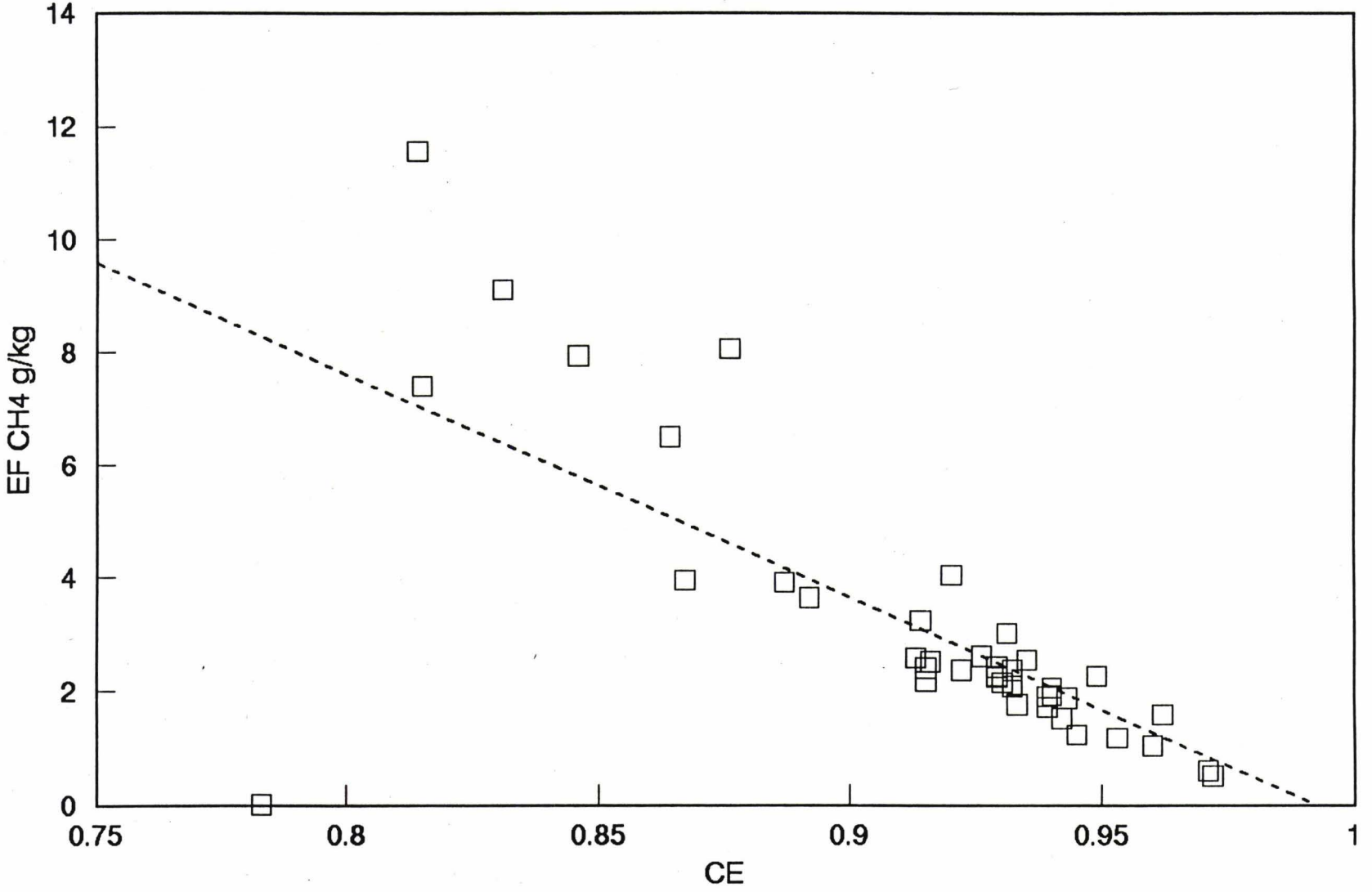

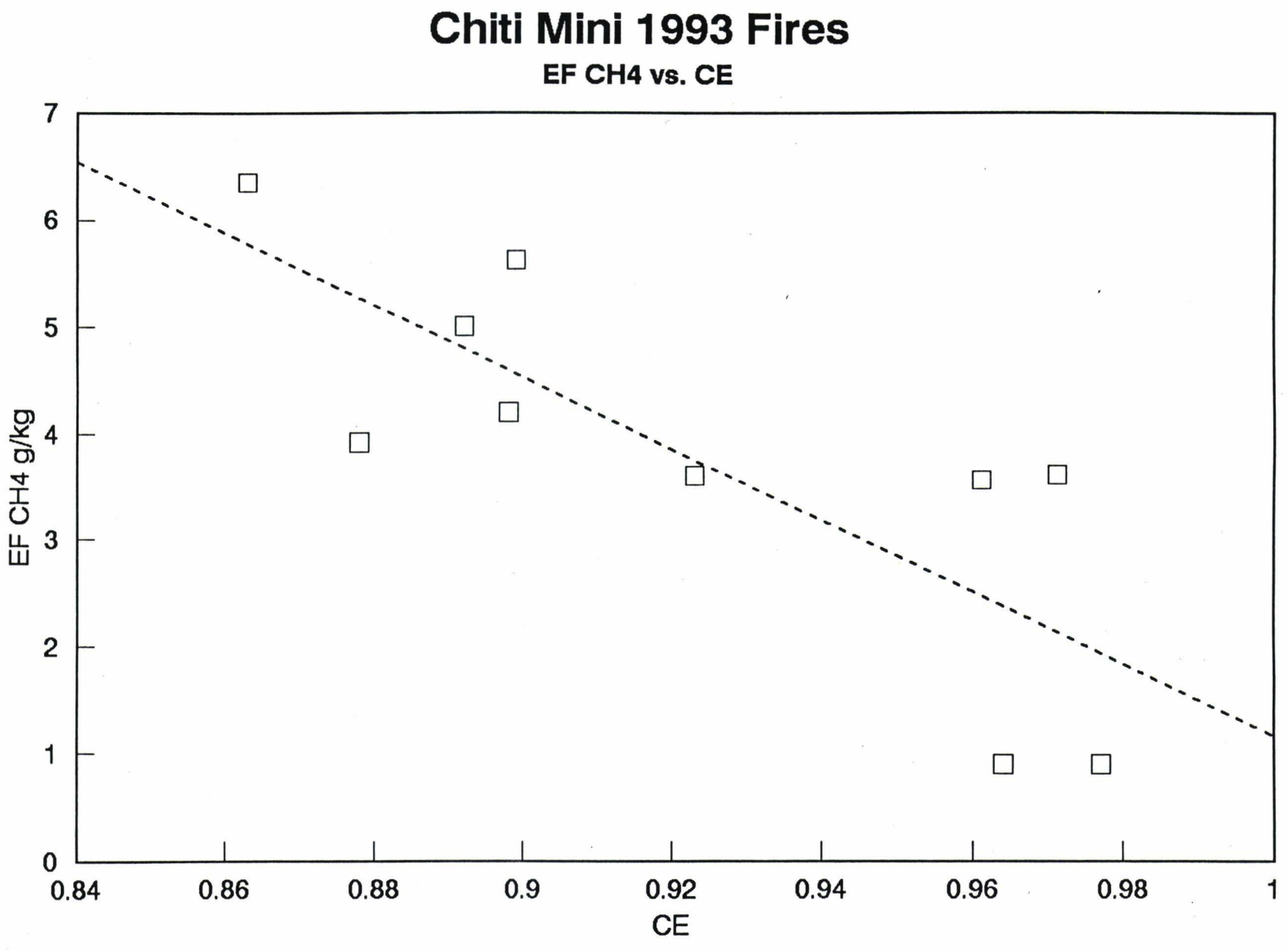
Chiti Mini 1993 Fires
EF CH4 vs. CE
EF CH4 g/kg
CE
0
1
2
3
4
5
6
7
0.84
0.86
0.88
0.9
0.92
0.94
0.96
0.98
1

SOME PROCESSES IN SMOLDERING COMBUSTION OF BIOMASS

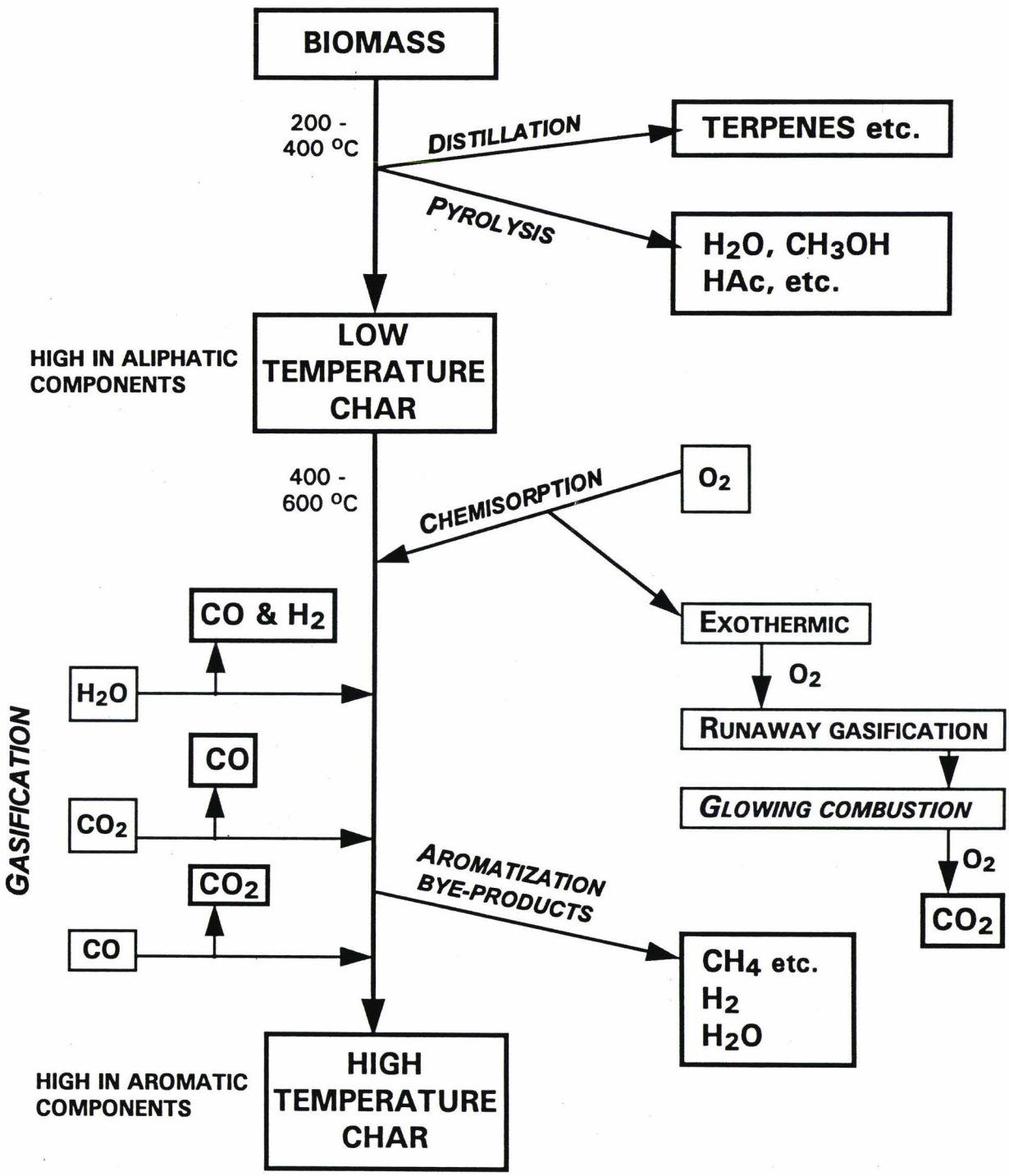

Executive Summary

This report summarizes the work accomplished as part of RJVA93847. It is divided into 4 parts.

Part 1 starts with a survey and cursory appraisal of some of the advanced instrumentation available to serve as combustion diagnostics with an emphasis on characterizing emissions. Based on the results of this survey a recommendation is made to invest in an FTIR multipass cell system. The expected benefits of this system are projected.

Part 2 consists of a detailed set of specifications for an FTIR system optimized for combustion emissions measurements. A system is currently being built according to these specifications.

Part 3 is a description of a pilot-scale study carried out in the IFSL using a prototype system with many similarities to the system we are having built. The potential of the FTIR-laboratory approach is clearly demonstrated and there is a preliminary presentation of the significant results. This section consists of a draft of a publication and a series of appendices on topics of special interest to IFSL scientists.

Part 4 is an outline of the installation schedule for the new system and also contains some simulated data from the new system compared to data from the system used in the pilot-scale study.